

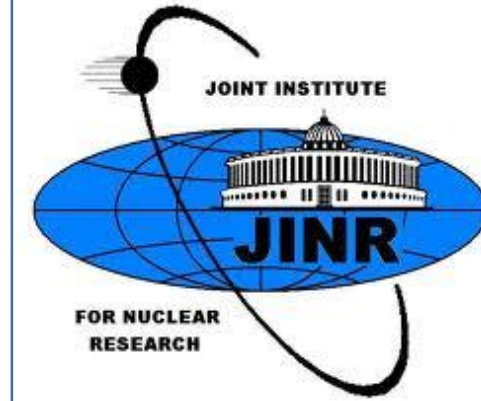


PROBING QCD AT HIGH ENERGY

Yuri Kulchitsky
for ATLAS Collaboration

JINR, Dubna, Russia

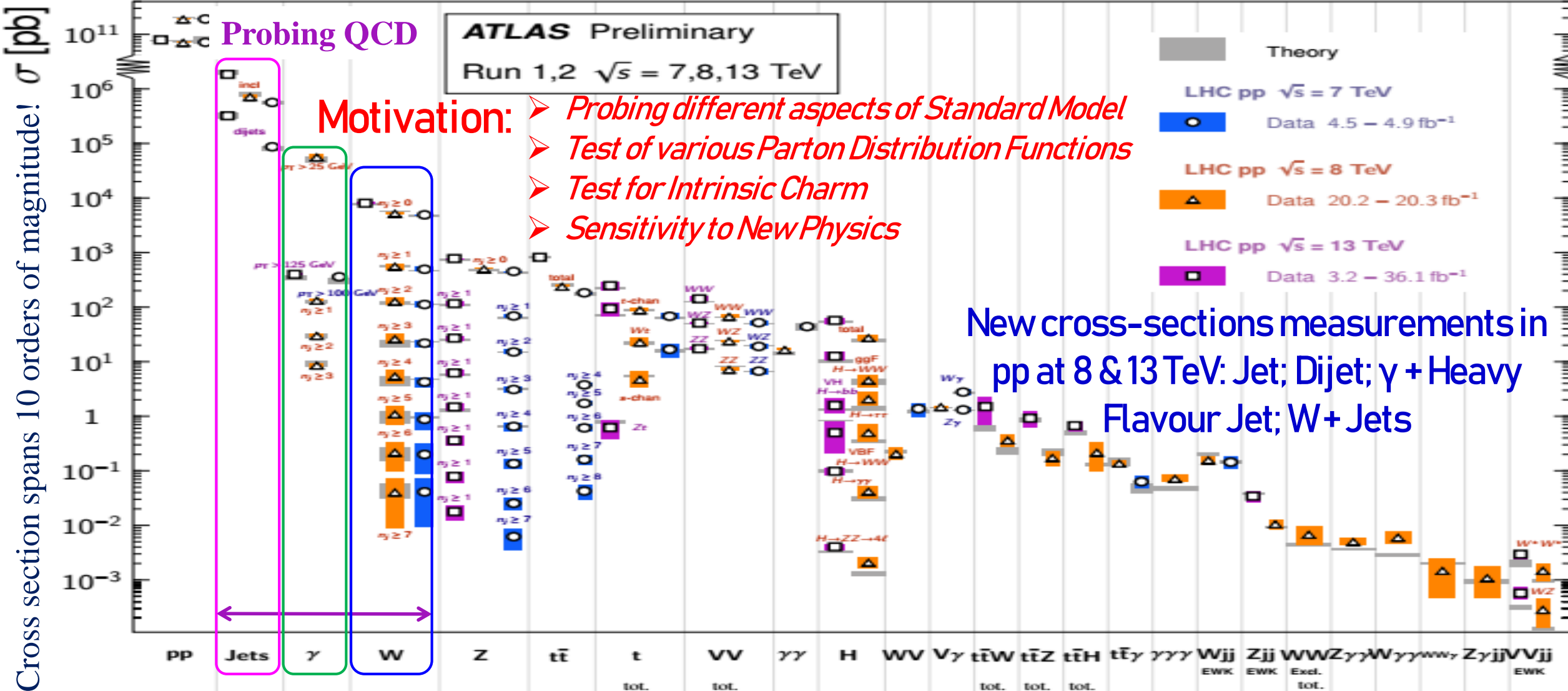
24-30 September 2018,
New Trends in High-Energy Physics,
Budva, Becici, Montenegro



STANDARD MODEL MEASUREMENTS

Standard Model Production Cross Section Measurements

Status: June 2018



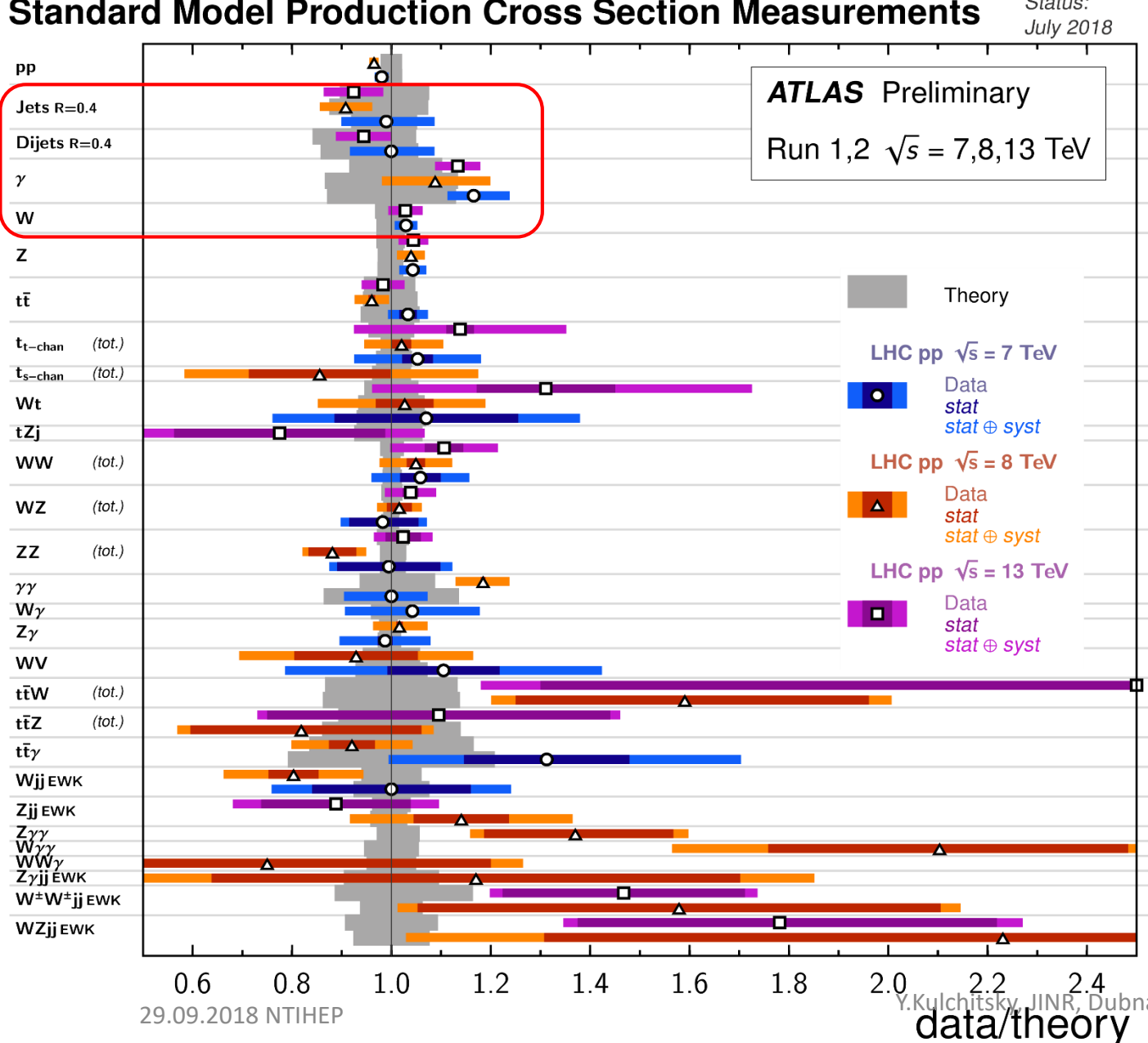
STANDARD MODEL X-SECTION MEASUREMENTS

Standard Model Production Cross Section Measurements

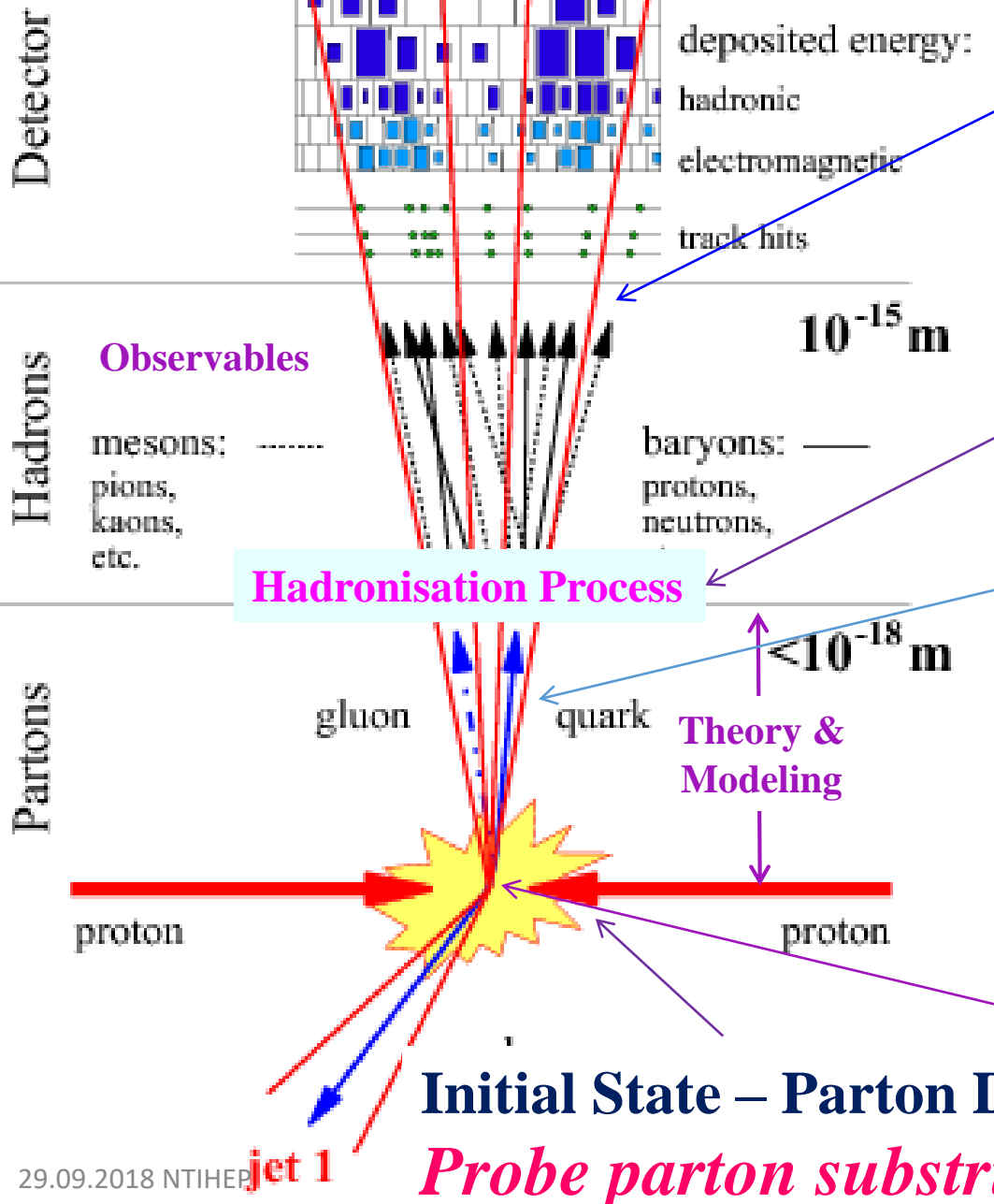
Status:
July 2018

ATLAS Preliminary

Run 1,2 $\sqrt{s} = 7,8,13$ TeV



The data/theory ratio for several SM total and fiducial production cross section measurements, corrected for leptonic branching fractions. *All theoretical expectations were calculated at NLO or higher.* The dark-color error bar represents the statistical uncertainty. The lighter-color error bar represents the full uncertainty, including systematics and luminosity uncertainties. The luminosity used and reference for each measurement are also shown. Uncertainties for the theoretical predictions are quoted from the original ATLAS papers. *They were not always evaluated using the same prescriptions for PDFs and scales.*



Jets: narrow collimated clusters of stable particles produced by the fragmentation of a hard parton

Probe highest $p_T \rightarrow$ best handles on searches for new physics

Parton fragmentation

- Phenomenological models (*PYTHIA*, *HERWIG*, ...)
- Matching to fixed order

Parton shower (PS)

- Soft- and collinear approximations
- Mismatch between kinematics of virtual and real corrections: *soft-gluon resummation*

Hard scattering – perturbative Quantum ChromoDynamics (pQCD) predictions at fixed-orders QCD calculations: Leading Order (LO), Next-to-LO (NLO), Next-to-Next-to-LO (NNLO)

Probe parton substructure \rightarrow test QCD through wide energy range

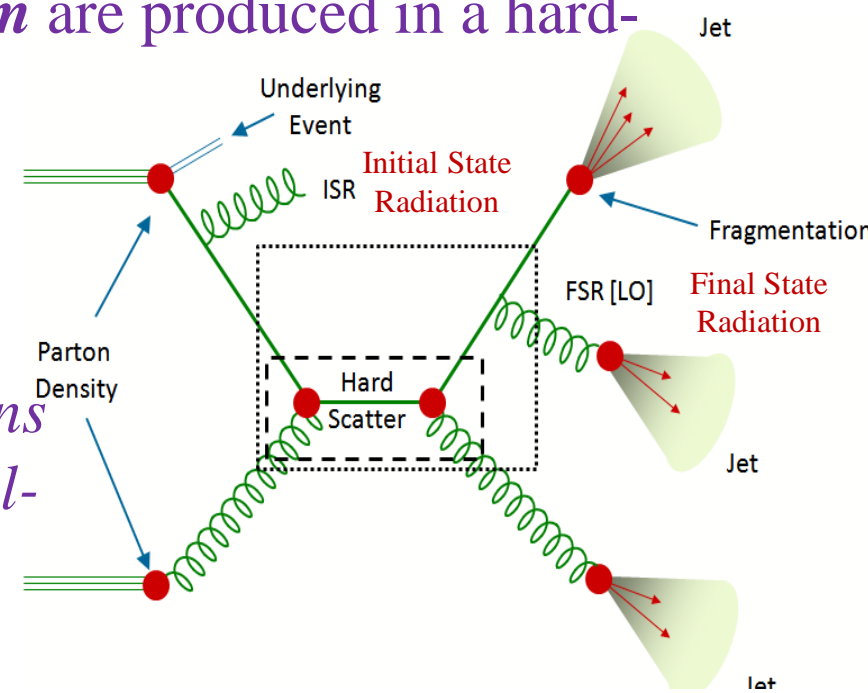
JET PHYSICS IN PP-COLLISIONS: MOTIVATION

Jets are crucial for our understanding of the Standard Model

Probing of the Quantum ChromoDynamics (QCD) → Jets are the result of fragmentation of partons produced in a scattering process

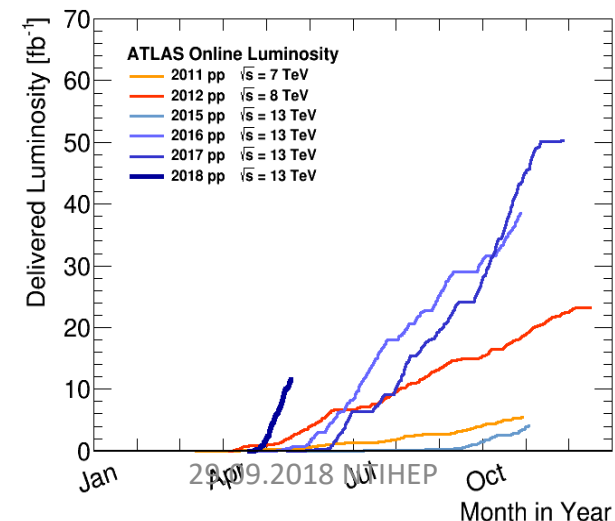
In High-Energy Particle collisions – two main phases:

- **Perturbative phase:** partons with *high-transverse momentum* are produced in a hard-scattering process at a scale Q
- **Non-perturbative phase:** partons convert in hadrons emitting gluons and $q\bar{q}$ -pairs an interplay between *Hadronization Process (HP)* and *Underlying Event (UE)*:
 - **Hadronization Process:** transition from partons to hadrons
 - **Underlying Event:** a) initial-state radiation (ISR), b) final-state radiation (FSR), c) multiple-parton interactions and d) colour-reconnection effects
- Effects of **HP** and **UE** depend on *Jet radius parameter* and are most pronounced at low p_T
 - ❖ All these aspects of high energy collisions can be Probed in the Jet Physics



A TOROIDAL LHC APPARATUS (ATLAS)

<u>Subdetector</u>	<u>Operational Fraction</u>
AFP	93.8%
ALFA	99.9%
CSC Cathode Strip Chambers	95.3%
Forward LAr Calorimeter	99.7%
Hadronic End-Cap Lar Cal	99.5%
LAr EM Calorimeter	100 %
LVL1 Calo Trigger	99.9%
LVL1 Muon RPC Trigger	99.8%
LVL1 Muon TGC Trigger	99.9%
MDT Muon Drift Tubes	99.7%
Pixels	97.8%
RPC Barrel Muon Chambers	94.4%
SCT Silicon Strips	98.7%
TGC End-Cap Muon Cha	99.5%
Tile Calorimeter	99.2%
TRT Transit Rad Tracker	97.2%



Air-core Muon spectrometer

(μ Trigger/tracking and Toroid Magnets)

Precision Tracking:

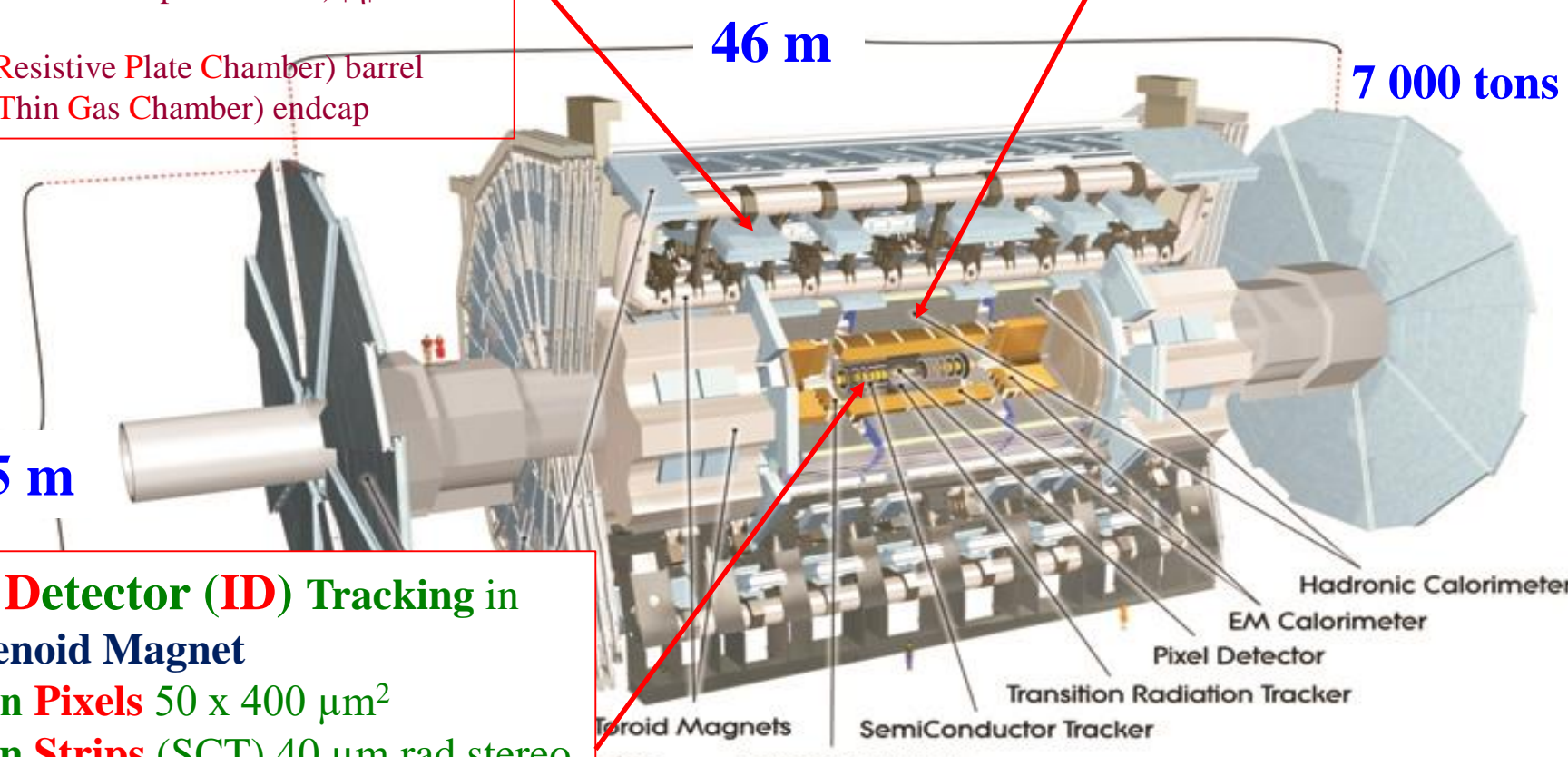
- MDT (Monitored Drift Tubes)
- CSC (Cathode Strip Chambers) $|\eta| > 2.4$

Trigger:

- RPC (Resistive Plate Chamber) barrel
- TGC (Thin Gas Chamber) endcap

Longitudinally segmented Calorimeter: EM and Hadronic energy

- LiquidAr EM barrel and End-cap & Hadronic End-cap
- Tile calorimeter (Fe-scintillator) Hadronic barrel



Inner Detector (ID) Tracking in

2T Solenoid Magnet

- Silicon **Pixels** $50 \times 400 \mu\text{m}^2$
- Silicon **Strips** (SCT) $40 \mu\text{m}$ rad stereo strips
- **Transition Radiation Tracker (TRT)** up to 36 points/track

Y.Kulchitsky, JINR, Dubna

Two Level Trigger system

- **L1** – hardware: 100 kHz, 2.5 μs latency
- **HLT** – farm: merge the former L2 and Event Filter 1.5 kHz, 0.2 s latency

ATLAS CALORIMETERS

- Lar & TileCal >> Very stable performance
- Improved stability of new Tile power supplies

- Good operation efficiency: ~100% for LAr & Tile
- LAr using 4 sample readout to achieve 100 kHz

Min. bias trigger scintillators (MBTS)

- Cu-LAr structure
- $1.5 < |\eta| < 3.2$

→ LAr hadronic end-cap (HEC)

LAr electromagnetic end-cap (EMEC)

- Pb-LAr accordion
- $|\eta| < 2.5$

LAr electromagnetic barrel

Cryostat (dead material)

(LAr: Liquid Argon)

Tile barrel

Tile extended barrel

LAr forward (FCal)

- Fe-Scintillating Tile structure
- $|\eta| < 1.7$

Muon Spectrometer

Hadronic Calorimeter

Electromagnetic Calorimeter

Solenoid magnet

Transition Radiation Tracker
Pixel/SCT detector

Photon

Neutron

Proton

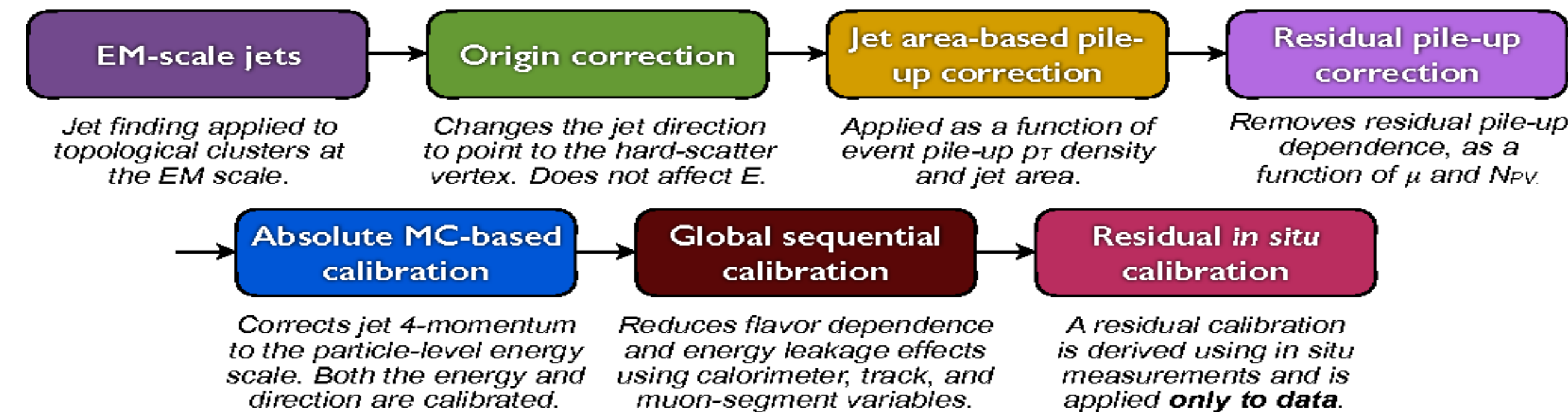
Neutrino

Electron

The dashed tracks are invisible to the detector

JET RECONSTRUCTION

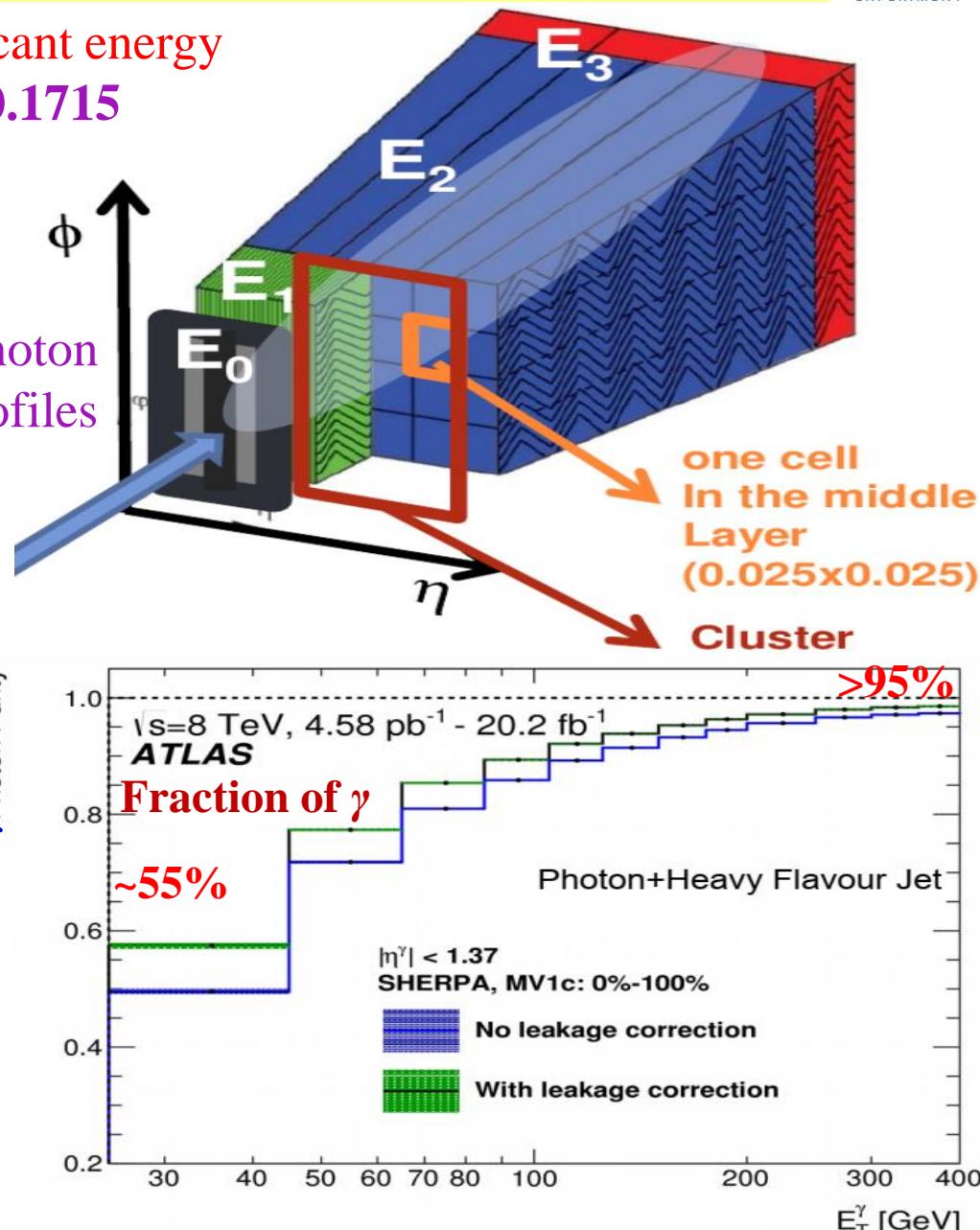
- ❑ A set of **Single-Jet Triggers** with different thresholds used to collect data
- ❑ Only events with **at least one Primary Vertex**, reconstructed ≥ 2 tracks with $p_T > 400$ MeV
- ❑ Primary Vertex with the highest $\sum p_T^2$ of associated tracks is selected as the hard-scatter vertex
- ❑ Jets reconstructed by the **anti- k_t** algorithm: jets are clustered using two values of **R=0.4 & 0.6**
- ❑ ***Multi-step process to an Jet Energy Calibration:***



- Jets corrected for experimental effects: *resolutions, efficiency, ...*
- Jets unfolding for cross-sections are defined at the ***particle-level final state***

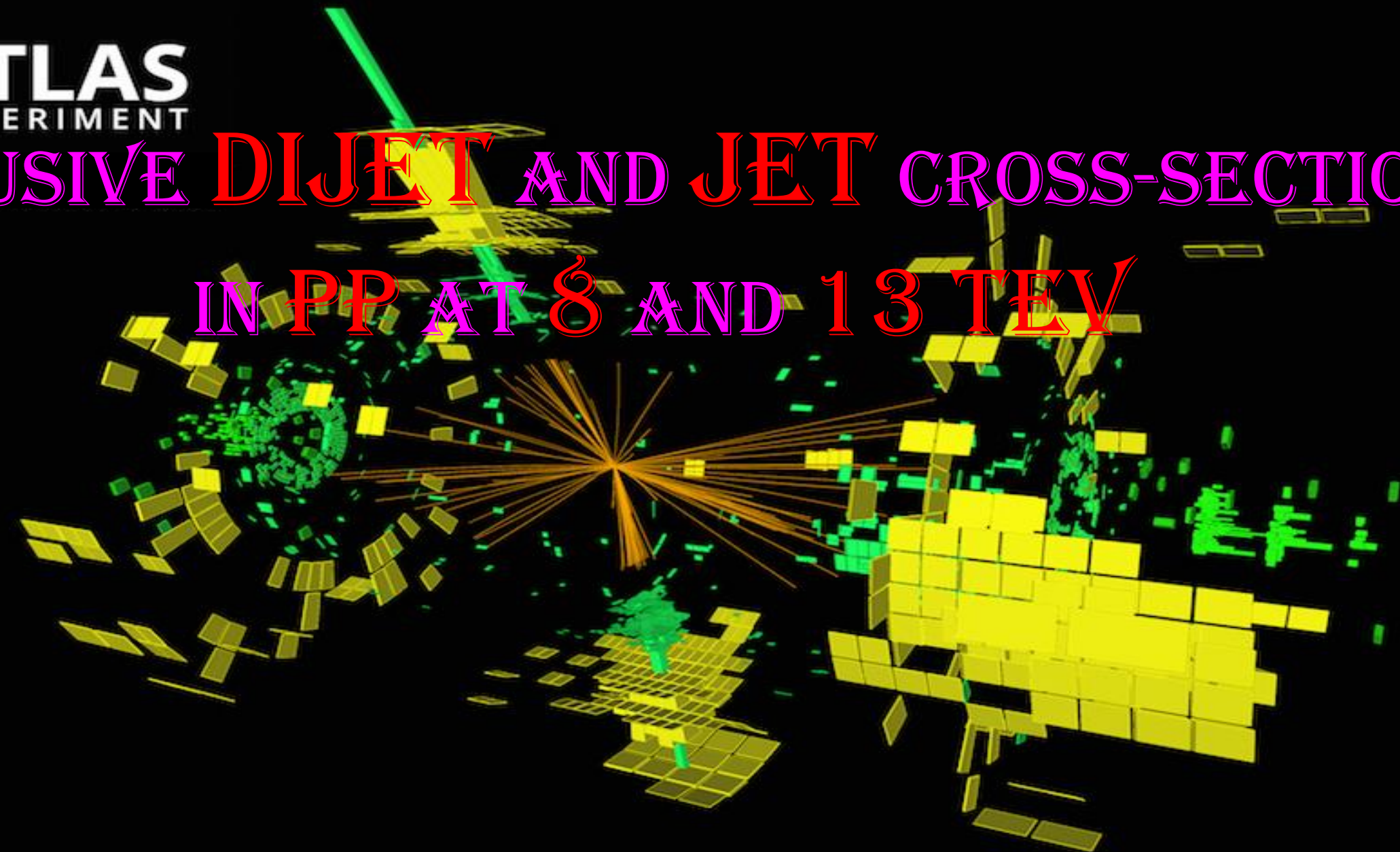
DIRECT PHOTON & ELECTRON RECONSTRUCTION

- Search for **seed energy clusters** in the EM calorimeter with significant energy
- Form a cluster from cells in a rectangular region $\Delta\eta \times \Delta\phi = 0.125 \times 0.1715$ around seed
- ❖ Selected in barrel $|\eta| < 1.37$ & end-cap $1.56 < |\eta| < 2.37$; excluding transition region between barrel & endcap ECAL $1.37 < |\eta| < 1.56$
- ✓ **Photon identification:** classify as electron, photon, or converted photon matching cluster with tracks; use lateral and longitudinal energy profiles of the photon/electron electromagnetic shower
- **Calorimeter isolation** in region $\Delta R = 0.4$ around photon with requirement $E_T^{iso} < 0.0042 \times E_T^\gamma + 4.8 \text{ GeV}$
- Converted and unconverted γ -s are calibrated separately use the tracking information to correct the Calorimeter response for upstream energy losses and leakage
- ❖ **Calculate energy and direction:** photon energy a weighted sum of layer energies, with corrections for detector effects
- ✓ Corrected for pileup using jet area method
- Use 2D-sidebands for remaining background
- ❖ Remove hadron and τ background
- ✓ Small electron background removed using MC





INCLUSIVE DIJET AND JET CROSS-SECTIONS IN PP AT 8 AND 13 TEV



□ *Dijet production allows to Probe for higher scales*

- The double-diff. inclusive **Jet** cross-section measurement vs. p_T^{jet} & $y \rightarrow 0.1 \text{ TeV} \leq p_T^{\text{jet}} \leq 4 \text{ TeV}$ & $|y| < 3$
- The double-differential inclusive **Dijet** cross-sections measurement vs. **dijet** mass $m_{\text{jj}} \rightarrow 0.3 \text{ TeV} - 9 \text{ TeV}$ & $y^* = |y_1 - y_2|/2 < 3$

□ **Motivation: a test of validity of pQCD and Probing of the Parton Distribution Functions (PDF) in the proton**

- ❖ Jets are identified with the anti- k_t using $R=0.4$
- ❖ Jet cross section refers to **Particle-Level Jets** and **to compare** them with **NLO pQCD** predictions with **Parton-Level Jets**, a correction for Non-Perturbative (NP) and ElectroWeak (EW) effects is done

□ **Theoretical predictions:** **NLO pQCD** calculated by **NLOJET++ 4.1.3** with

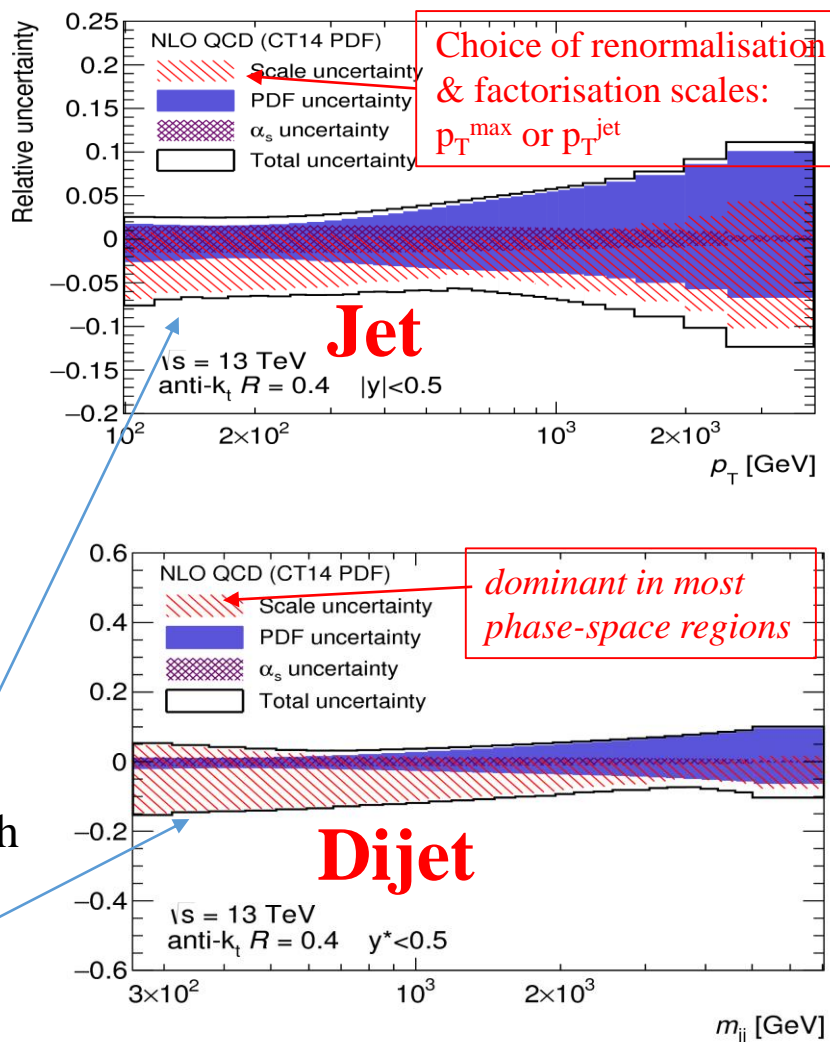
several PDFs and different **Renormalisation** (μ_R) and **Factorisation** (μ_F) scales
 $\mu_R = \mu_F = p_T^{\text{jet}, \text{max}}$ for **Jet** & $\mu_R = \mu_F = p_T^{\text{max}} \times \exp(0.3y^*)$ for **Dijet**

- The difference between the predictions obtained with the p_T^{max} and p_T^{jet} scale choice is **treated as an additional uncertainty**

p_T^{max} is the transverse momentum of the leading jet in the event

Y.Kulchitsky, JINR, Dubna

p_T^{jet} is the p_T of each individual jet in the event



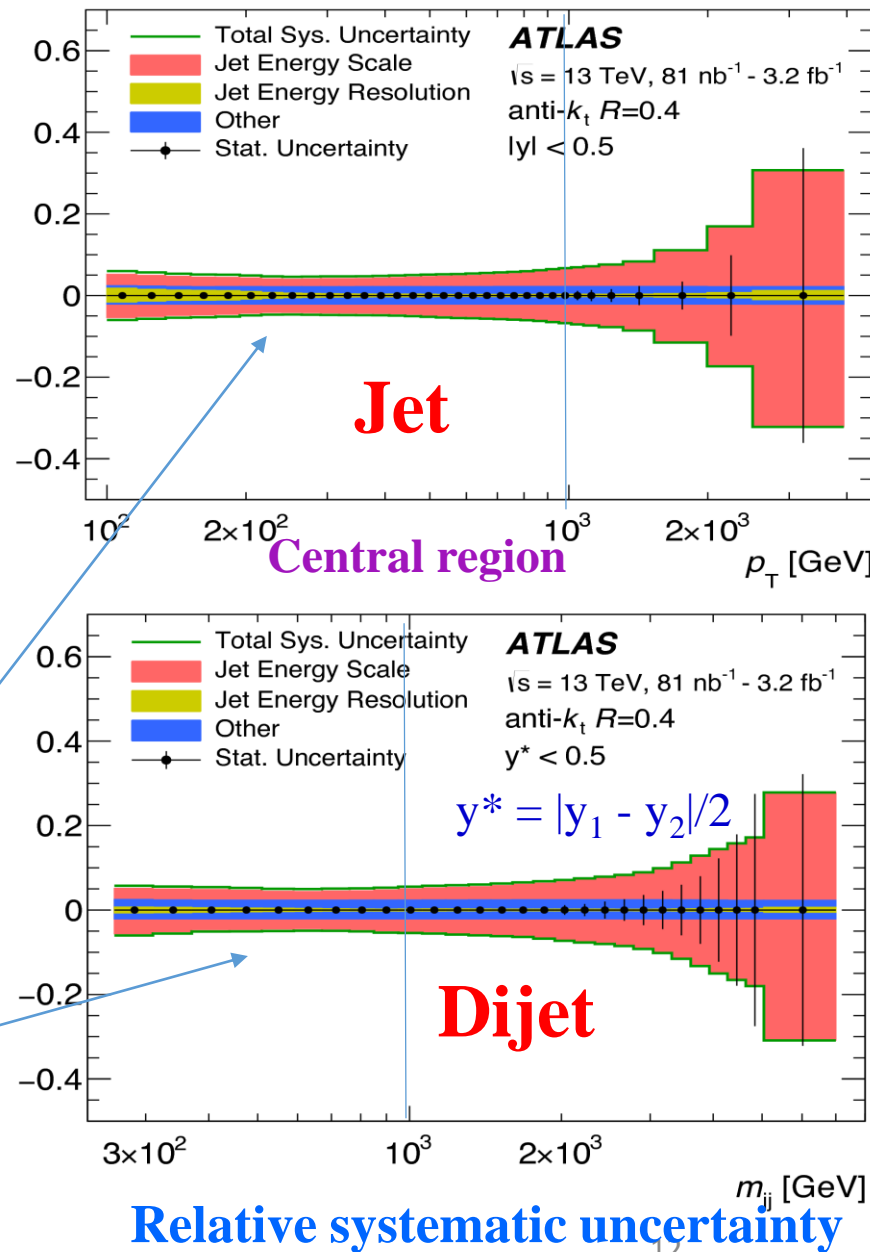
Uncertainty in the **NLO pQCD** inclusive jet & dijet cross-sections

EVENT AND JET SELECTION AT 13 TeV

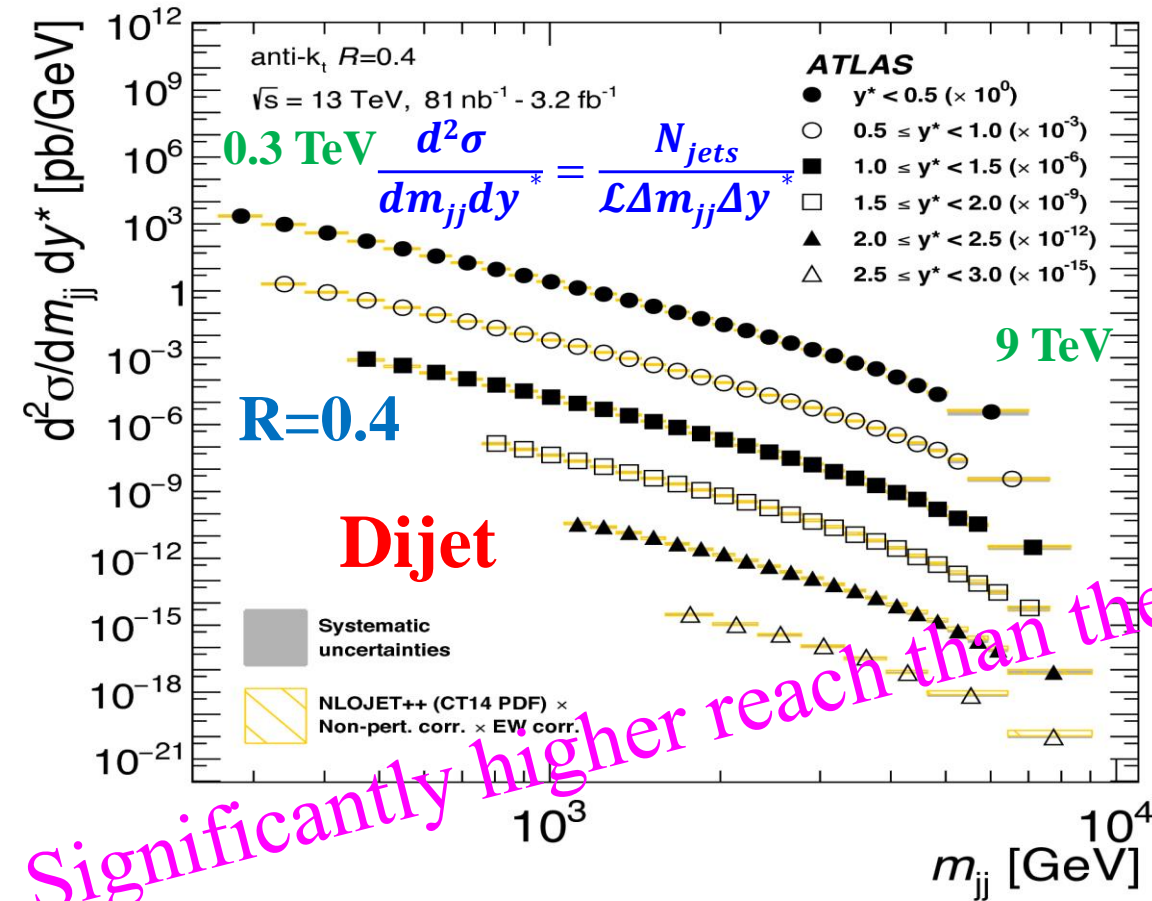
JHEP 05 (2018) 195



- Dataset used for measurement: pp at 13 TeV; $L_{\text{int}} = 3.2 \text{ fb}^{-1}$
- **Pile-up:** $\langle \mu \rangle$ increases from $\langle \mu \rangle \sim 10$ to $\langle \mu \rangle \sim 36$
- **Two-level Jet trigger.** Events with Jet: $|\eta| < 3.2$, p_T^{jet} over a threshold. Offline data selection and **Jet correction**: similar to **Dijet case**
- ❖ Cross-sec. are measured for **6 rapidity bins** as funct. p_T^{jet}, m_{jj}
- ❖ Data are **unfolded** to the **particle level** in a 3-step procedure:
 - correction for the sample **impurities**;
 - unfolding for the **p_T migration**;
 - correction for the analysis **inefficiencies**
- **Sources of systematic uncertainty:** those associated with Jet
 - reconstruction &
 - calibration,
 - unfolding procedure,
 - luminosity measurement
- **Main sources:** ► **Jet Energy Scale (JES)** & ► **Jet Energy Resolution (JER)**: for $|y| < 0.5$ & $p_T < 1 \text{ TeV}$ less than 10%

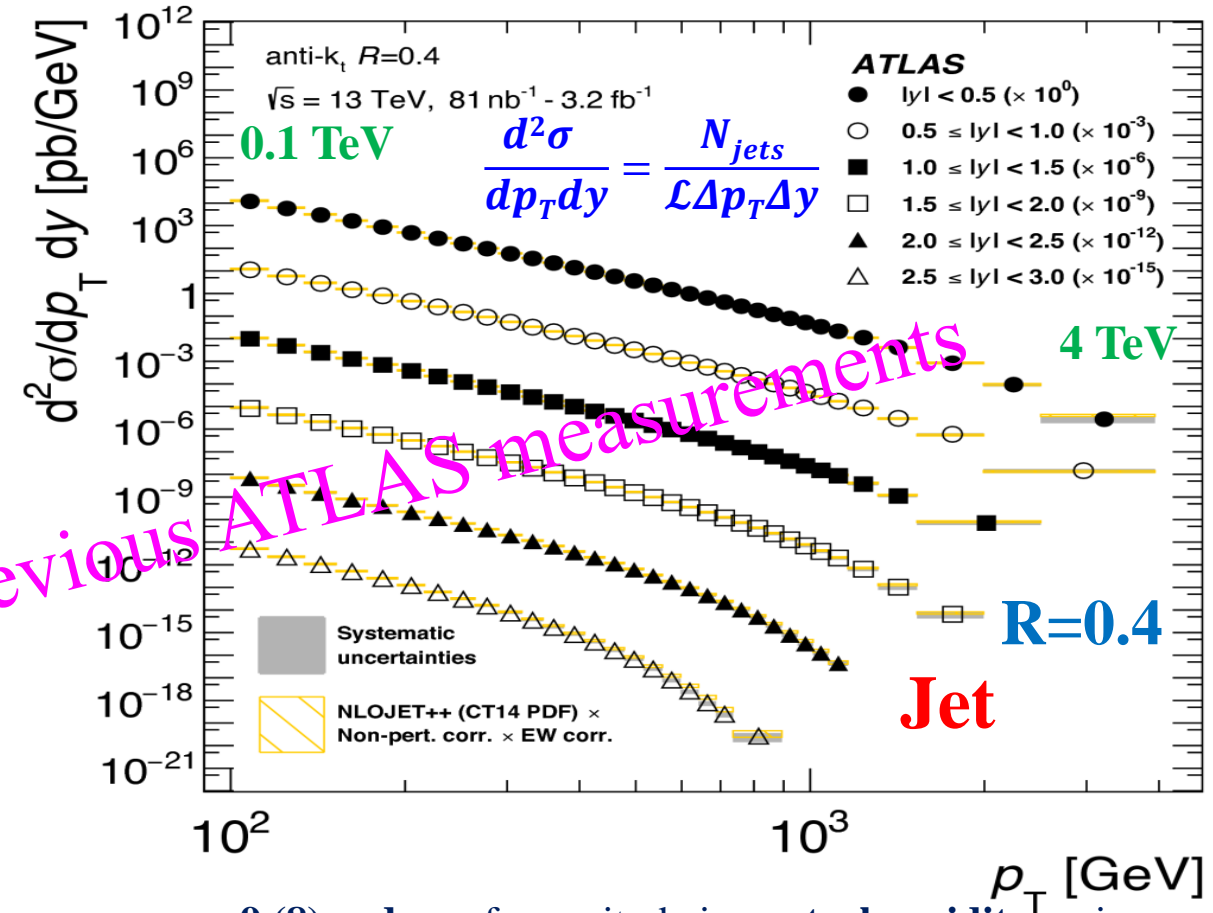


Dijet double-diff. cross-sections vs. **dijet mass (m_{jj})** and **rapidity separation ($y^* = |y_1 - y_2|/2$)**



□ Data are compared to **NLOJET++ predictions** with various **PDFs (CT14)**, corrected for *non-perturbative* and *EW* effects, scale: $\mu = \mu_R = \mu_F = p_T^{\max} e^{0.3y^*}$

Jet double-diff. cross-sections vs. **jet p_T** and **rapidity separation $|y| < 3$**

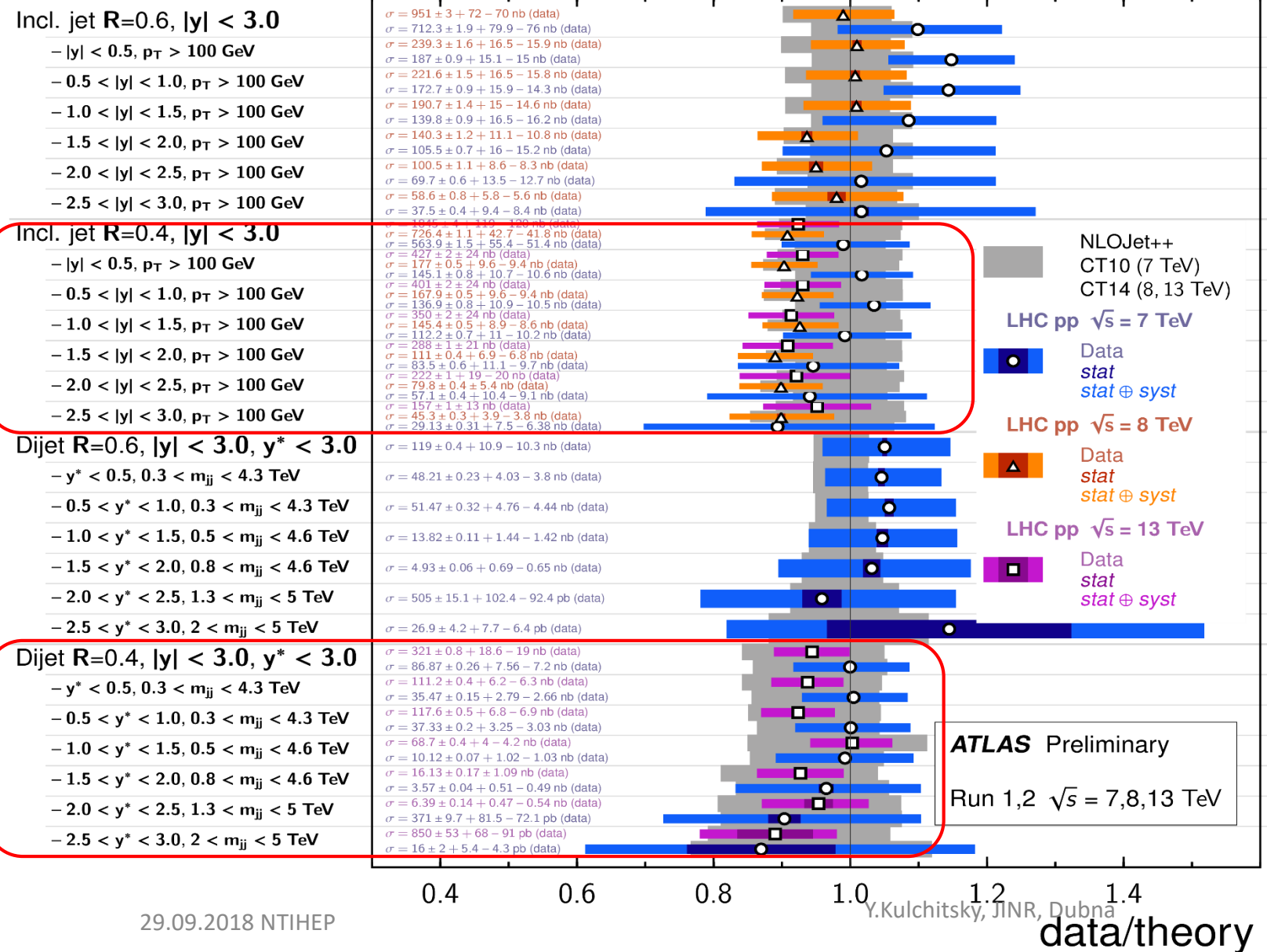


9 (8) orders of magnitude in central rapidity region;
□ **Adequate description** of data by **NLO QCD** calculations

INCLUSIVE JETS & DIJETS X-SECTION MEASUREMENTS

Inclusive Jet Cross Section Measurements

Status: July 2018

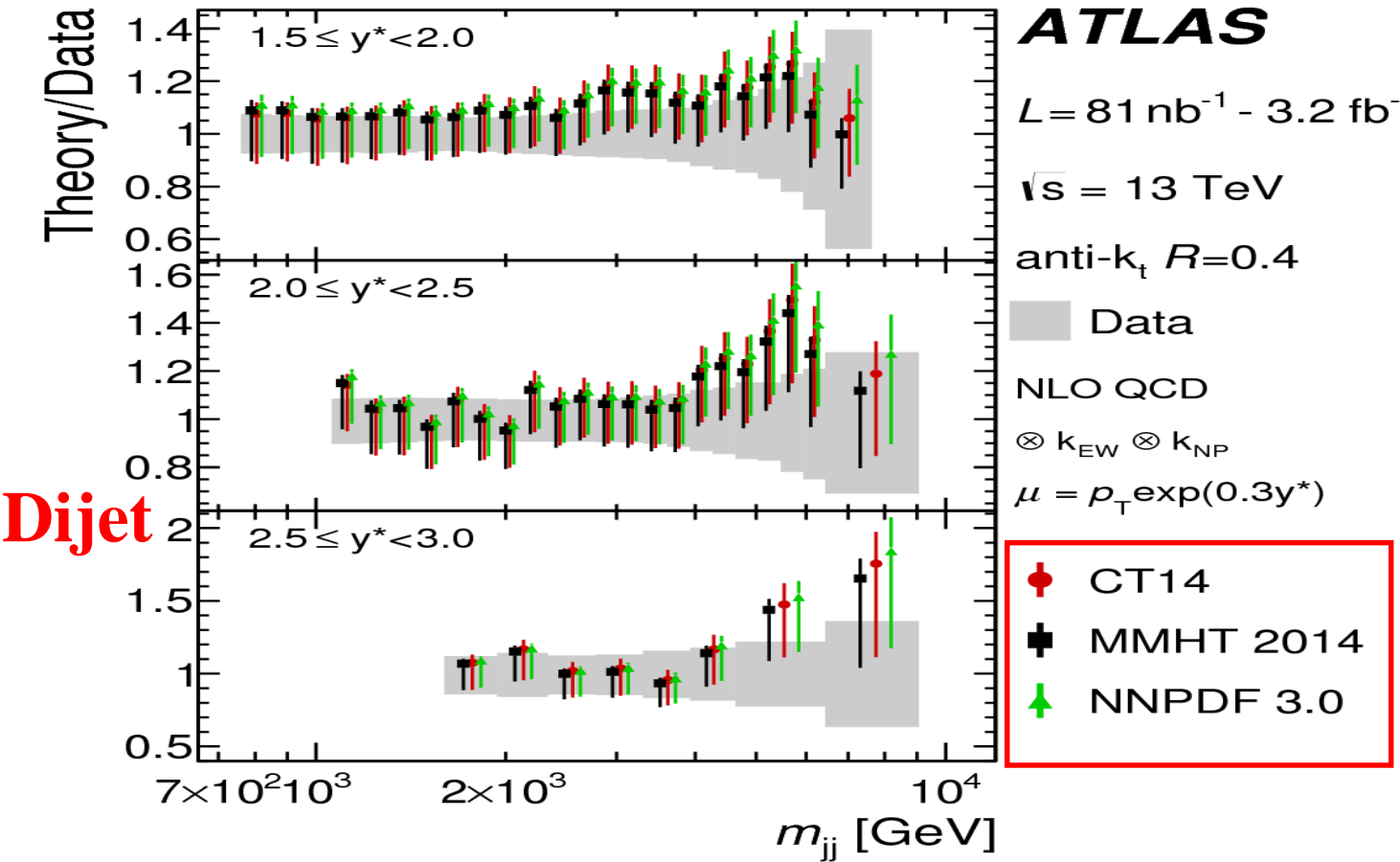
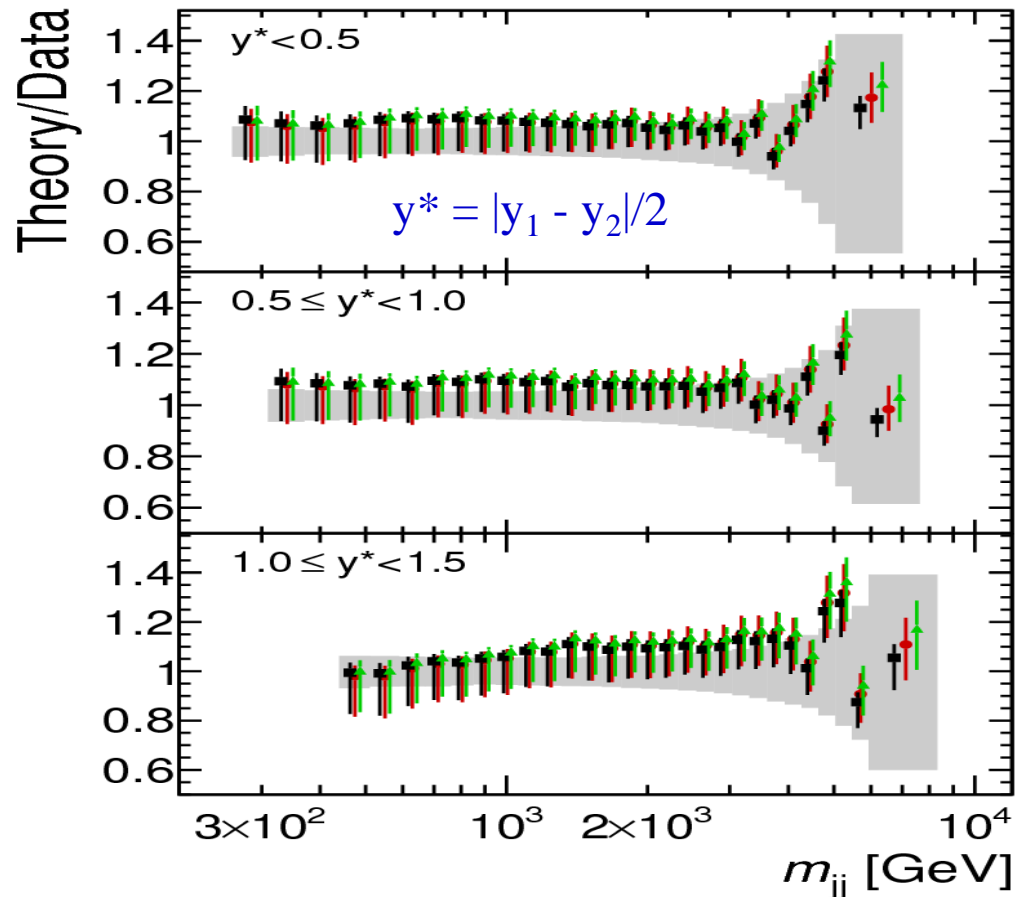


29.09.2018 NTIHEP

14

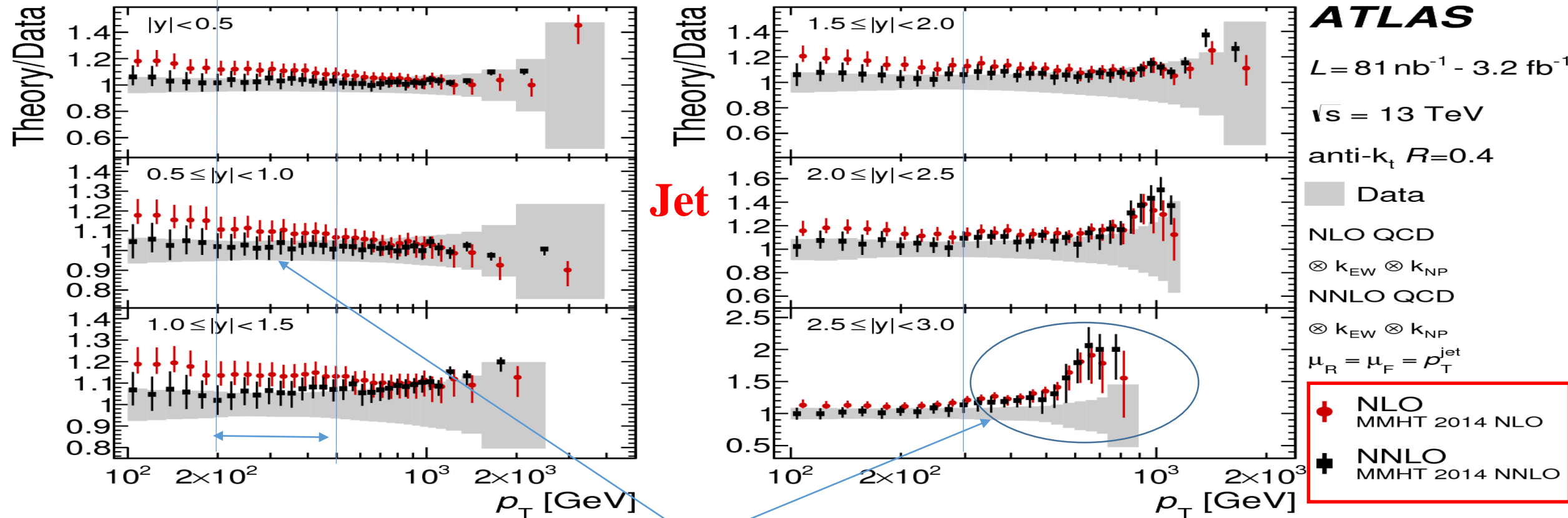
The data/theory ratio for several inclusive jet fiducial production cross section measurements. All theoretical expectations were calculated at NLO or higher. The dark-color error bar represents the statistical uncertainty. The lighter-color error bar represents the full uncertainty, including systematics and luminosity uncertainties. The luminosity used and reference for each measurement are also shown. Uncertainties for the theoretical predictions are quoted from the original ATLAS papers. At 7 TeV the **CT10 PDF** set and at 8 TeV and **13 TeV CT14 PDF** was used in the calculation of the theory prediction. For the dijets measurement, $y^* = |y_1 - y_2|/2$.

Ratio of **NLOJET++ prediction** to measurements of Dijet double-diff. cross-sec. vs. Dijet mass
& y^* PDF sets used: **CT14, MMHT 2014, NNPDF 3.0**



- Good description of data by NLO pQCD within the uncertainties
 - Similar shape predicted by the studied PDF sets
 - For $|y^*| > 2$, tendency for the NLO pQCD prediction to overestimate the measured cross-section in the high m_{jj}
- The CT14 case is repeated to serve as a reference for comparison

Ratio of **NLOJET++** (p_T^{jet} QCD scale) *prediction* to measurements of Jet double-diff. cross-sec.
vs. jet p_T and y : PDF sets used: **MMHT 2014 NLO, MMHT 2014 NNLO**



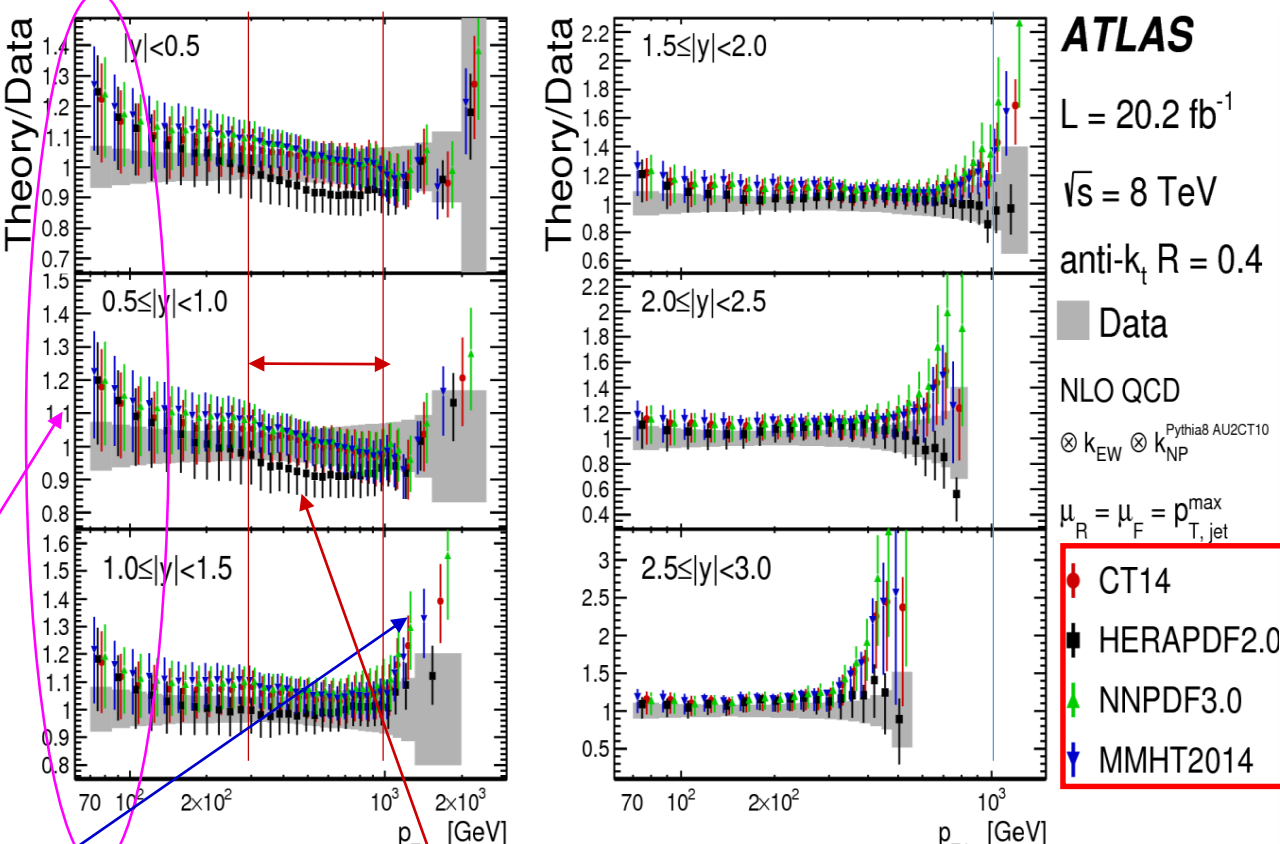
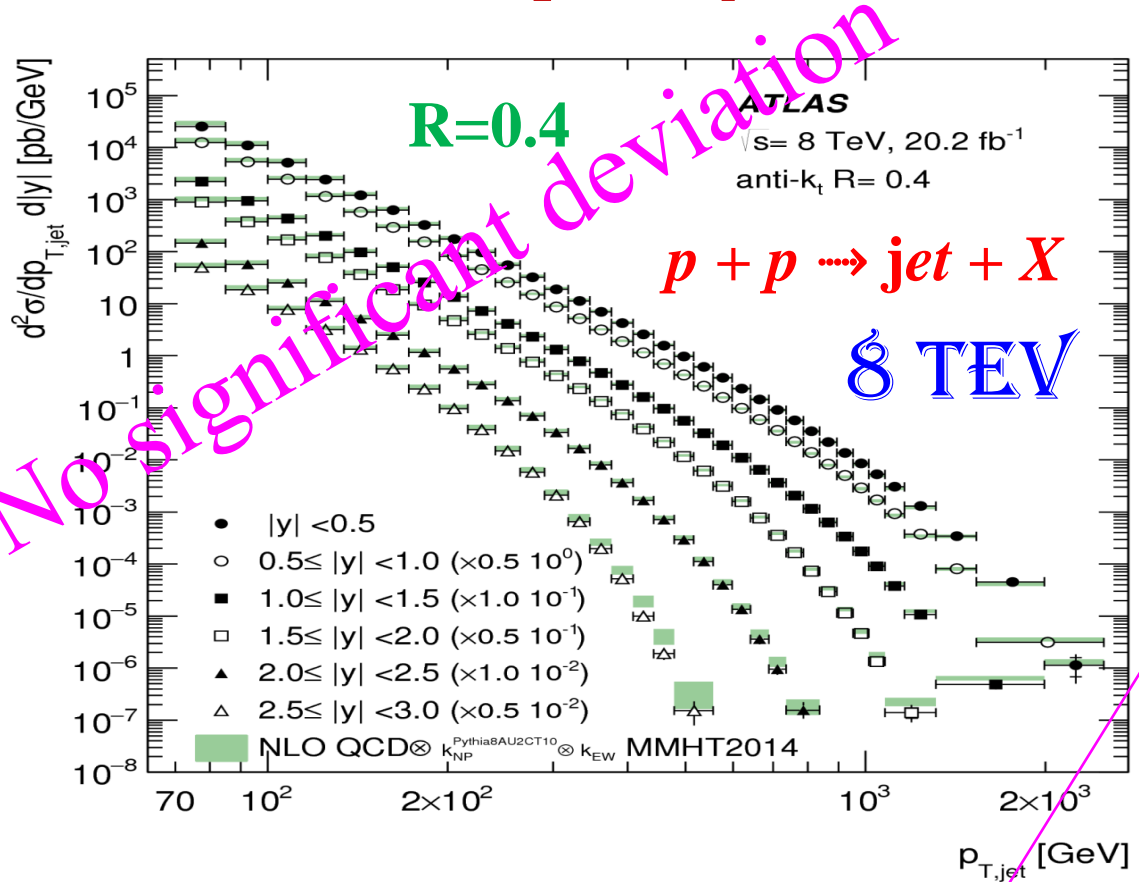
- NLO pQCD above the measurements for $p_T \lesssim 200\text{-}500 \text{ GeV}$
- Toward higher p_T NLO pQCD closer to data
- $p_T > 300 \text{ GeV}$ and high y rise of NLO pQCD with respect to data ($>20\%$)
- Similar behaviour for different PDF sets
- Good description by NNLO
- The differences between data and the theoretical predictions at NNLO are smaller than at NLO for the p_T^{jet} scale
- The predictions change quite a bit when considering a different renormalisation scale: $p_T^{\text{jet}} \rightarrow p_T^{\text{max}}$

THEORY/DATA COMPARISON FOR $p + p \rightarrow \text{jet} + X$ AT 8 TeV



JHEP 09 (2017) 020

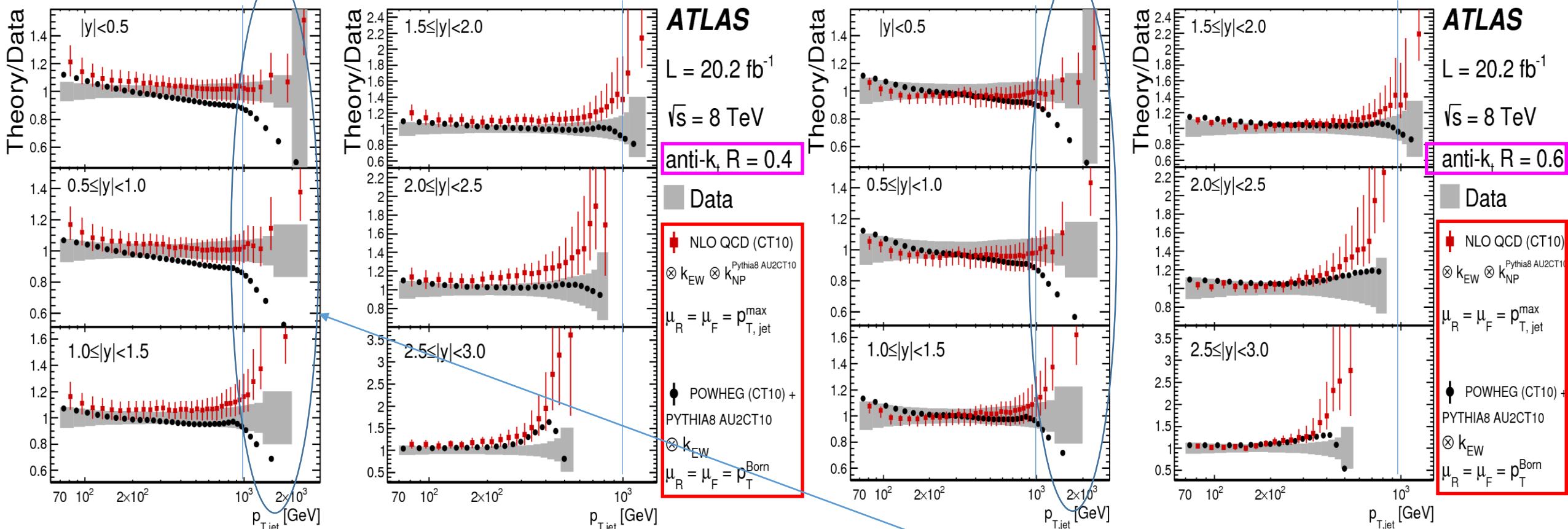
Double-differential *inclusive Jet* cross-sections for jets with $R=0.4$ vs. jet p_T and rapidities data vs. NLO pQCD prediction corrected for *non-perturbative (NP)* and *EW effects*



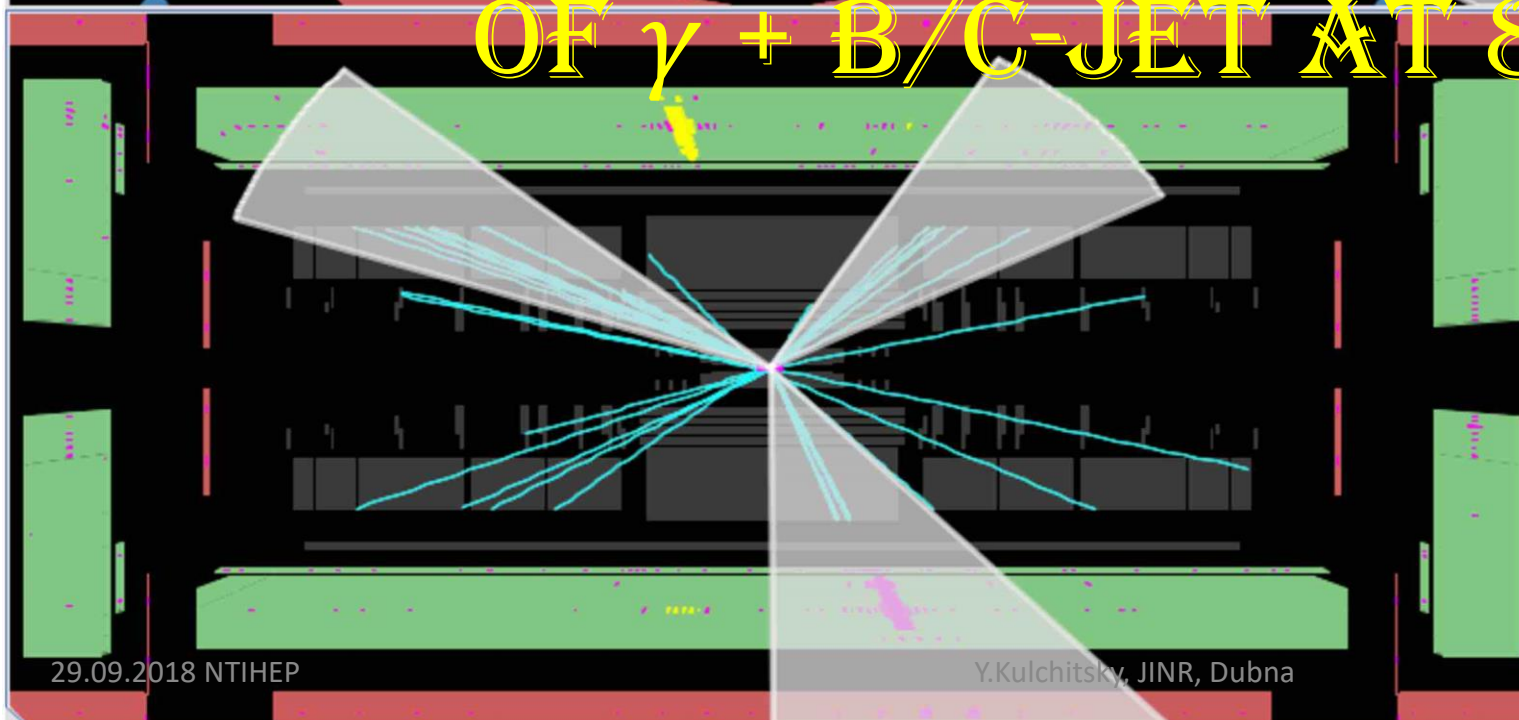
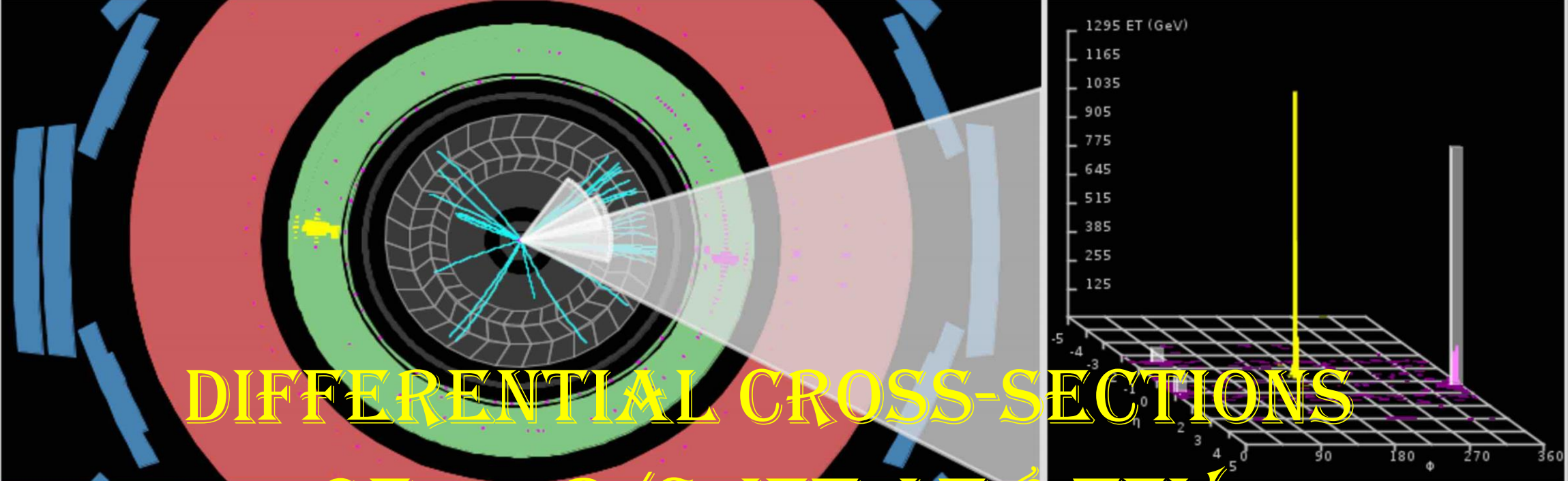
No significant deviation

- NLO pQCD above the measurements for $p_{T,\text{jet}} < 100 \text{ GeV}$
- Toward higher $p_{T,\text{jet}}$ NLO pQCD closer to data
- For $p_{T,\text{jet}} > 1 \text{ TeV}$ rise of NLO pQCD respect to data on 10-20%
- Similar behaviour for *different PDF sets*
- **HERAPDF2.0** significantly lower than data in $0.3 < p_{T,\text{jet}} < 1 \text{ TeV}$

Ratio of **POWGEN** predictions to measured double-diff. *inclusive Jet* cross-section vs. jet p_T
 and *jet rapidity* – **POWGEN (C10)+PYTHIA8 AU2CT10** and **NLO QCD (CT10)**



- **POWGEN(NLO+PS)** below **NLOJET++** at low p_T
- Toward higher p_T tendency to be *below* the data
- For $p_T > 1$ TeV different behaviour than NLO QCD
 - **POWGEN** prediction less dependent on the jet radius



□ **Deep probe of proton structure, mainly gluon PDF**

□ **Prompt photons** represent a *cleaner probe* of a **hard interaction** than jet production

➤ Prompt photon production at LHC dominated by $qg \rightarrow q\gamma$ for $\text{pp} \rightarrow \gamma + \text{jet} + \text{X}$ events

➤ Inclusive photons can be produced by **two main mechanism**:

- ✓ **Direct-photon** – γ produced in the hard interaction

- ✓ **Fragmentation** – γ coming from the fragmentation of a high- p_T parton

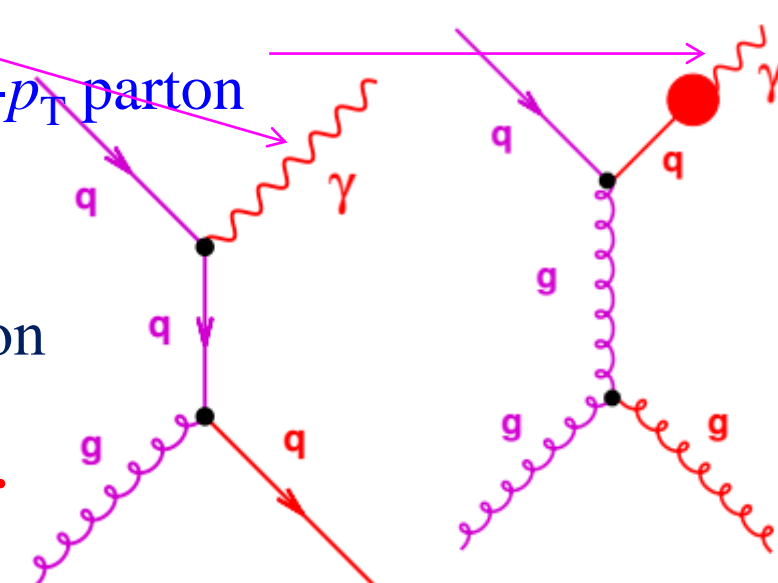
➤ **Essential to require the photon to be isolated:**

- Calorimeter isolation $E_T^{\text{iso}} < E_T^{\text{max}}$ in a cone of radius $R=0.4$ with $E_T^\gamma > 25 \text{ GeV}$ (suppress $\pi^0 (\eta^0 \dots) \rightarrow \gamma\gamma$ and fragmentation contribution)

➤ **The measurement is performed in bins of E_T^γ for 2 regions of $|\eta^\gamma|$:**

- **central region** with $|\eta^\gamma| < 1.37$ for $25 \leq E_T^\gamma \leq 400 \text{ GeV}$
- **forward region** with $1.56 < |\eta^\gamma| < 2.37$ for $25 \leq E_T^\gamma \leq 350 \text{ GeV}$

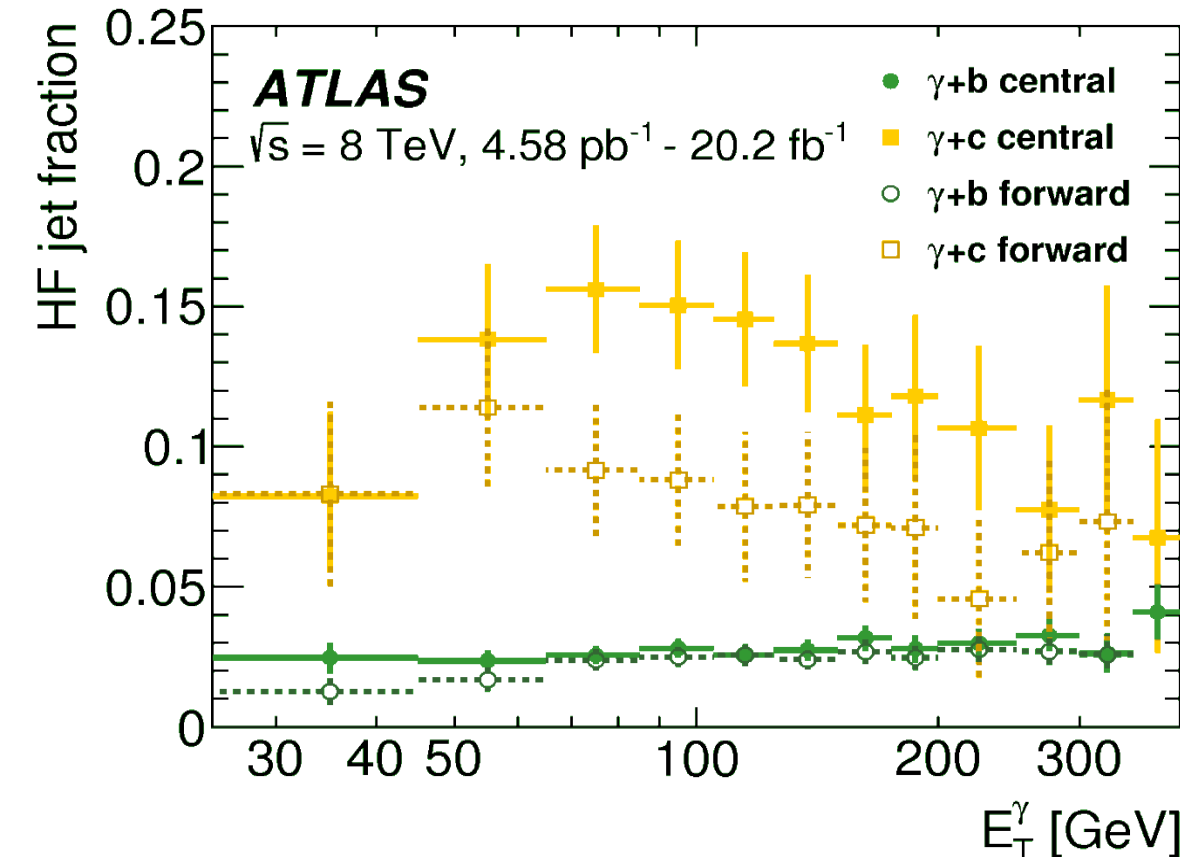
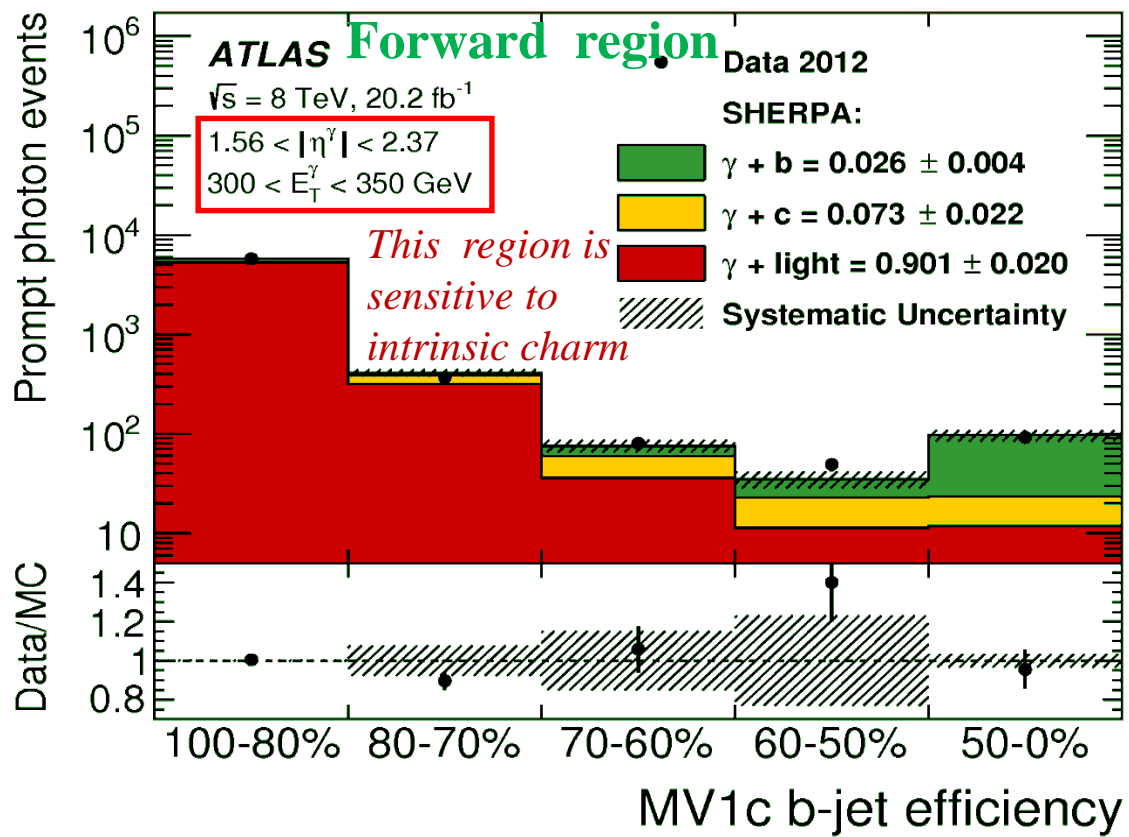
➤ **Jet p_T reduced to $p_T^{\text{jet}} > 20 \text{ GeV}$**



- Strictly distinguishable only at **Leading Order (LO)**
- Precise measurements are testing ground for **pQCD**

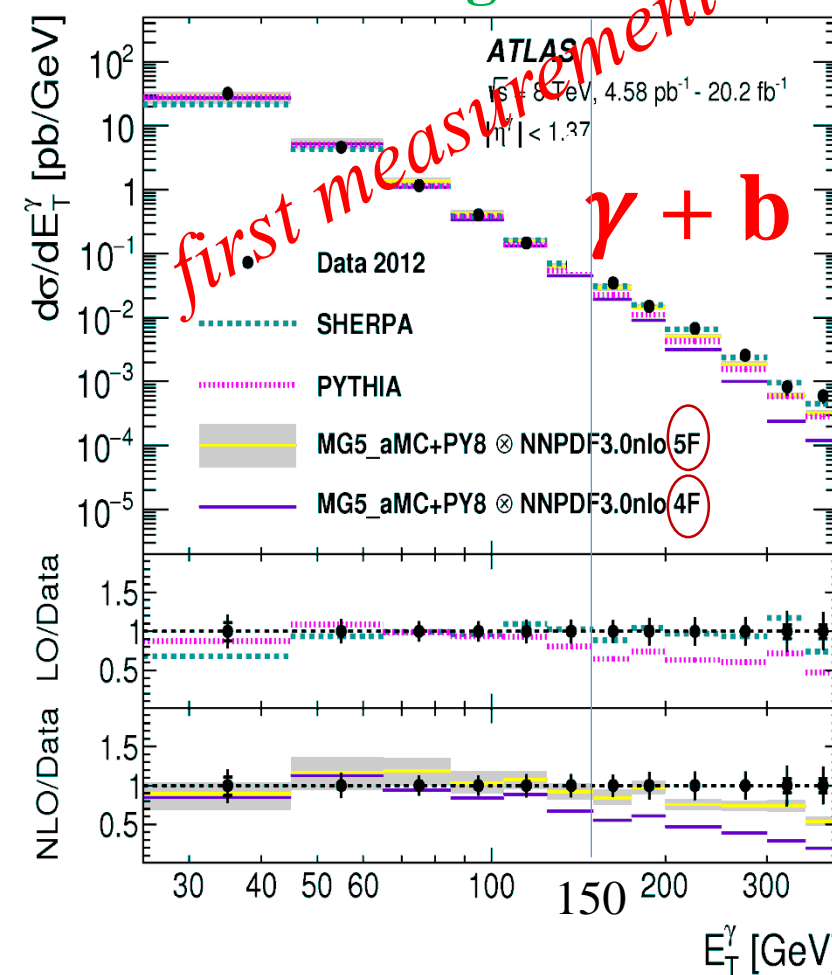
The addition of Heavy Flavour (HF) Jet using MV1c (neural network) algorithm:

- *Is trained* to specifically identify *b-jets* with enhanced rejection of *c-jets*
- *Uses discriminants* from **3 other algorithms** based on different aspects of **jet tracking** information from *Secondary Vertices*
- Perform maximum likelihood template fit



- Leading γ : $E_T^\gamma \geq 25 \text{ GeV}$, $|\eta^\gamma| < 1.37$, $1.56 < |\eta^\gamma| < 2.37$; $E_T^{\text{iso}} < 0.0042 \times E_T^\gamma + 4.8 \text{ GeV}$
- Leading Jet: $\Delta R^{\gamma\text{-jet}} = \sqrt{(\Delta y)^2 + (\Delta \phi)^2} > 1$, $p_T^{\text{jet}} > 20 \text{ GeV}$, $|\eta^{\text{jet}}| < 2.5$

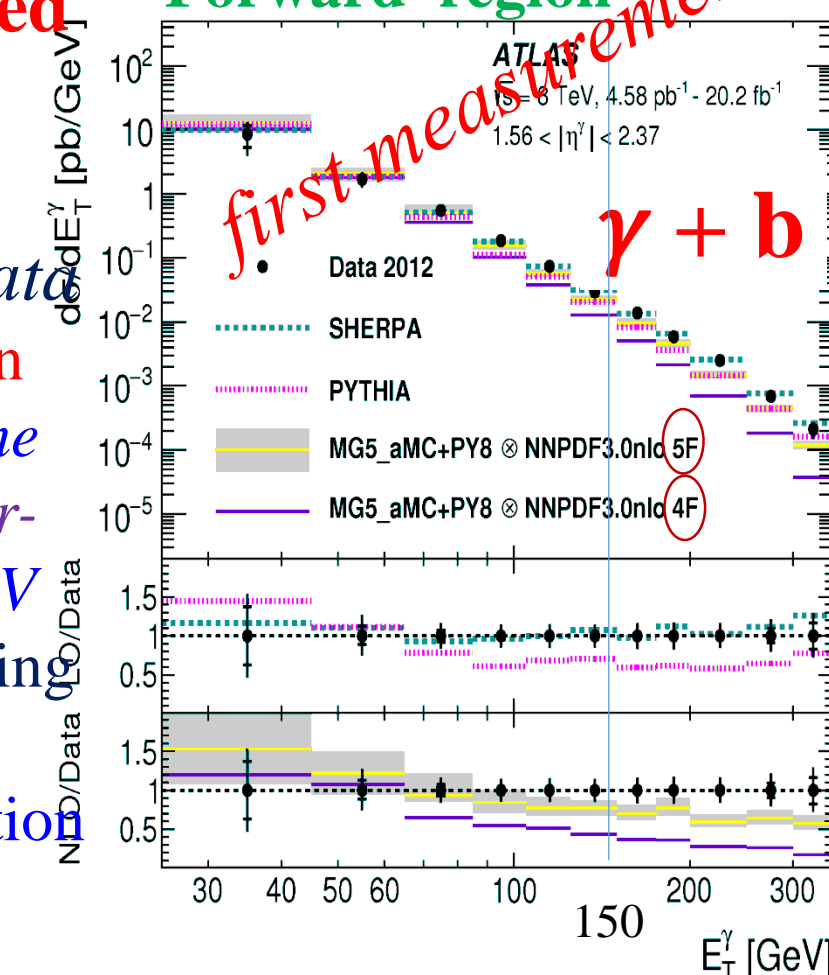
Central region



Best description is provided by **SHERPA** for $\gamma + b$

- ❖ Above 150 GeV in $\gamma + b$ **PYTHIA** underestimates data
- ❖ Both **NLO** agree at low E_T in $\gamma + b$; **5F (five-flavour) scheme** performs better than **4F (four-flavour)** for $125 < E_T < 200 \text{ GeV}$
 - At higher E_T gluon splitting is important
 - High order (HO) calculation needed at higher E_T

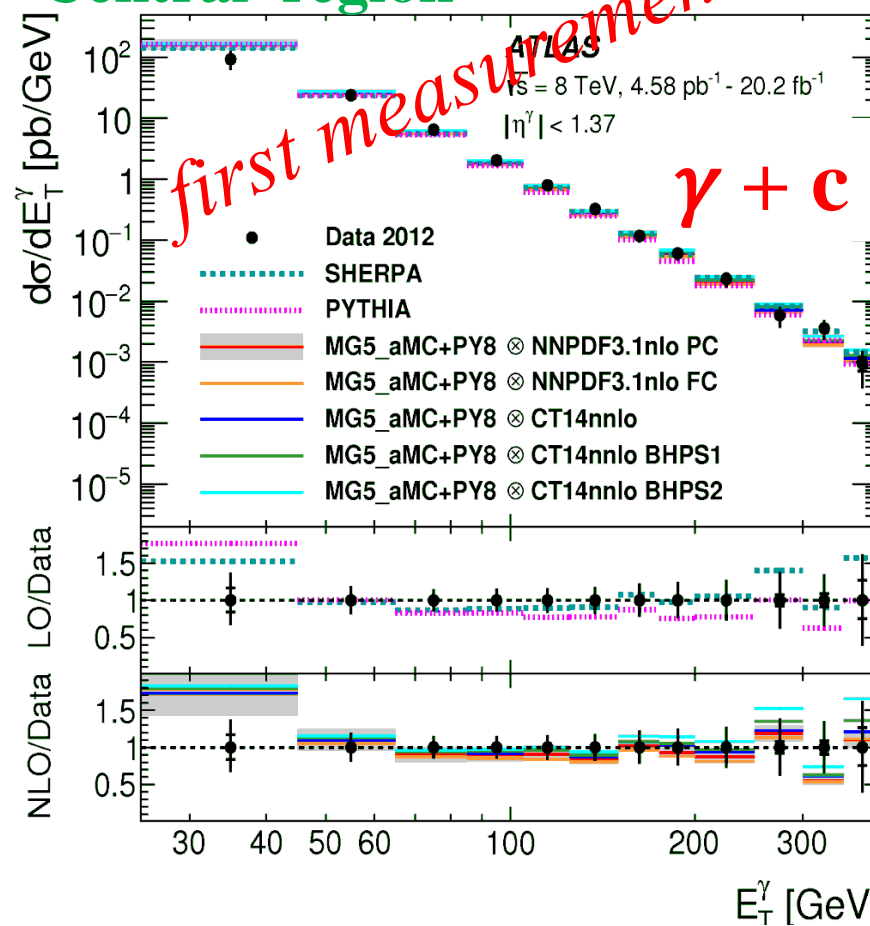
Forward region



□ ***MADGRAPH5_AMC@NLO*** with several *PDF* sets → with different *intrinsic charm (IC)* content/ model and *5F/4F* (five-flavour)/(four-flavour) flavor-schemes comparison

➤ **4F worse description at high E_T^γ** (large $\log(m_b/E_T^\gamma)$ terms)

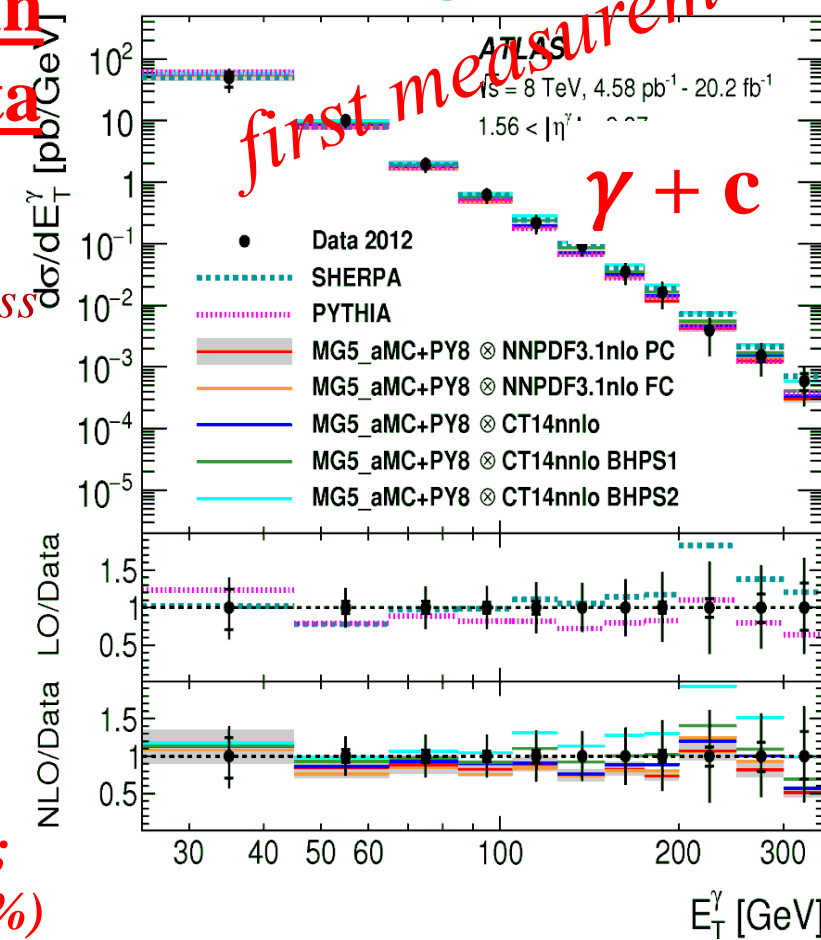
Central region



□ **All the predictions are in agreement with $\gamma+c$ data**

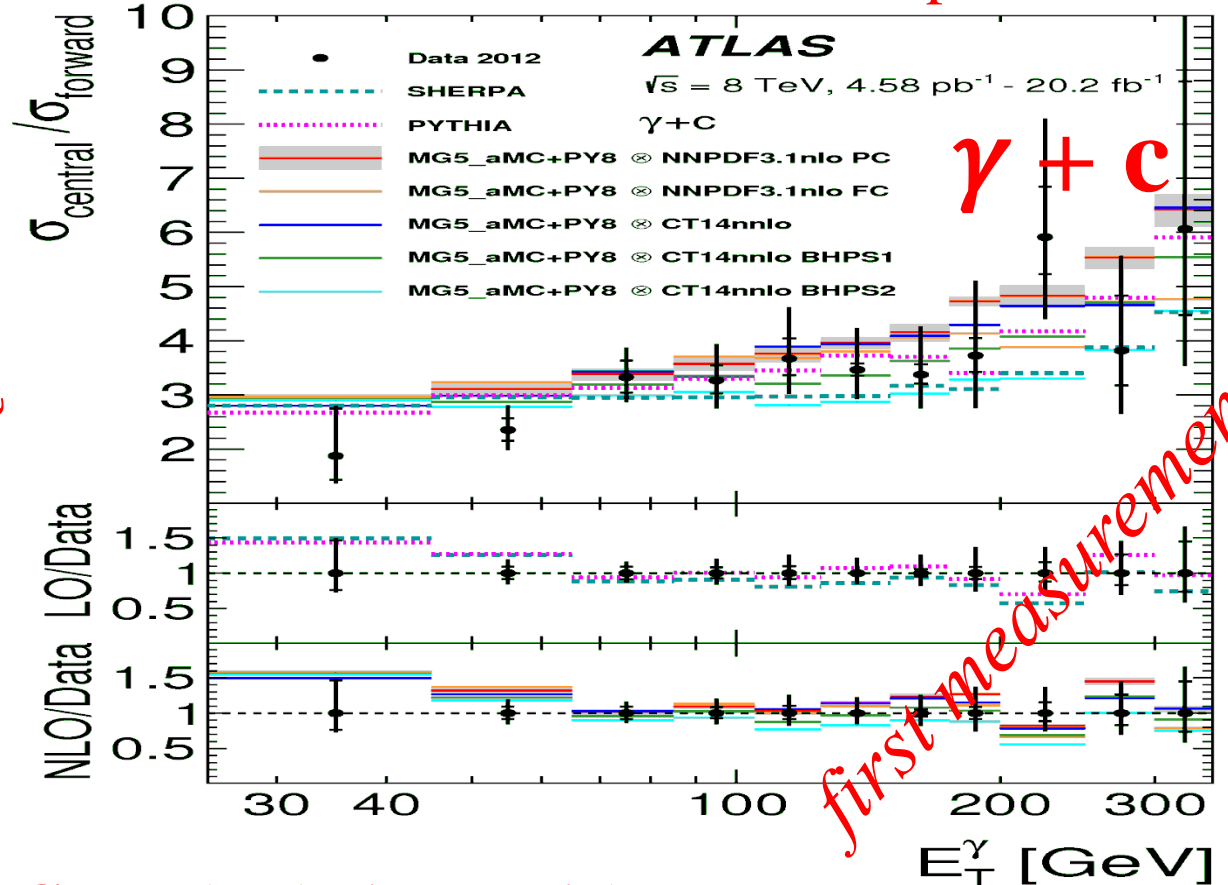
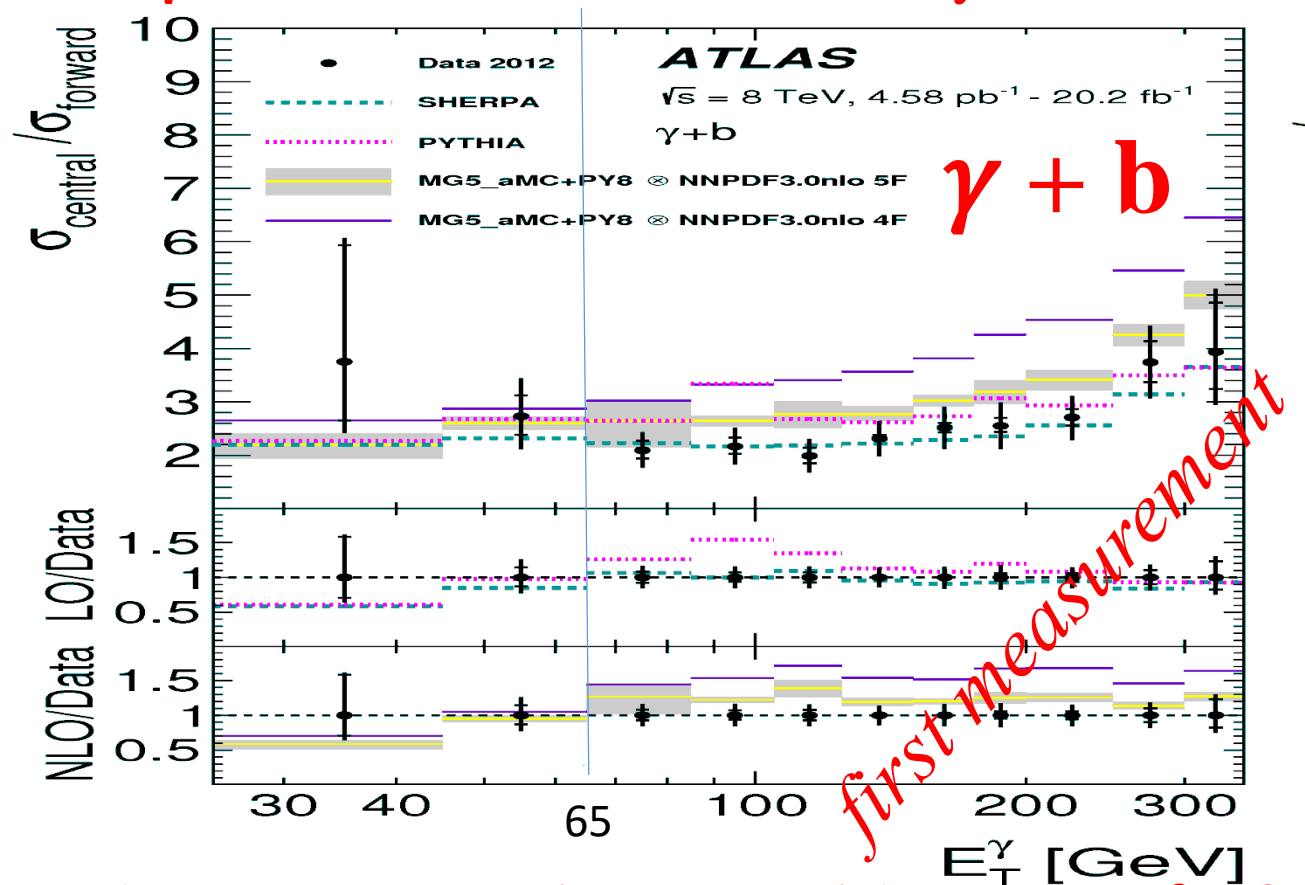
- ❖ Gluon splitting less important at this E_T^γ region
- All IC predict **higher forward cross section as expected**
- ❖ BHPs2 deviates the most from nominal PDF by factor 1.5
- ❖ BHPs1 give intermediate values
- **PDFs with/without IC give deviations similar to the measurement uncertainties**
PDFs: NNPDF3.1nlo (IC 0.26%); BHPs1 (IC 0.6%); BHPs2 (IC 2.1%)

Forward region



$\Delta_{\text{sys}} \sim 15\%$: main contribution due to jet flavour determination. Stat. dominated in the E_T^γ tails 10-40%²³

- SHERPA**, which generates additional partons in the matrix element and uses a massive *5F scheme*, provides a better description of the measured cross sections and cross-section ratios than **MADGRAPH5_AMC@NLO**
- ❖ The *4F and 5F NLO* predictions for the cross-section ratios consistently overestimate the data for $E_T^\gamma > 65 \text{ GeV}$
- In $\gamma + \text{c}$ the measurement accuracy matches the deviations between the theoretical predictions



These cross sections provide a *test of pQCD* calculations with Heavy Quarks and are sensitive to the *b- and c-quark PDFs*

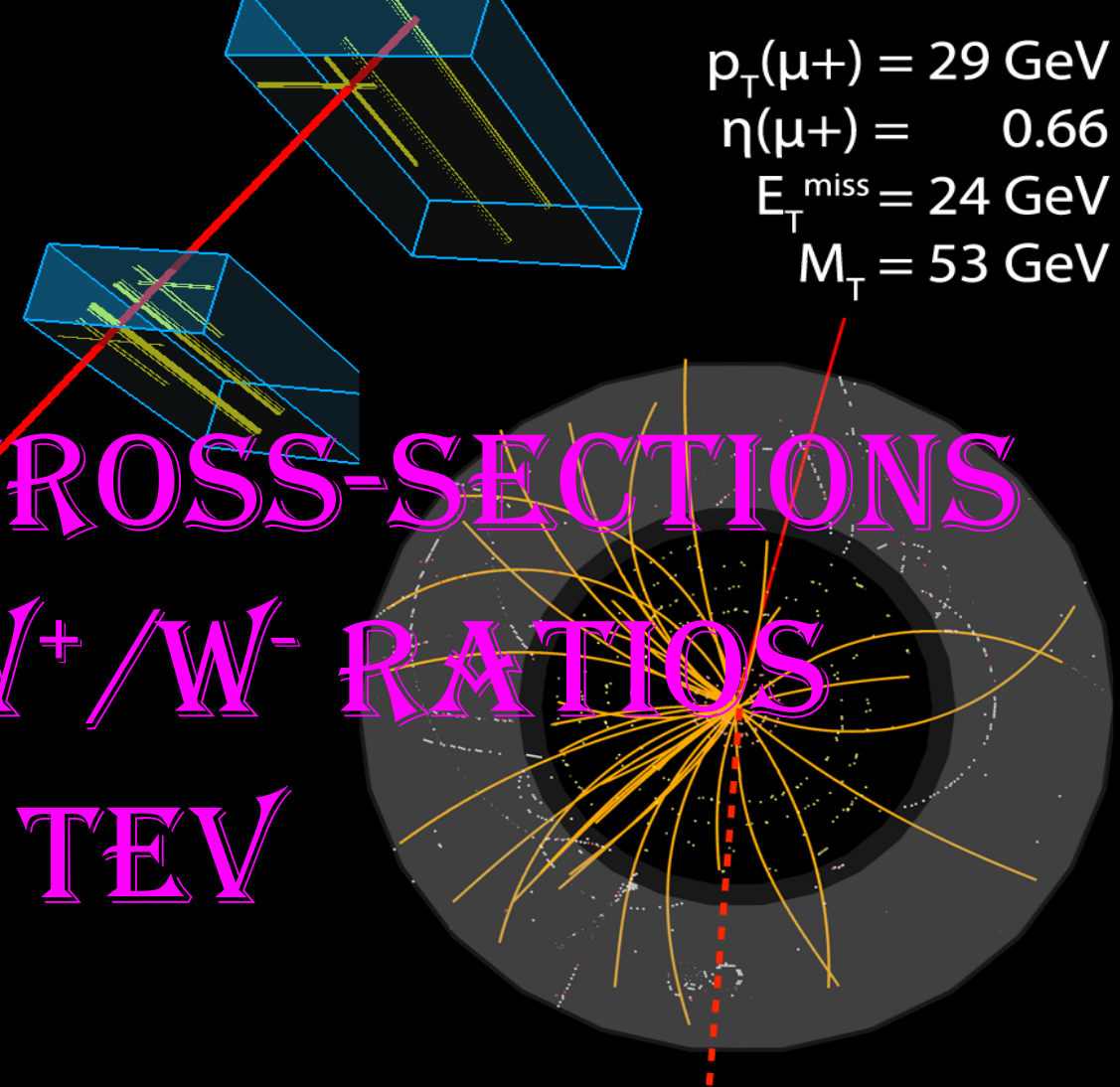
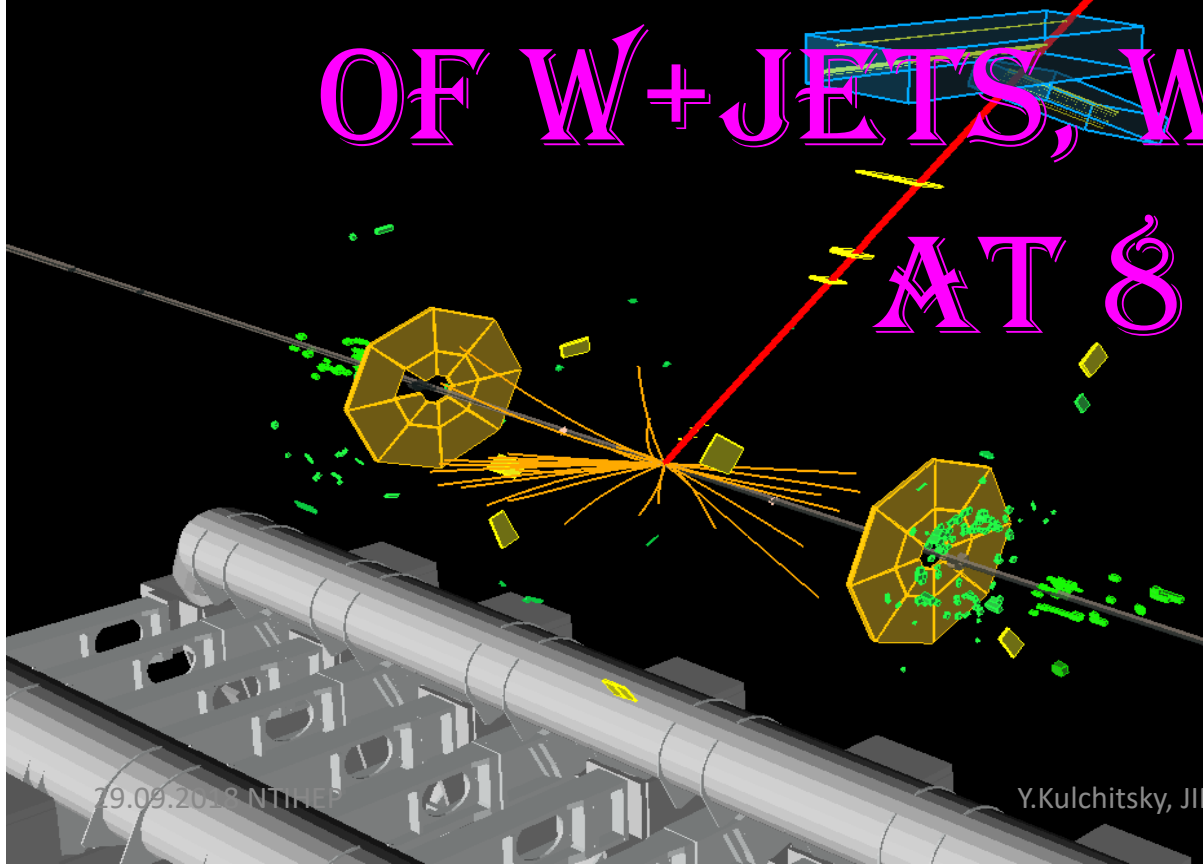


**ATLAS
EXPERIMENT**

$p_T(\mu^+) = 29 \text{ GeV}$
 $\eta(\mu^+) = 0.66$
 $E_T^{\text{miss}} = 24 \text{ GeV}$
 $M_T = 53 \text{ GeV}$

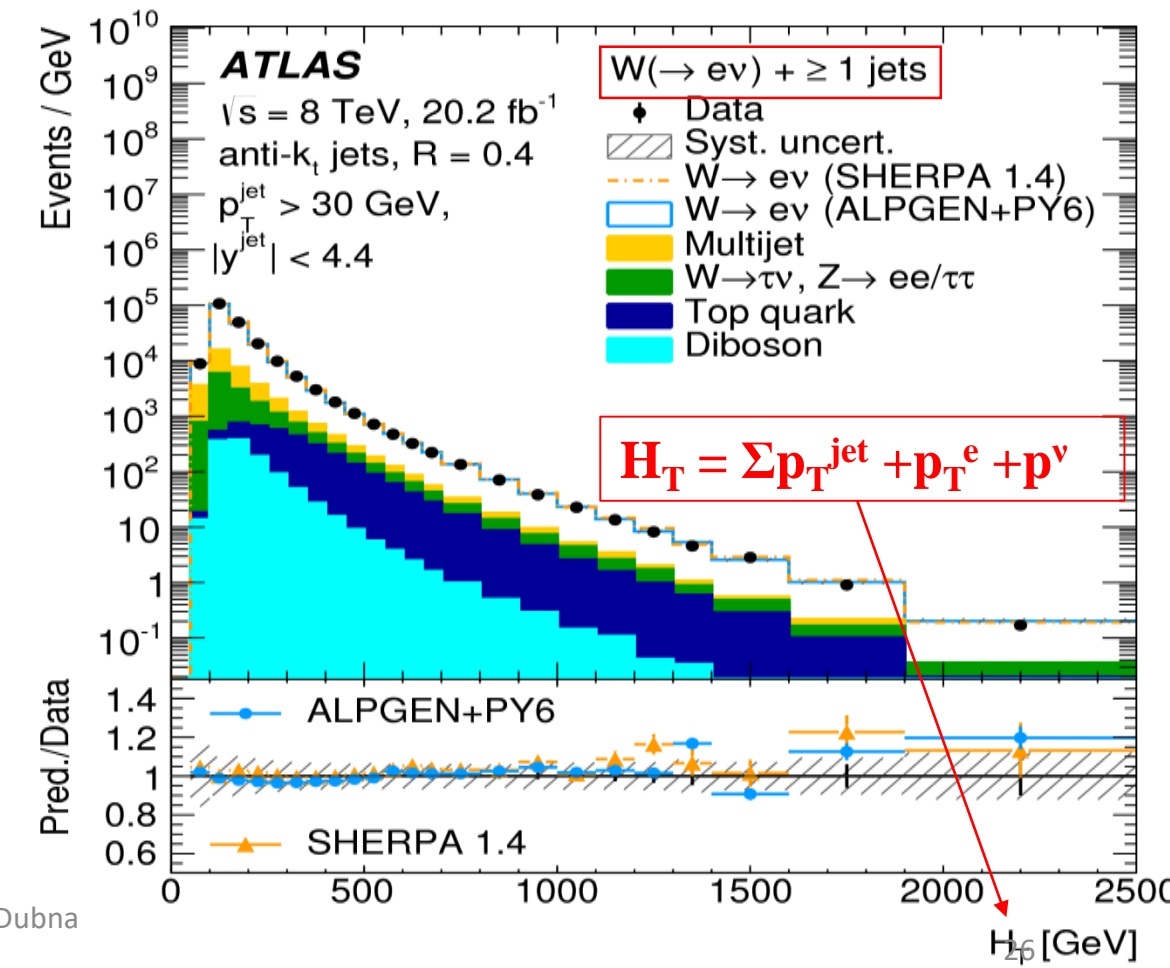
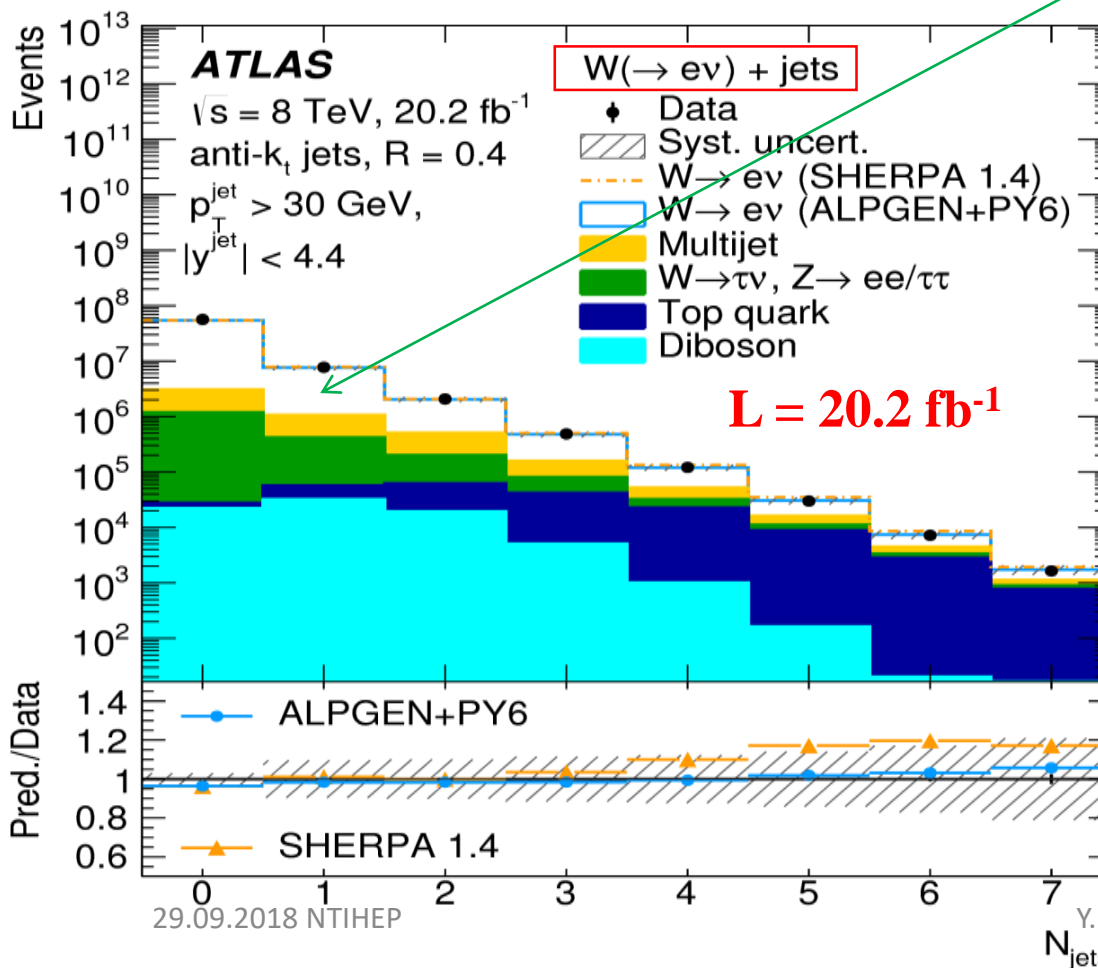
DIFFERENTIAL CROSS-SECTIONS OF $W^+ + \text{JETS}$, W^+ / W^- RATIOS AT 8 TEV

$W \rightarrow \mu\nu$ candidate



- W \rightarrow ev production with Jets association**
- One Electron: $|\eta^e| < 2.47$ (excl. $1.37 < |\eta^e| < 1.52$), $p_T^e > 25\text{ GeV}$
- Jet: anti- k_T , $R = 0.4$, $p_T^{\text{jet}} > 30\text{ GeV}$, $|y| < 4.4$, b-veto
- Track (Calorim.) e isolation: $\Sigma p_T(\Delta R < 0.3)/p_T^e < 0.07$ (**0.14**)

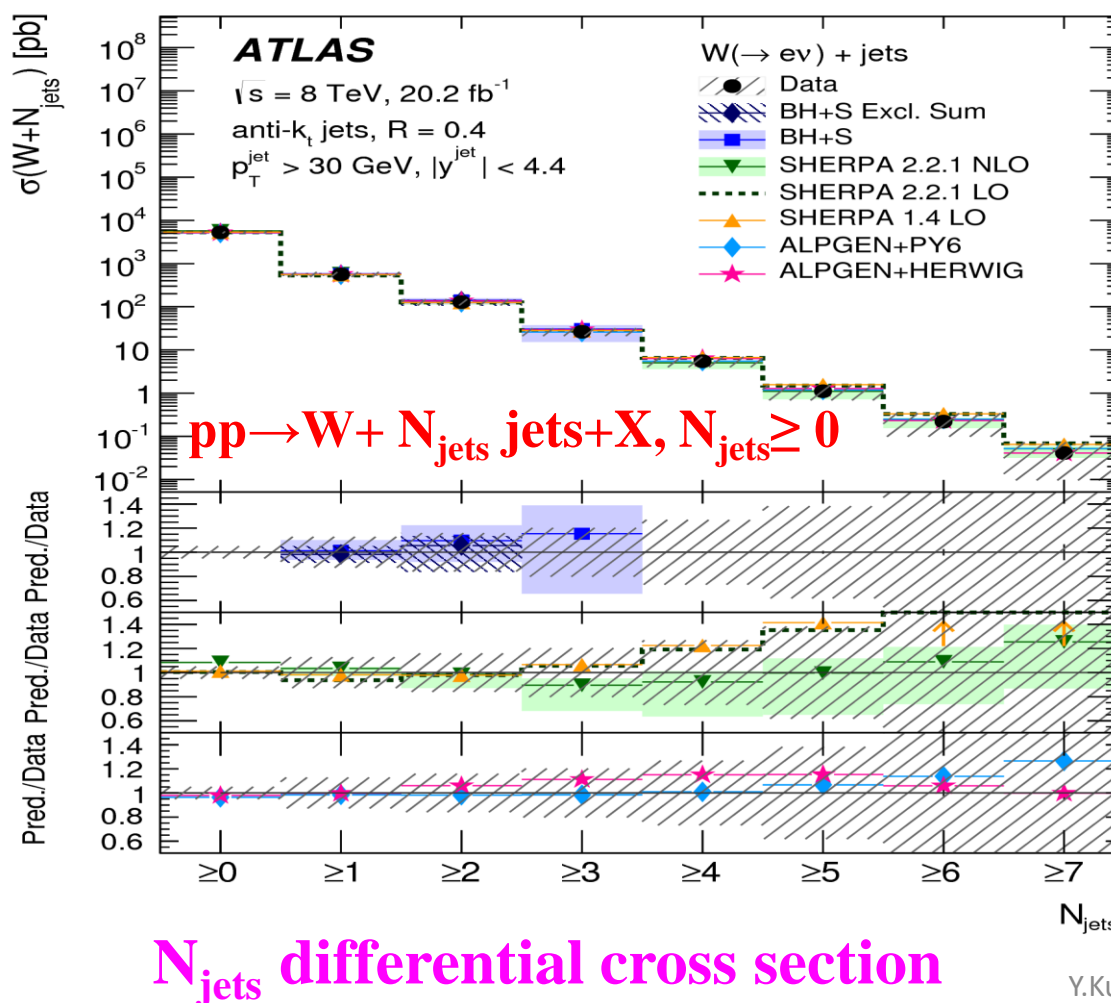
- Electron-Jet distance: $\Delta R(e, \text{jet}) > 0.4$
- $E_T^{\text{miss}} > 25\text{ GeV}$; $m_T = \sqrt{2p_T^e p_T^v [1 - \cos(\phi^e - \phi^v)]} > 40\text{ GeV}$
- Suppress by electron isolation & low momentum contributions to E_T^{miss} from tracks, not calorimeter deposits
- Challenge–Backgrounds \rightarrow **Multijet is dominant at low N_{jets}**



□ Cross section at *High Jet multiplicity* is sensitive to *differences in MC generators*

❖ Cross section measured differentially as a function of characteristic variables:

➤ jet p_T , jet y , N_{jets} , H_T (*scalar sum of the p_T of all visible objects*) and W boson p_T

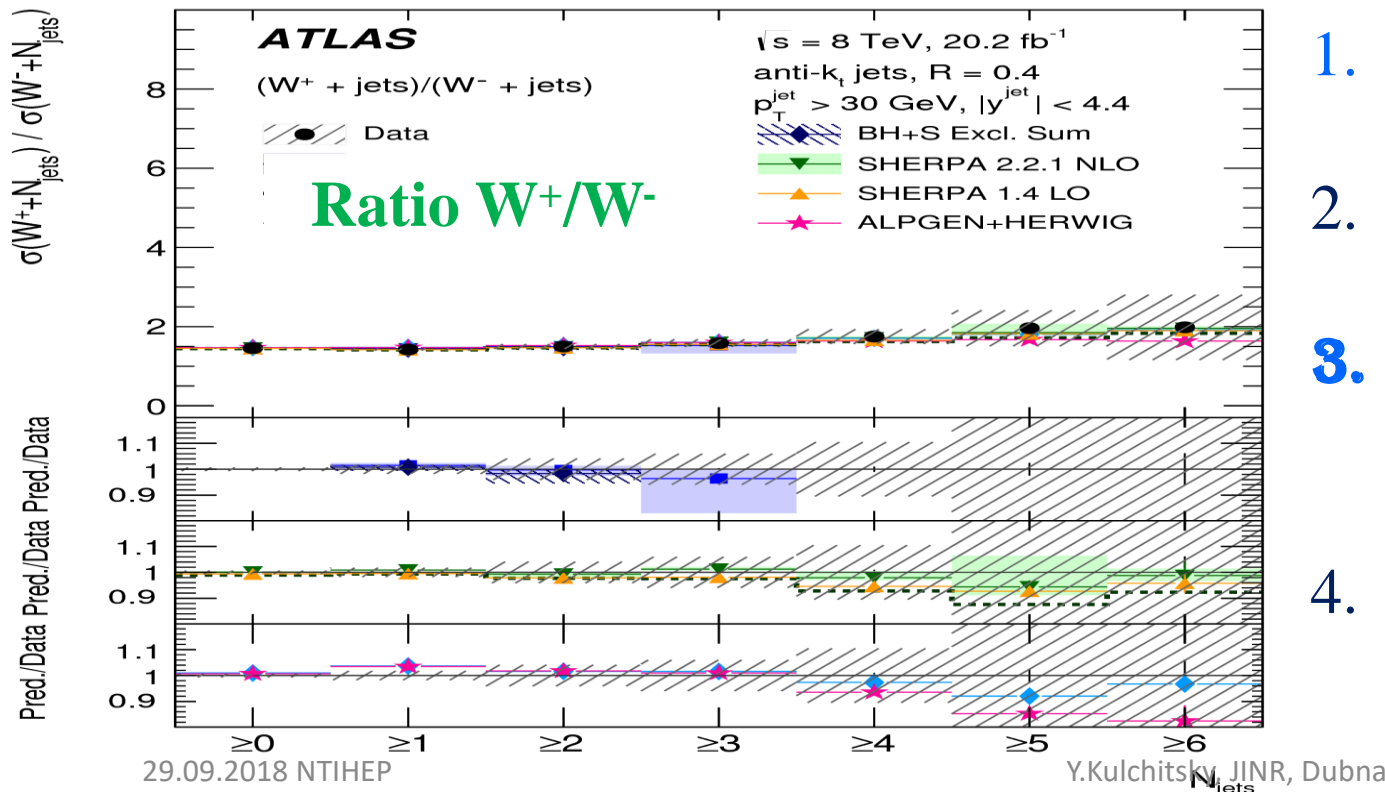


Differential cross section as a function of Jet multiplicity in comparison with MCs:

1. **BLACKHAT+SHERPA NLO** with ≤ 3 partons with Non-perturbative corrections applied
2. **SHERPA 2.2.1 NLO** is NLO for ≤ 2 partons + LO for ≤ 3 partons + Parton Shower (PS)
3. **SHERPA 2.2.1 LO** is LO for ≤ 3 partons + PS
4. **SHERPA 1.4 LO** is LO for ≤ 4 partons + PS
5. **ALPGEN+PY6** is LO for ≤ 5 partons + PS
6. **ALPGEN+HERWIG** is LO for ≤ 5 partons + PS

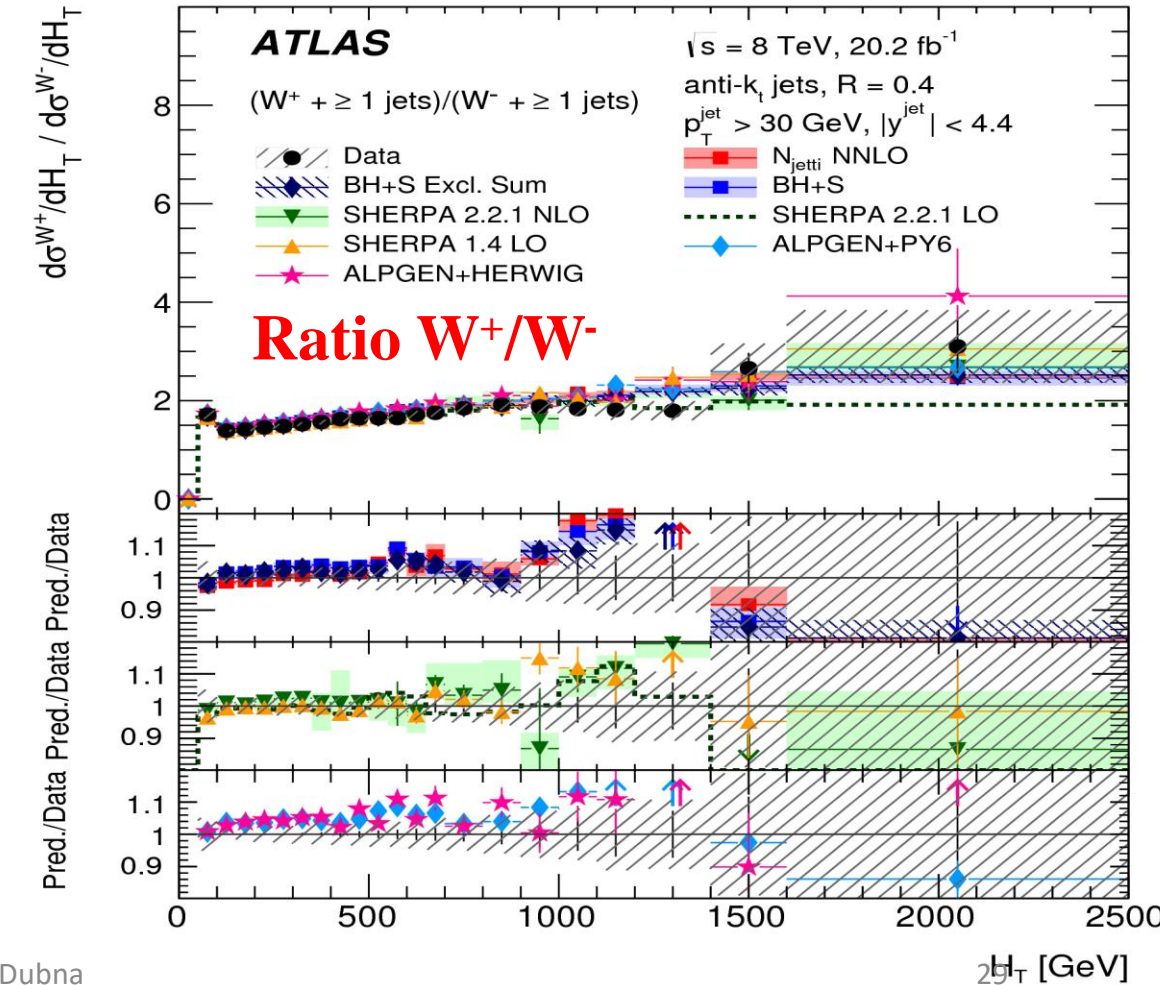
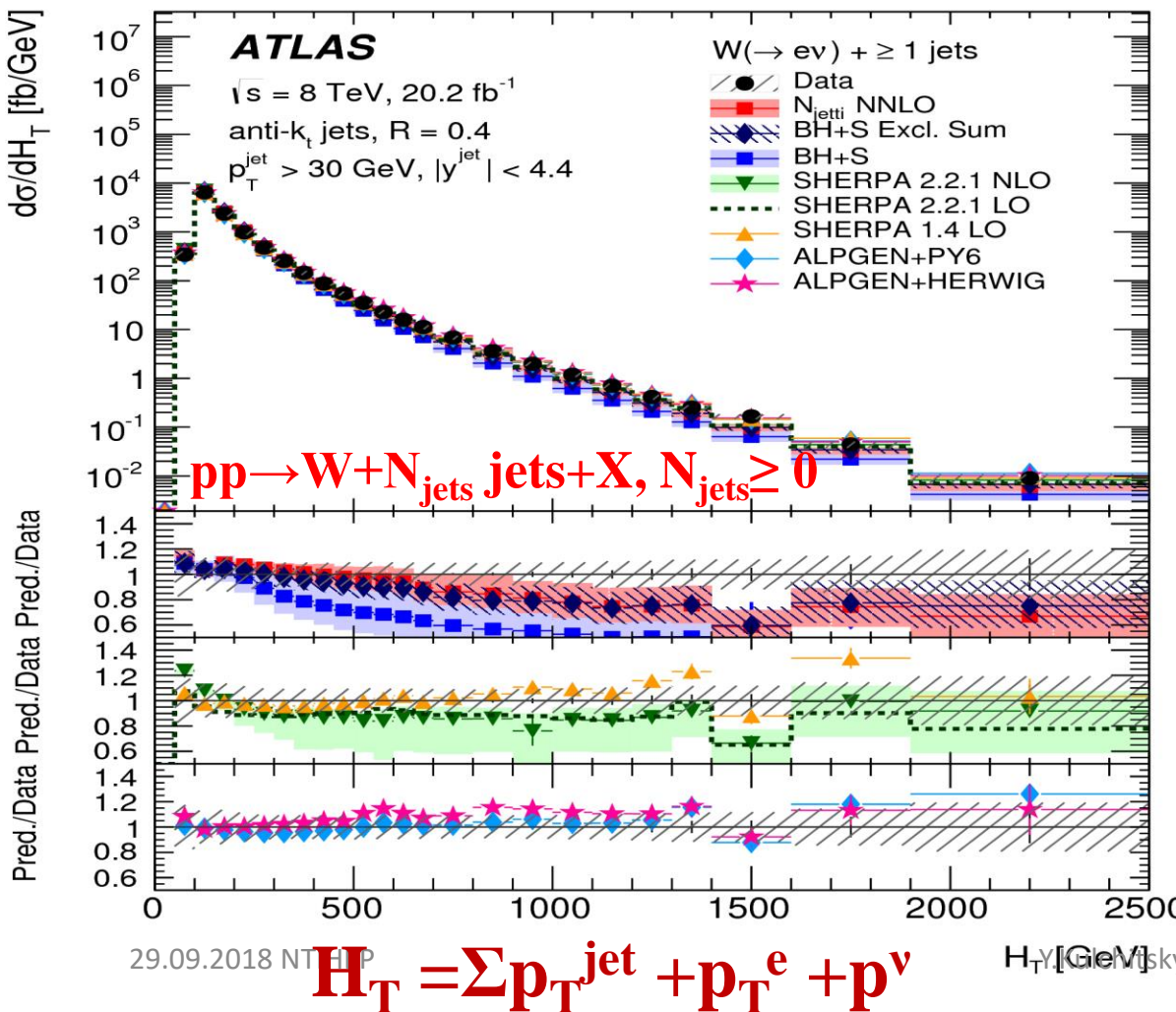
Predictions vary substantially once the **Number of Jets** exceeds the **Number of Partons** included in the matrix element calculation

- The W^+/W^- cross-section ratio can be measured to high precision as many of the experimental and theoretical uncertainties cancel out
- NLO **SHERPA** provides a good description
- ❖ LO **SHERPA** diverges from the data at high multiplicities



- ❖ Offset in **ALPGEN+PS** for $W^+/W^- + \geq 1 \text{ jet}$: due to matrix element (ME) calculation and/or u/d -ratio in the LO PDF
- Data/predictions agreement much improved in W^+/W^- : theory mismodelling related to jet emission cancels out in the ratio
 1. Overall the jet mismodelling cancels out in the ratio
 2. Previously dominant Jet Energy Scale (JES) uncertainty cancels out
 3. **ALPGEN-LO** predictions have an offset in the $\geq 1 \text{ jet}$ bin in the W^+/W^- ratio outside the experimental uncertainties
 4. Suggests that there is a problem in the matrix element calculation or with the u/d -ratio in the LO PDF

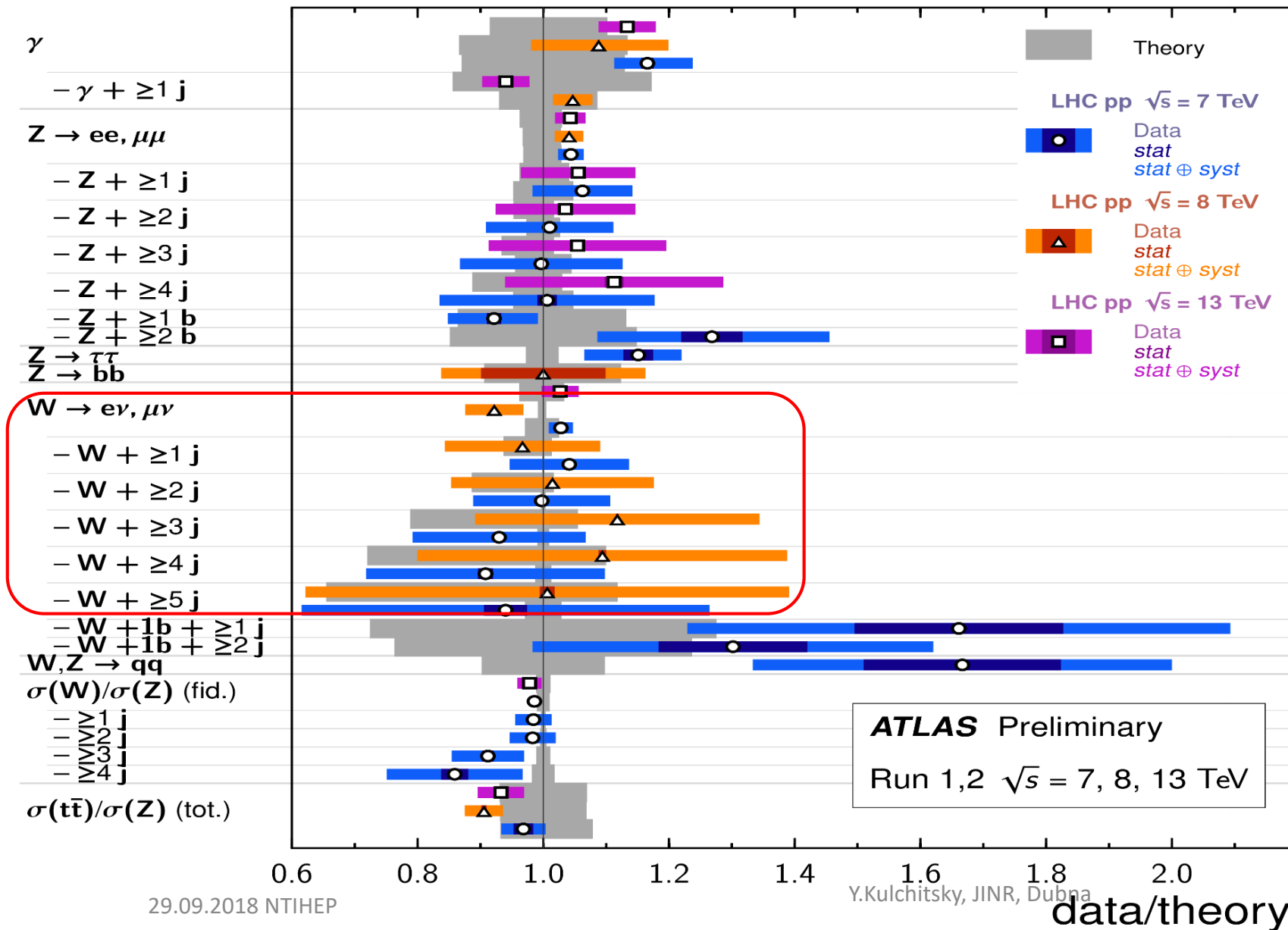
- Large, well understood dataset *Probing up to a few TeV scale*
- W^+/W^- cross-section-ratio observables: *Jet energy scale on other uncertainties mostly cancel*
- ***ALPGEN+PY6 and SHERPA 2.2 NLO*** (Run 2 ATLAS default) *describe data well*



VECTOR BOSONS + X CROSS SECTION MEASUREMENTS

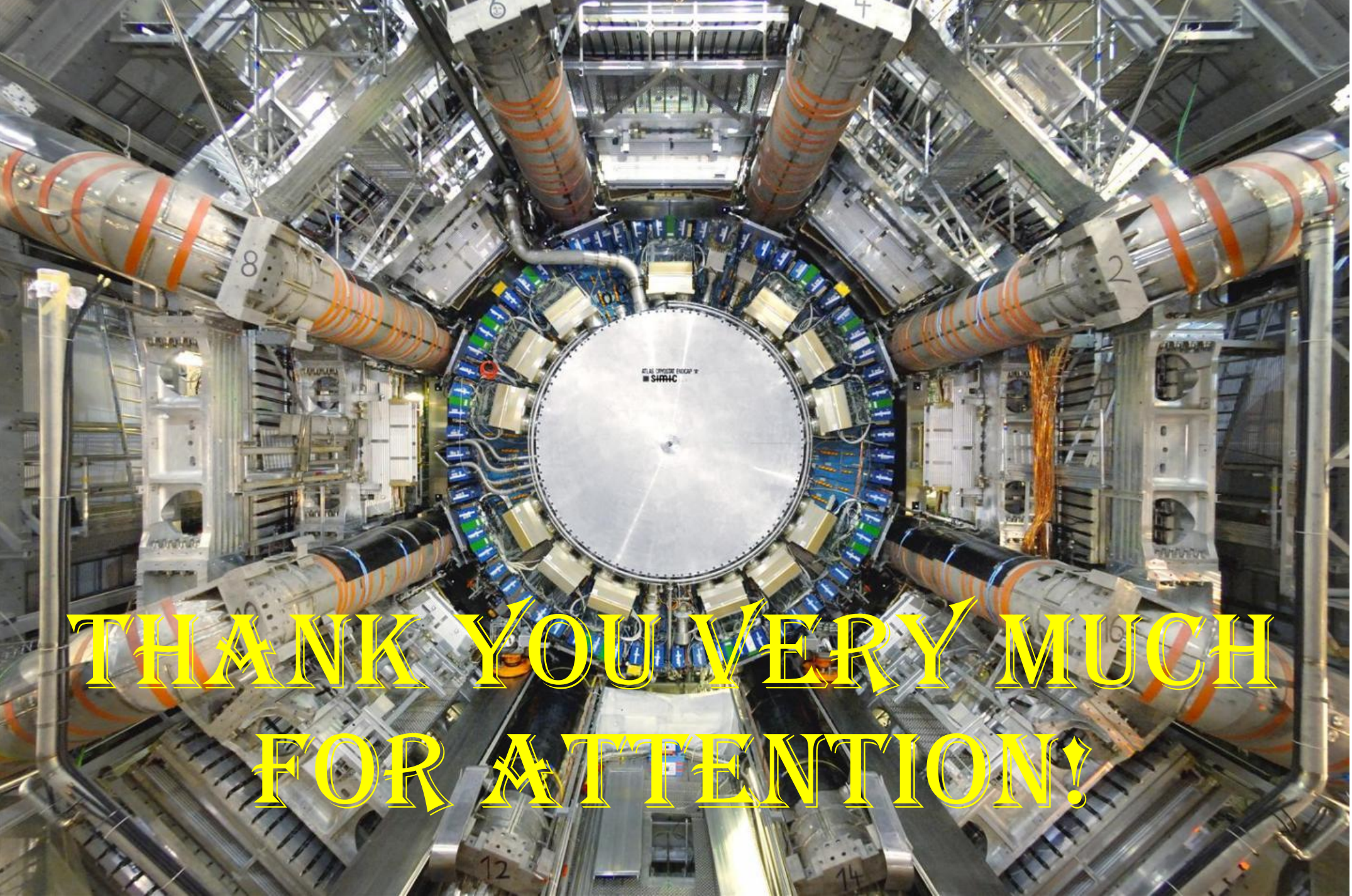
Vector Boson + X fid. Cross Section Measurements

Status: July 2018



The data/theory ratio for several single-boson fiducial production cross section measurements, corrected for leptonic branching fractions. All theoretical expectations were calculated at NLO or higher. The dark-color error bar represents the statistical uncertainty. The lighter-color error bar represents the full uncertainty, including systematics and luminosity uncertainties. The luminosity used and reference for each measurement are also shown. Uncertainties for the theoretical predictions are quoted from the original ATLAS papers. They were not always evaluated using the same prescriptions for PDFs and scales.

- *Probing different aspects of our understanding of the Stand Model*
- *Great variety of precision QCD results*
- The latest results from the ATLAS involving *jets, dijets, photons in association with heavy flavors jets and vector bosons in association with jets*, measured at center of mass energies of 8, 13 TeV obtained
- All measured cross-sections are compared to state-of-the art **theory predictions**
- The *first measurement of γ +Heavy Flavour jet* at the LHC
 - ❖ For $\gamma + b$ the best description is provided by *Sherpa*; the *NLO* underestimates the data
 - ❖ The $\gamma + c$ measurement has *larger experimental uncertainties: PDFs with/without intrinsic charm give deviations similar to the measurement uncertainties*

An aerial photograph of the ATLAS particle detector at the Large Hadron Collider (LHC) at CERN. The detector is a complex, circular structure composed of various sub-detectors. In the center is the Inner Detector (ID), surrounded by the Pixel, Silicon Microstrip, and Strip detectors. Beyond the ID is the muon system, featuring large cylindrical solenoids labeled '8' and '2'. The entire detector is situated within a massive steel and concrete structure, with the LHC ring visible around it.

THANK YOU VERY MUCH
FOR ATTENTION!

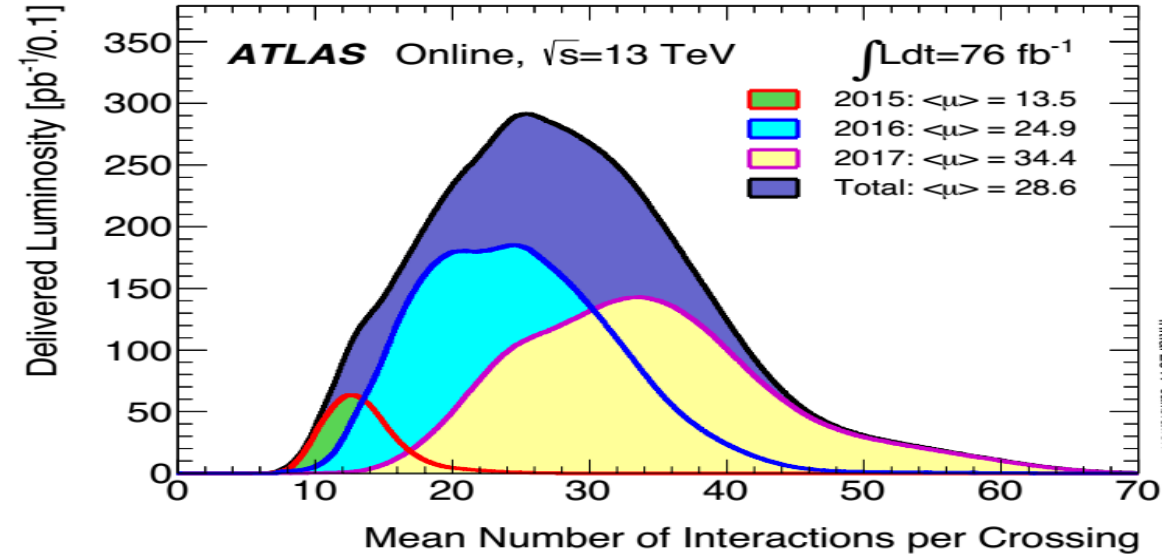
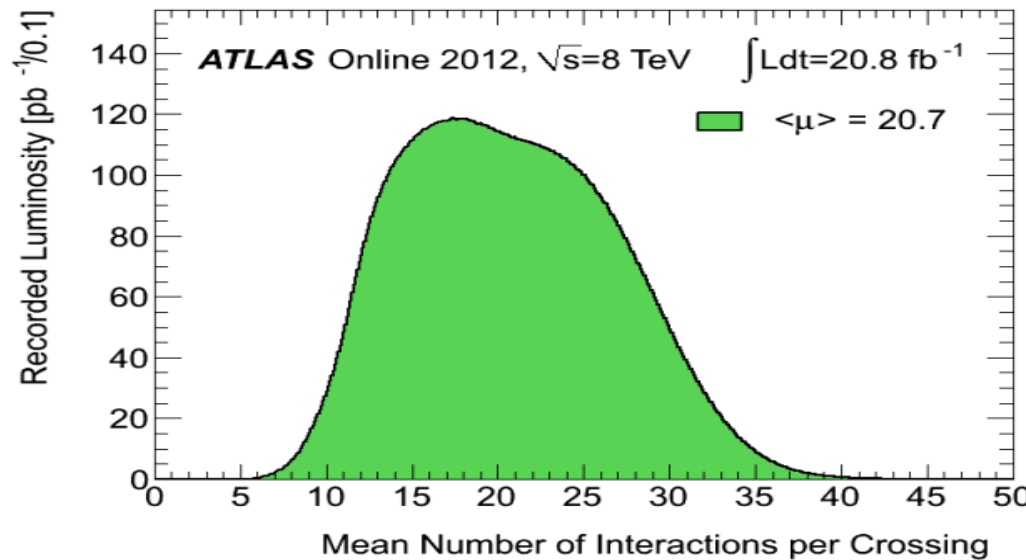
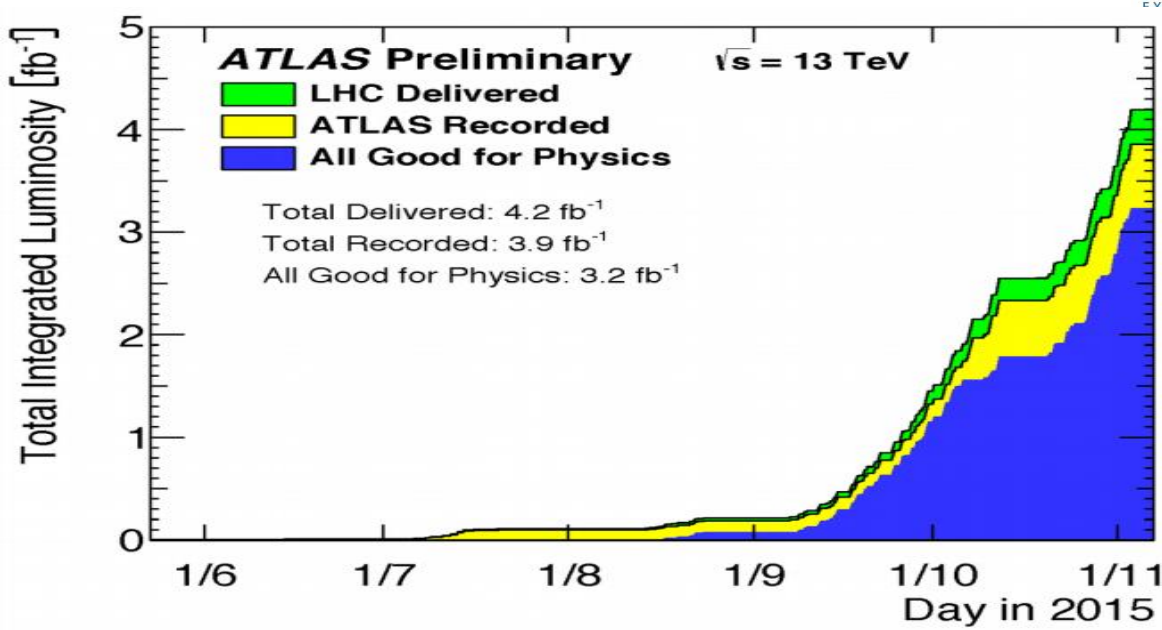
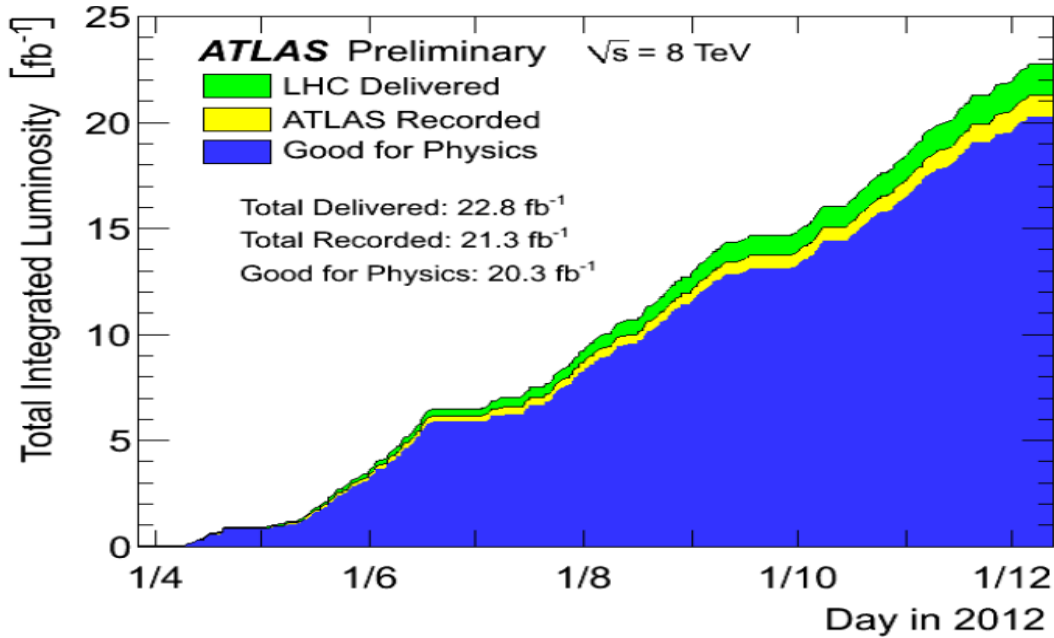


OUTLINE OF THE TALK

- New Standard Model results
- Motivation: Jet physics
- ATLAS detector
 - Reconstruction of physical objects: Jets, photons/electrons
- Jet physics in pp-collisions at 8 & 13 TeV
 - ❖ Inclusive Jet and Dijet cross-sections at 13 TeV (*JHEP 05 (2018) 195*)
 - *Comparison inc. Dijet & inc. Jet at 13 TeV*
 - ❖ Inclusive Jet cross-section at 8 TeV (*JHEP 09 (2017) 020*)
 - ❖ Differential cross-sections of γ +heavy-flavour Jet at 8 TeV (*Phys.Lett.B776(2018) 295*)
 - *Comparison $\gamma + b$ and $\gamma + c$ at 8 TeV*
 - *Intrinsic charm*
 - ❖ Differential cross-sections of $W+\text{Jets}$ & W^+/W^- ratios at 8 TeV (*JHEP 05 (2018) 077*)
 - ❖ Soft-drop Jet mass at 13 TeV (*Phys. Rev. Lett. 121 (2018) 092001*)
- Conclusions

- Measurement of *inclusive jet and dijet* cross-sections in proto-proton collisions at $\sqrt{s}=13\text{ TeV}$ with the ATLAS detector, *arXiv:1711.02692, JHEP 05 (2018) 195*
- Measurement of the *inclusive jet* cross-sections in proton–proton collisions at $\sqrt{s}=8\text{ TeV}$ with the ATLAS detector, *arXiv:1706.03192, JHEP 09 (2017) 020*
- Measurement of differential cross sections of *isolated-photon plus heavy-flavour jet* production in pp collisions at $\sqrt{s}=8\text{ TeV}$ using the ATLAS detector; *arXiv:1710.09560, Phys. Lett. B 776 (2018) 295*
- Measurement of differential cross sections and W^+/W^- cross-section ratios for W *boson production in association with jets* at $\sqrt{s}=8\text{ TeV}$ with the ATLAS detector, *arXiv:1711.03296, JHEP 05 (2018) 077*
- A measurement of the *soft-drop jet mass* in pp collisions at $\sqrt{s}=13\text{ TeV}$ with the ATLAS detector, *arXiv:1711.08341, PRL 121, 092001 (2018)*

ATLAS DATA AT 8 AND 13 TEV

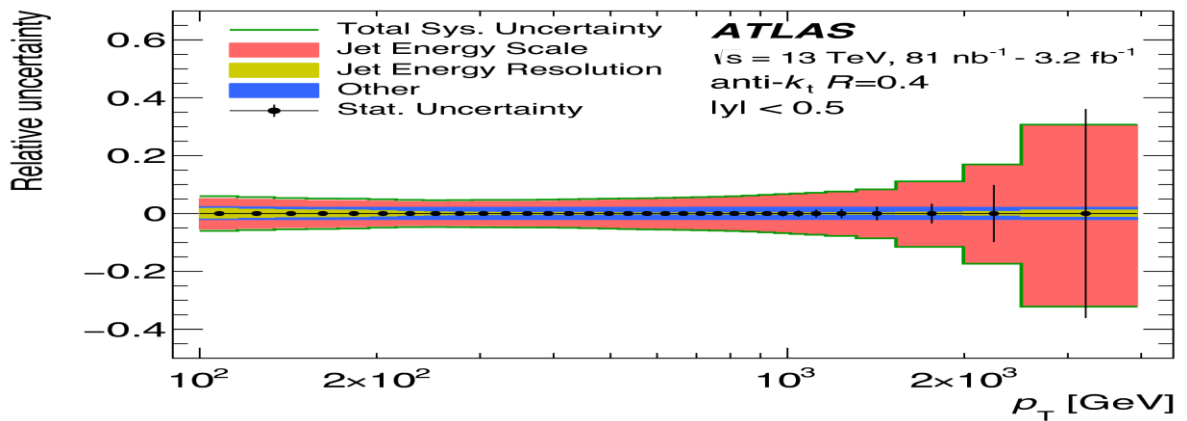


RELATIVE SYSTEMATIC UNCERTAINTIES: $\text{pp} \rightarrow \text{JET, DIJET + X}$ AT 13 TeV

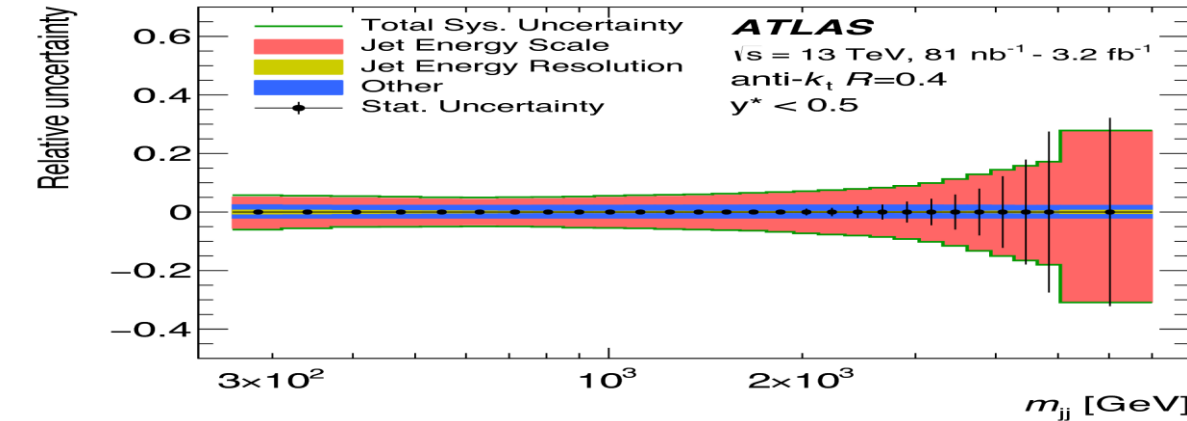
arXiv:1711.02692



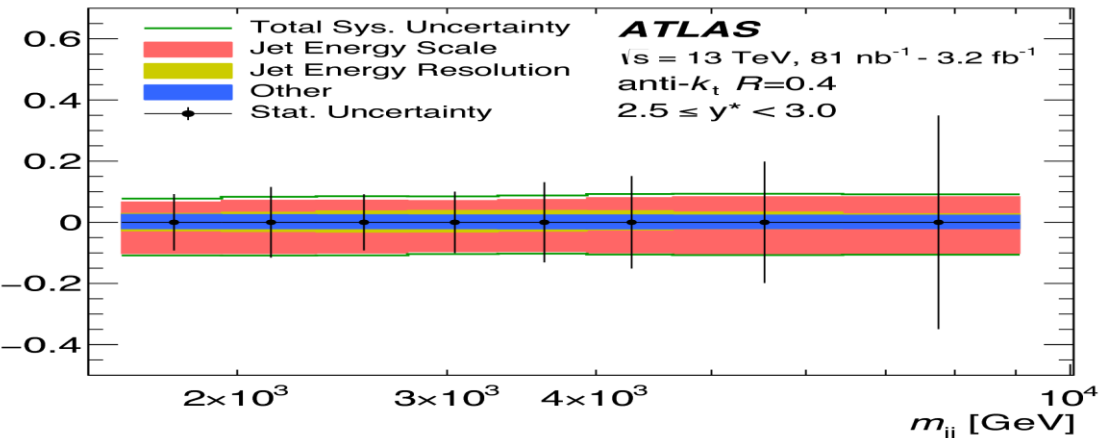
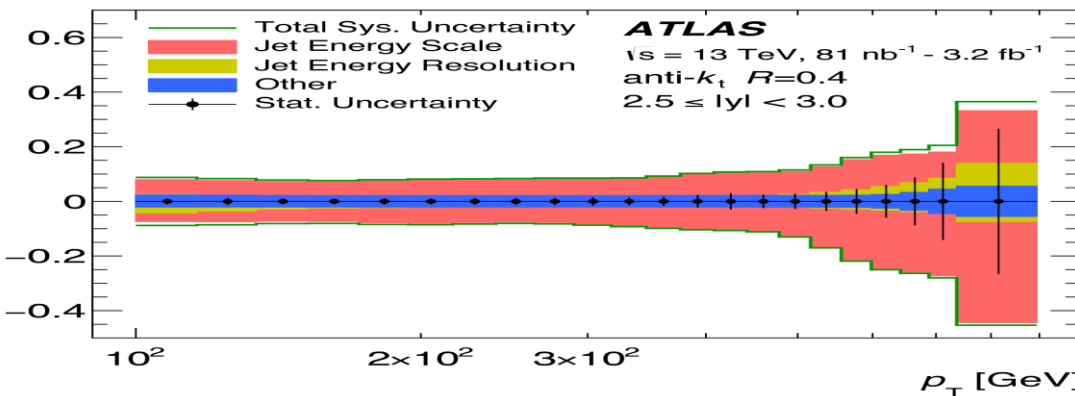
Relative systematic uncertainty for the inclusive jet cross-section as a function of the jet (dijet) p_T (m_{jj}) for the first (left) and last (right) $|y|$ (y^*) bins. The individual uncertainties are shown in different colours: the JES, JER, jet cleaning, luminosity & unfolding.



Jet



Dijet

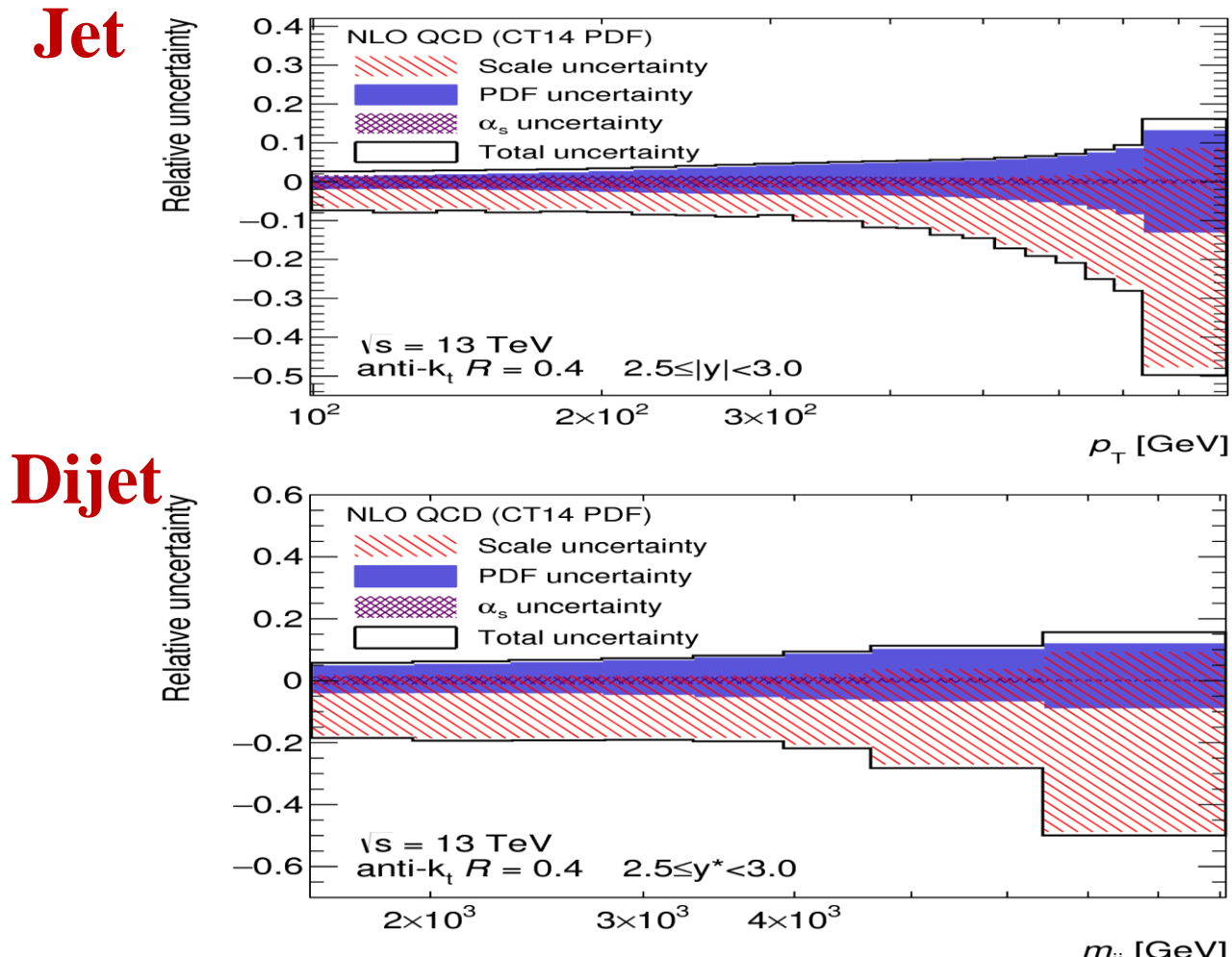
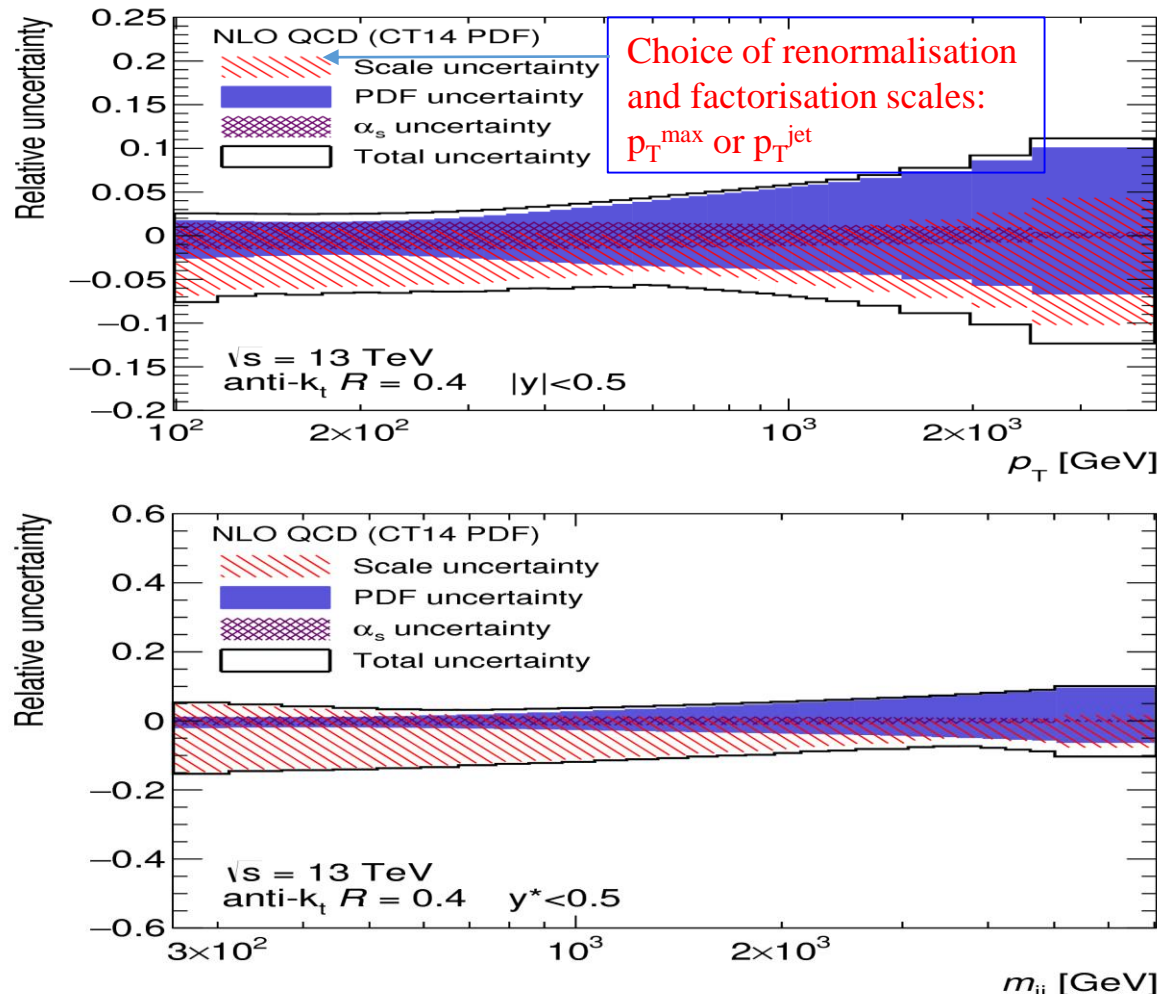


In the central (forward) region the total uncertainty in the inclusive jet measurement is about 5%(8%) at medium p_T of 300-600 GeV. The uncertainty increases towards both lower and higher p_T reaching 6%(10%) at low p_T and 30% $([-45\%, +40\%])$ at high p_T . The total uncertainty in the dijet measurement is about 5%(10%) at medium m_{jj} of 500-1000 GeV (2000-3000 GeV) in the first (last) y^* bin. The uncertainty increases towards both lower and higher m_{jj} reaching 6% at low m_{jj} and 30% at high m_{jj} in the first y^* bin. In the last y^* bin no significant dependence on m_{jj} is observed.

RELATIVE NLO QCD UNCERTAINTIES: $\text{PP} \rightarrow \text{JET, DIJET} + X$ AT 13 TeV

arXiv:1711.02692

Relative NLO QCD uncertainties in the jet cross-sections calculated using **CT14 PDF**. Top (bottom) panels correspond to the first and last $|y|$ (y^*) bins for the jet (dijet). The uncertainties: renormalisation and factorisation scale, the α_s , PDF & total are shown.



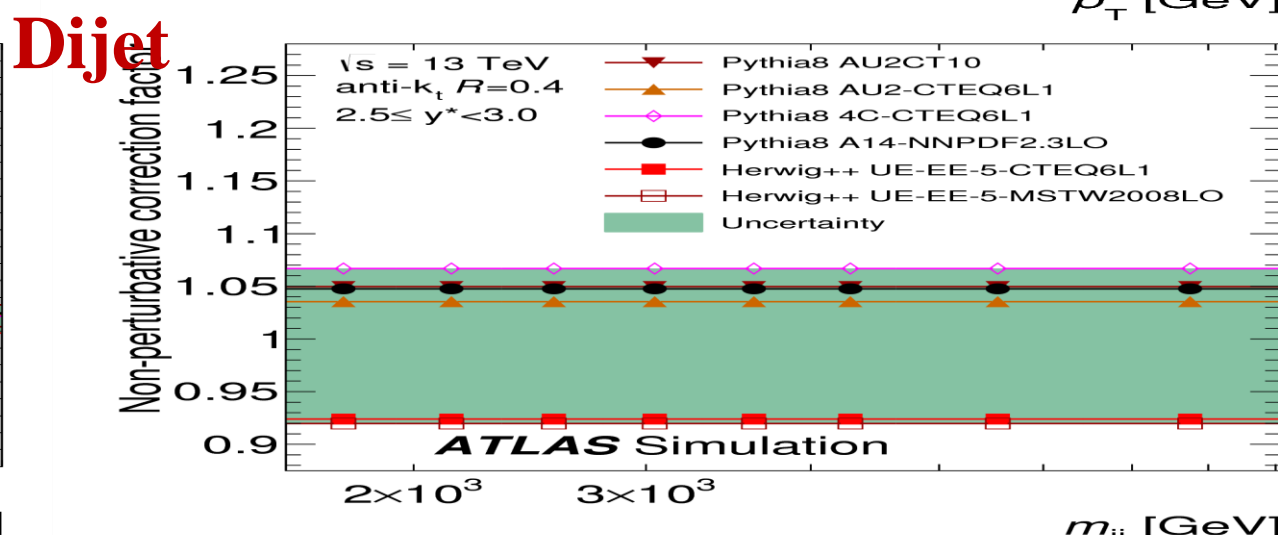
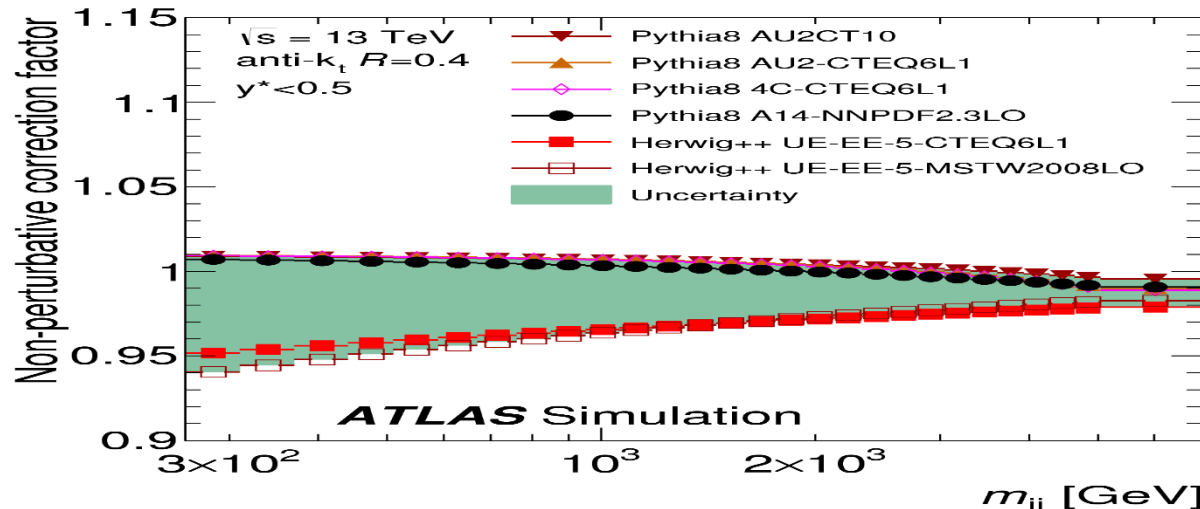
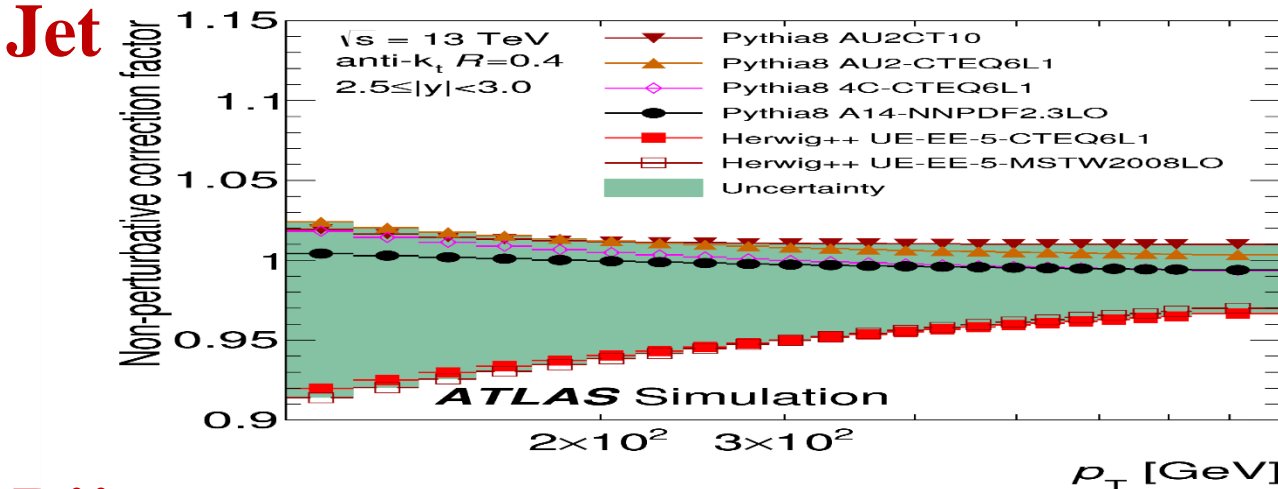
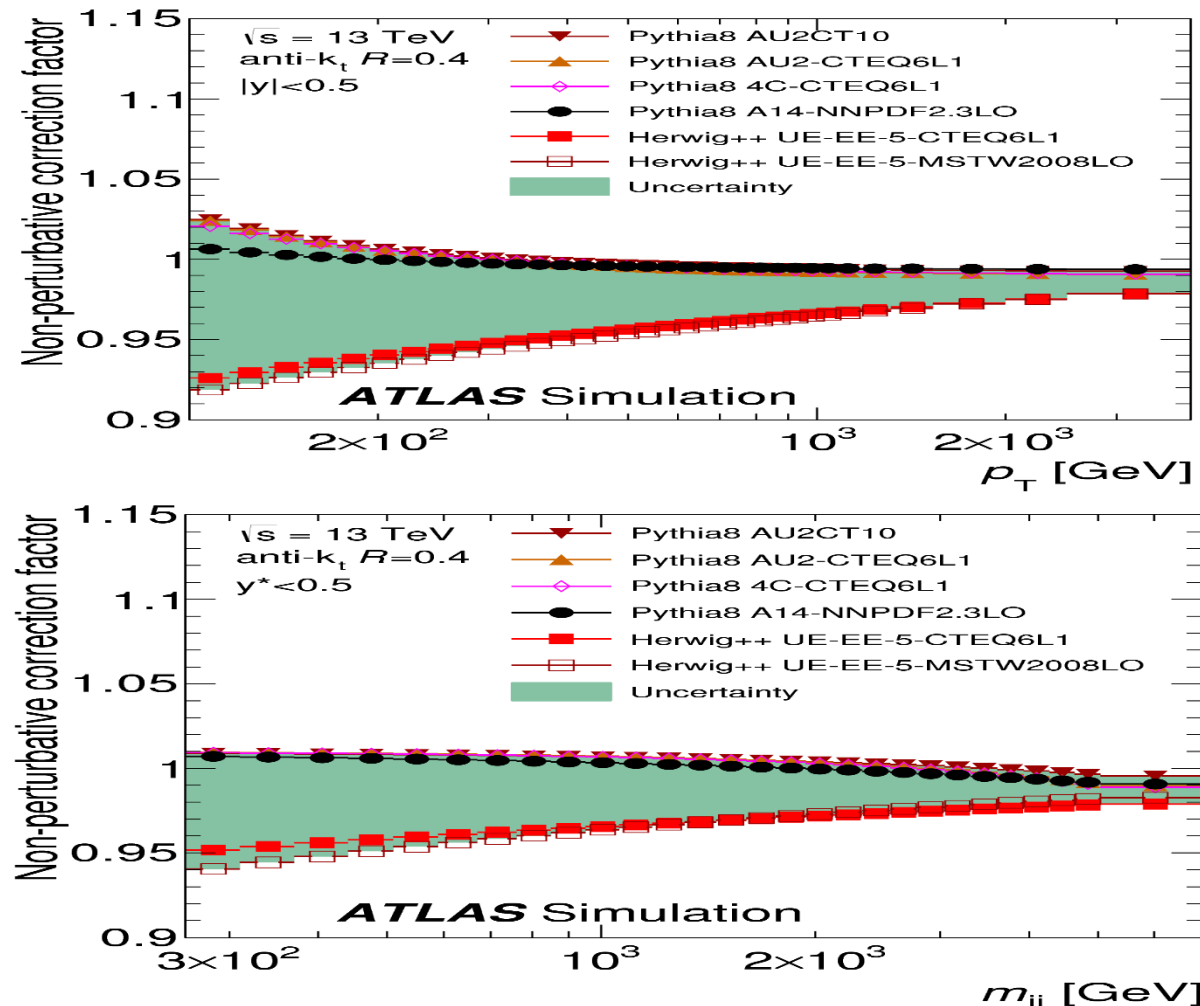
The uncertainty due to the [1] choice of renormalisation and factorisation scale is **dominant in most phase-space regions**, rising from 10% (20%) at about $p_T=100$ GeV ($m_{jj}=300$ GeV) in the central $|y|$ (y^*) bin to about 50% in the highest p_T (m_{jj}) bins in the most forward $|y|$ (y^*) region. The [2] PDF uncertainties vary 2-12% depending on the jet p_T & $|y|$ (m_{jj} , y^*). The contribution

NON-PERTURBATIVE CORRECTION FACTORS: $\text{PP} \rightarrow \text{JET, DIJET + X}$ AT 13 TeV



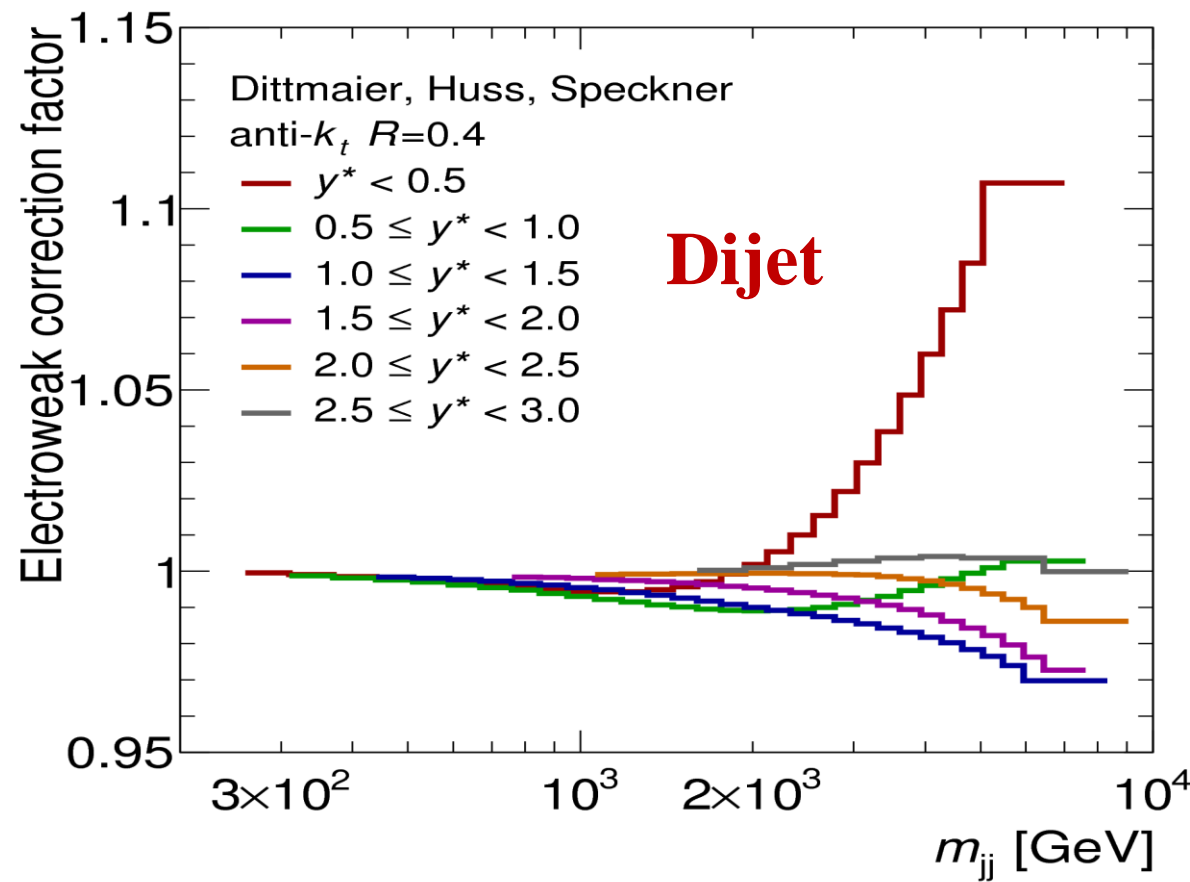
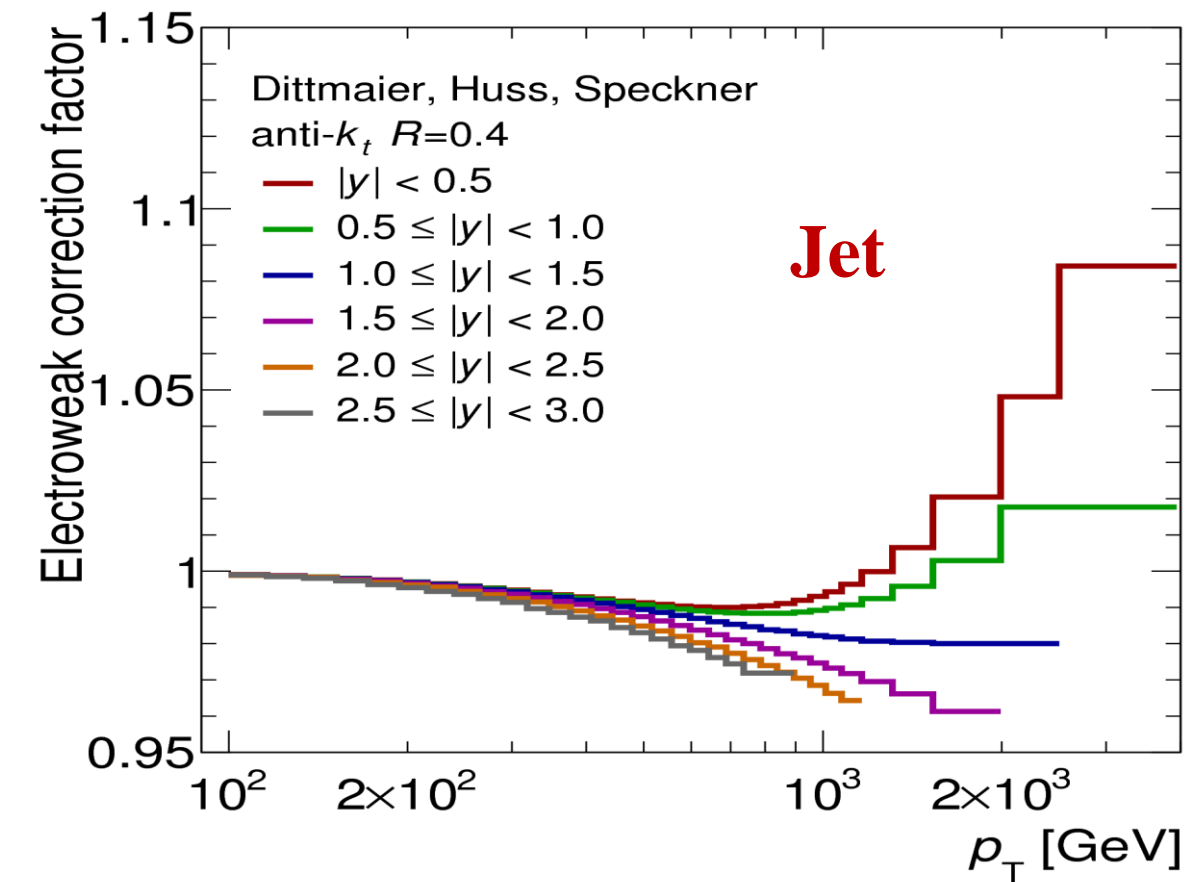
arXiv:1711.02692

Non-perturbative correction factors for the (jet, dijet) NLO pQCD prediction as a function of $(p_T^{\text{jet}}, m_{jj})$ for (left) the first ($|y|, y^*$) bin and for (right) the last ($|y|, y^*$) bin. The corrections are derived using Pythia 8 A14 with the NNPDF2.3 LO PDF set



The values of the correction are: for jet $\rightarrow 0.92\text{-}1.03$ at low p_T and $0.98\text{-}0.99$ ($0.97\text{-}1.01$) at high p_T for the first (last) $|y|$ bin & for dijet $\rightarrow 0.94\text{-}1.01$ ($0.98\text{-}0.99$) at low (high) m_{jj} for the first y^* bin and for the last y^* bin is a fixed range $0.92\text{-}1.07$

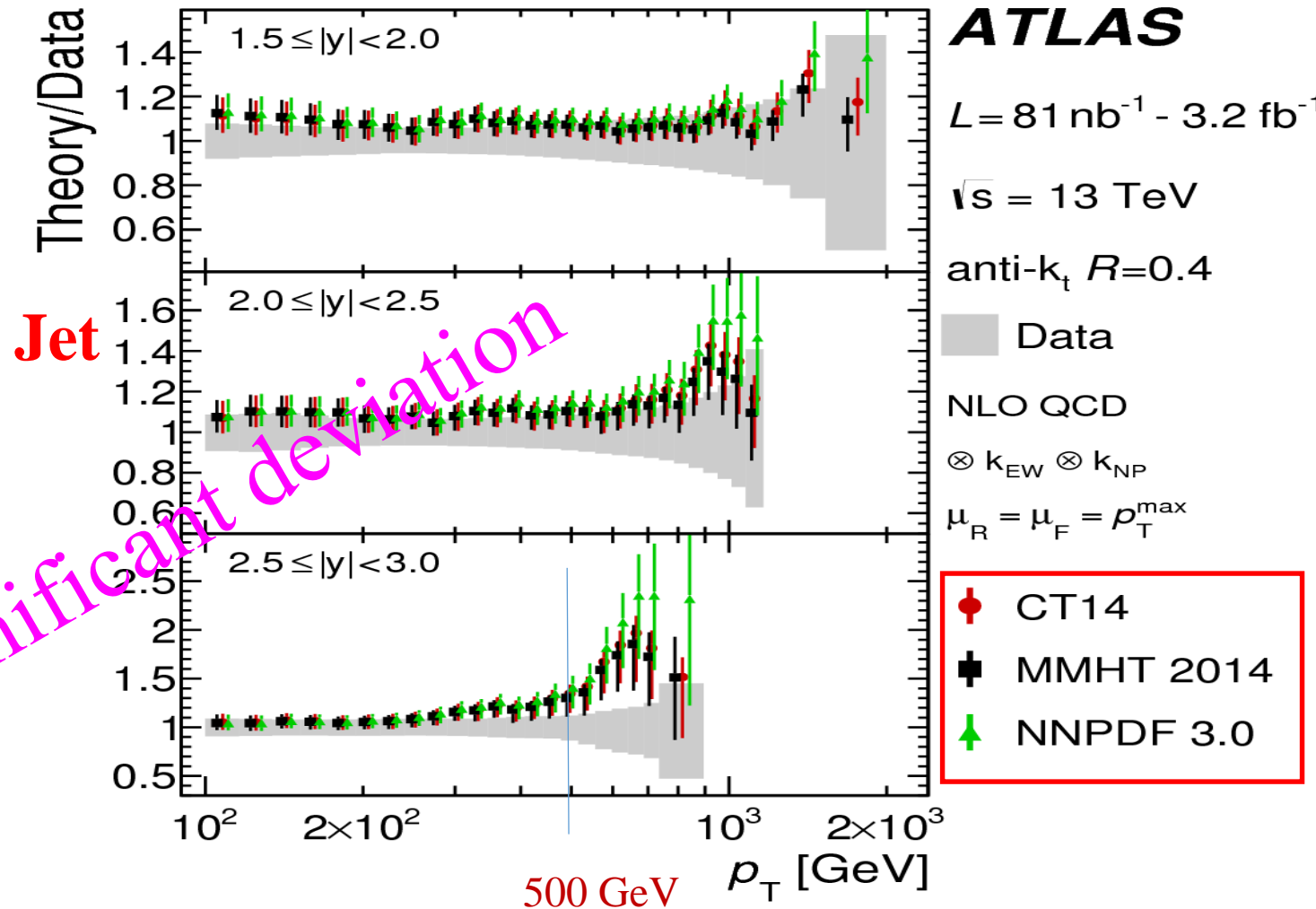
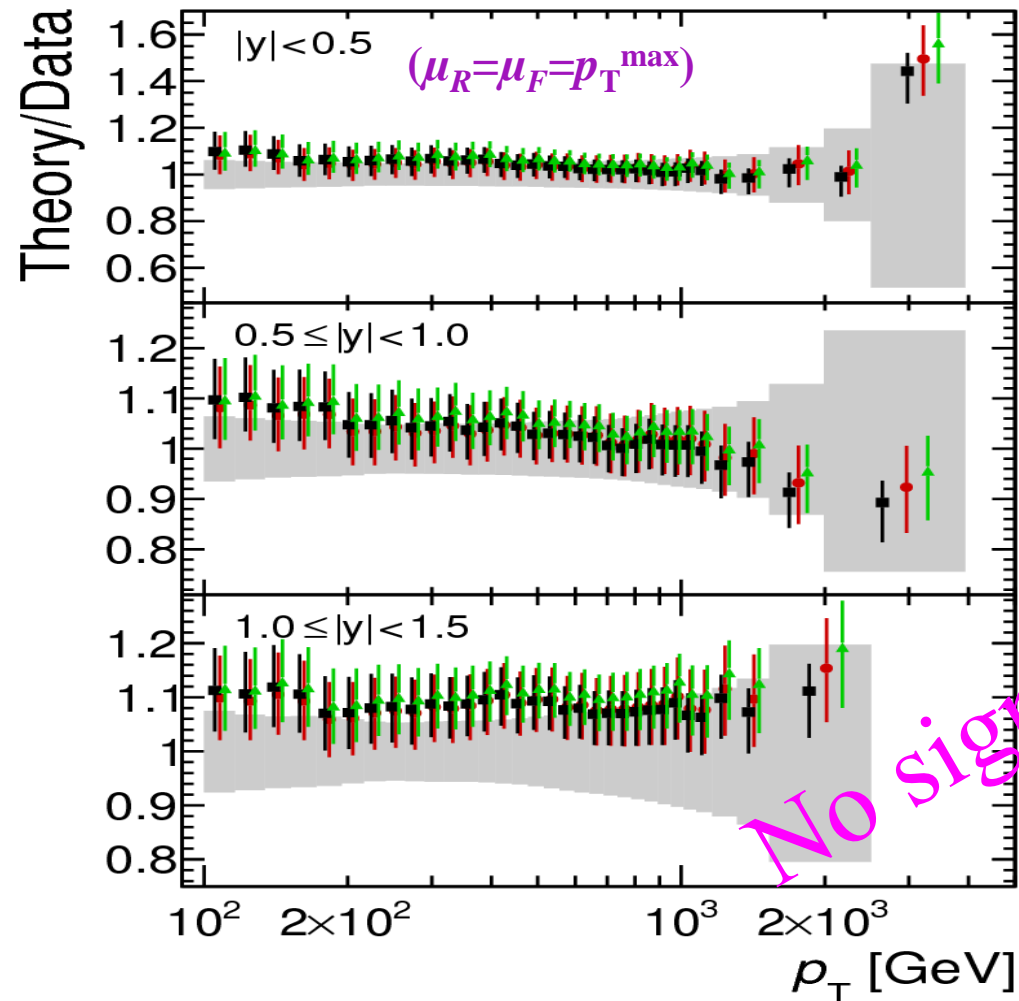
- The NLO pQCD predictions are corrected for the **effects of γ and W^\pm/Z interactions** at tree and one-loop level
- Electroweak correction factors for the inclusive jet (dijet) cross-section as function of **jet p_T (m_{jj})** for $|y|$ (y^*) bins



- The electroweak correction is small for low jet p_T and for low m_{jj}
- For jets the correction reaches 8% at the highest p_T (3 TeV) for the central $|y|$ bin and is less than 4% for the rest of the $|y|$ bins
- For dijets the EW correction reaches 11% at $m_{jj}=7$ TeV for the central y^* bin and less than 3% for the rest of the y^* bins

Ratio of **NLOJet++ prediction** to measurements of Jet double-diff. cross-sec. vs. Jet p_T and y

PDF sets used: **CT14, MMHT 2014, NNPDF 3.0**



- ❖ Good description of data by **NLO pQCD** within the uncertainties
- ❖ Similar shape predicted by the studied **PDF sets**

The **CT14** case is repeated to serve as a reference for comparison⁴¹

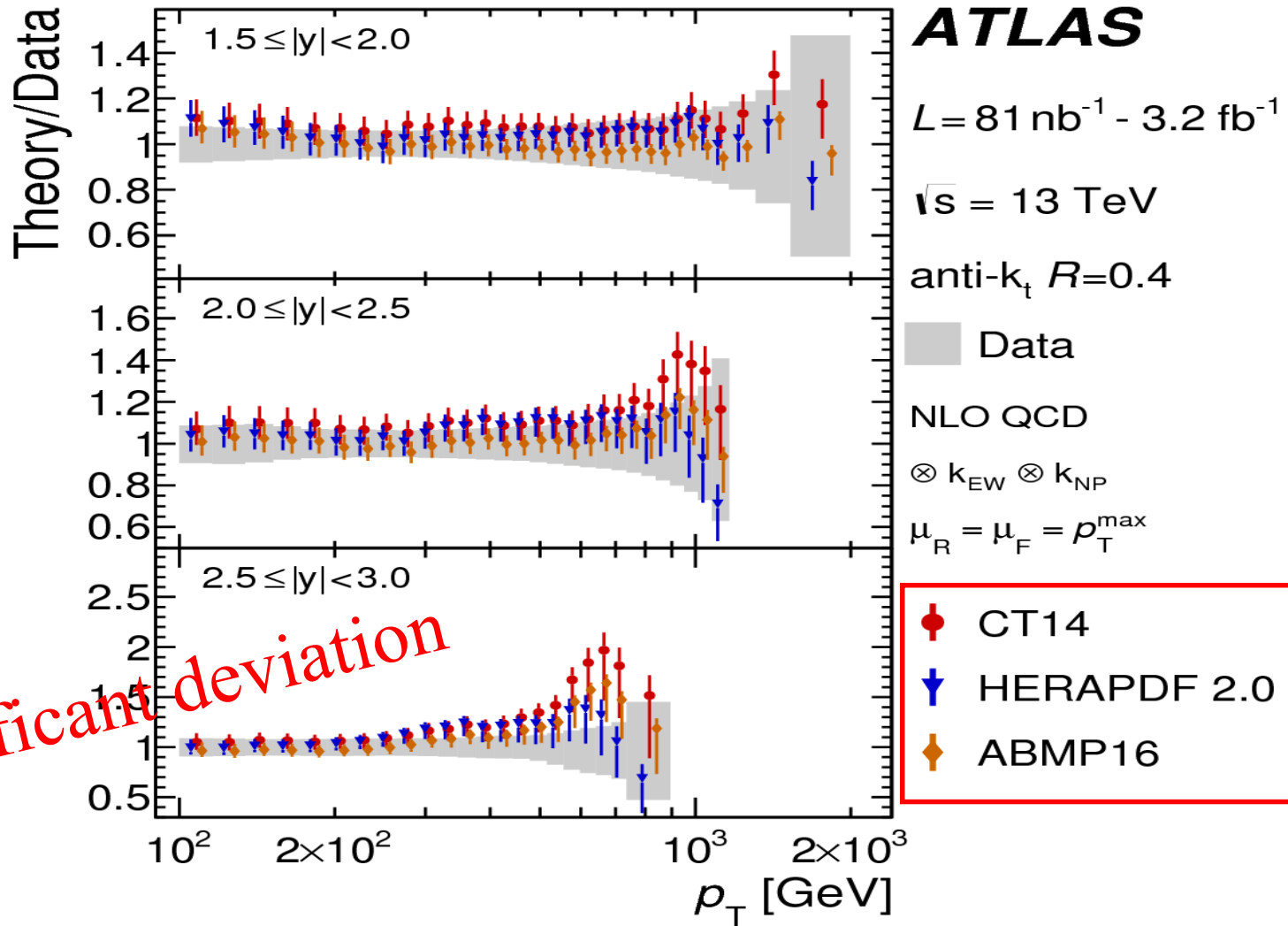
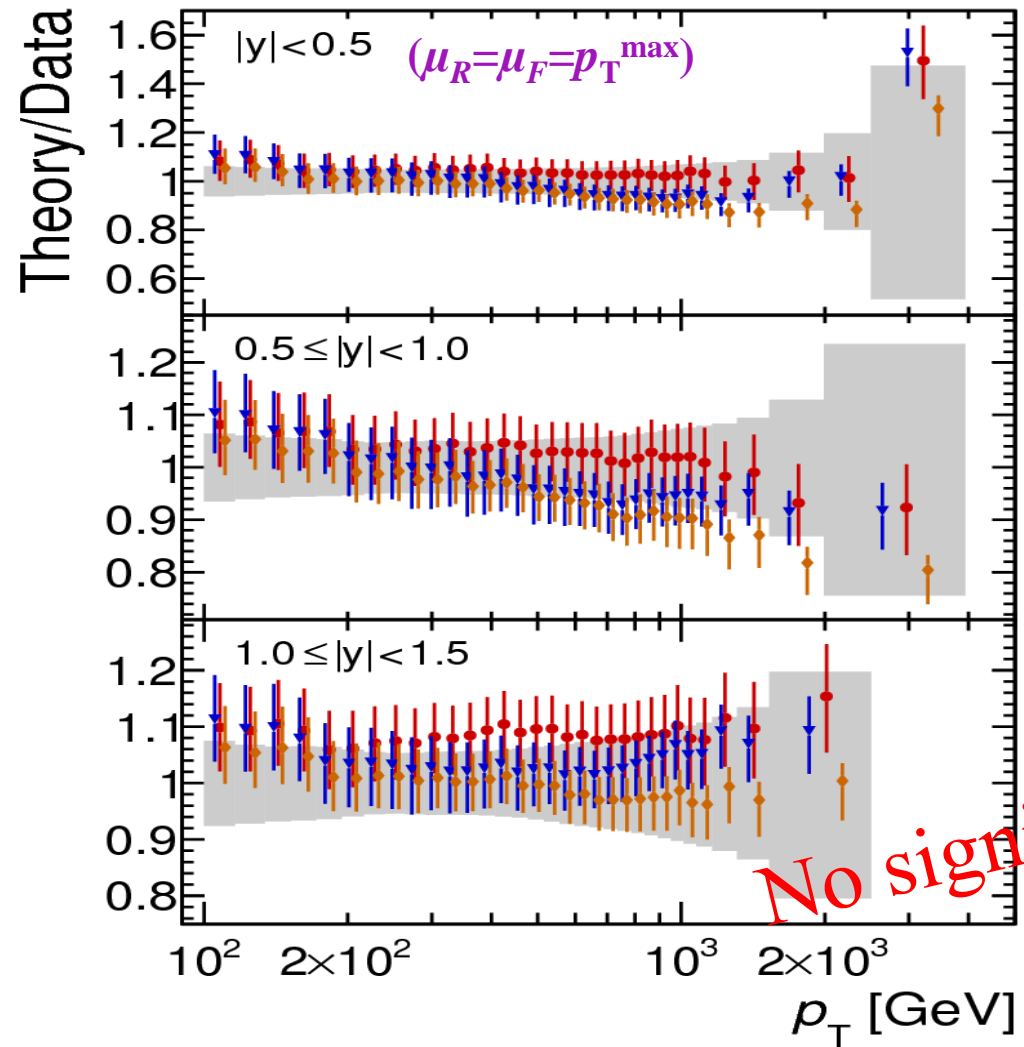
THEORY/DATA COMPARISON FOR JET CROSS SECTION AT 13 TeV

arXiv:1711.02692



Ratio of NLOJet++ prediction to measurements of Jet double-diff. cross-sec vs jet p_T and y

PDF sets used: CT14, HERAPDF 2.0, ABMP16



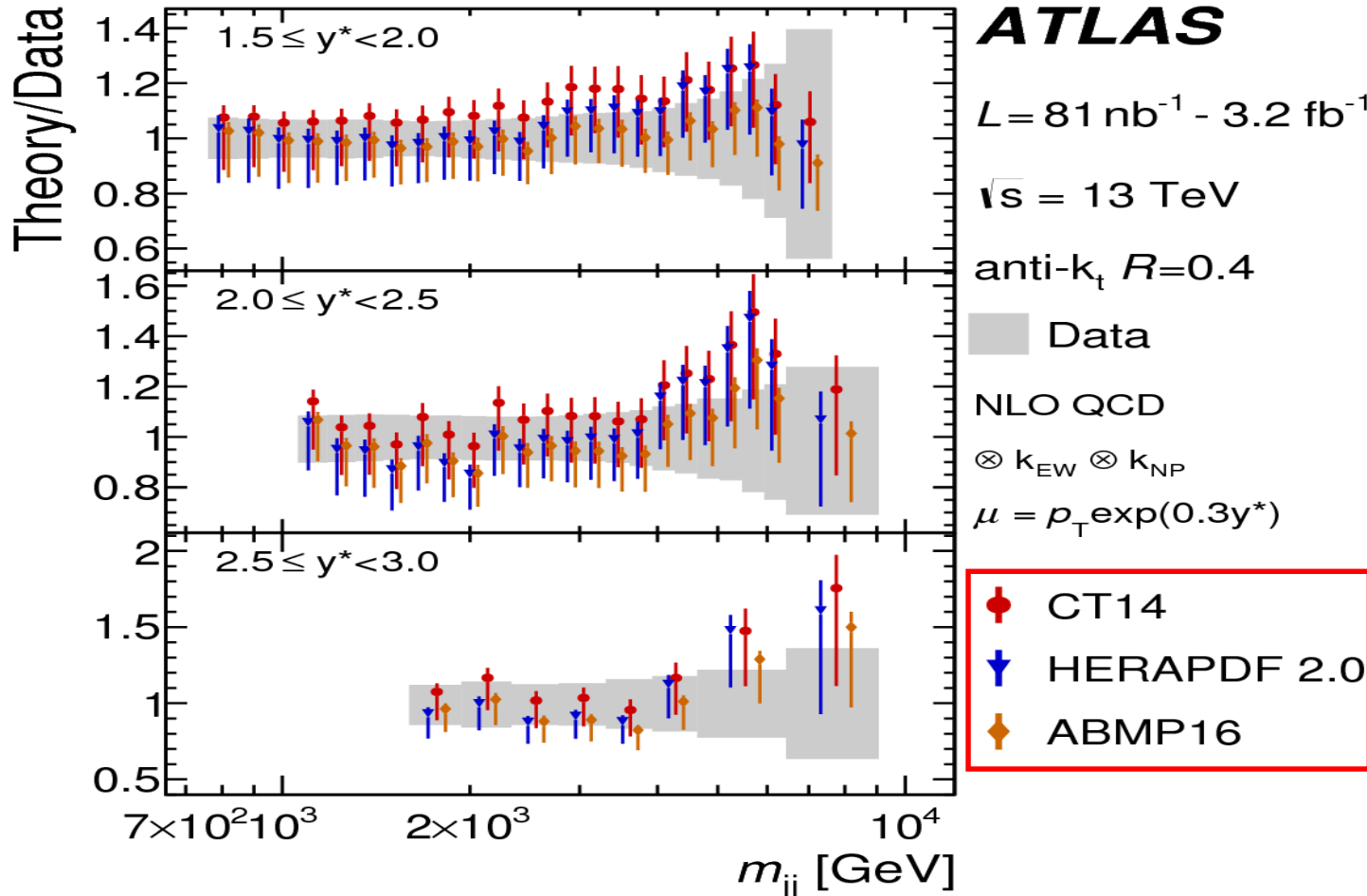
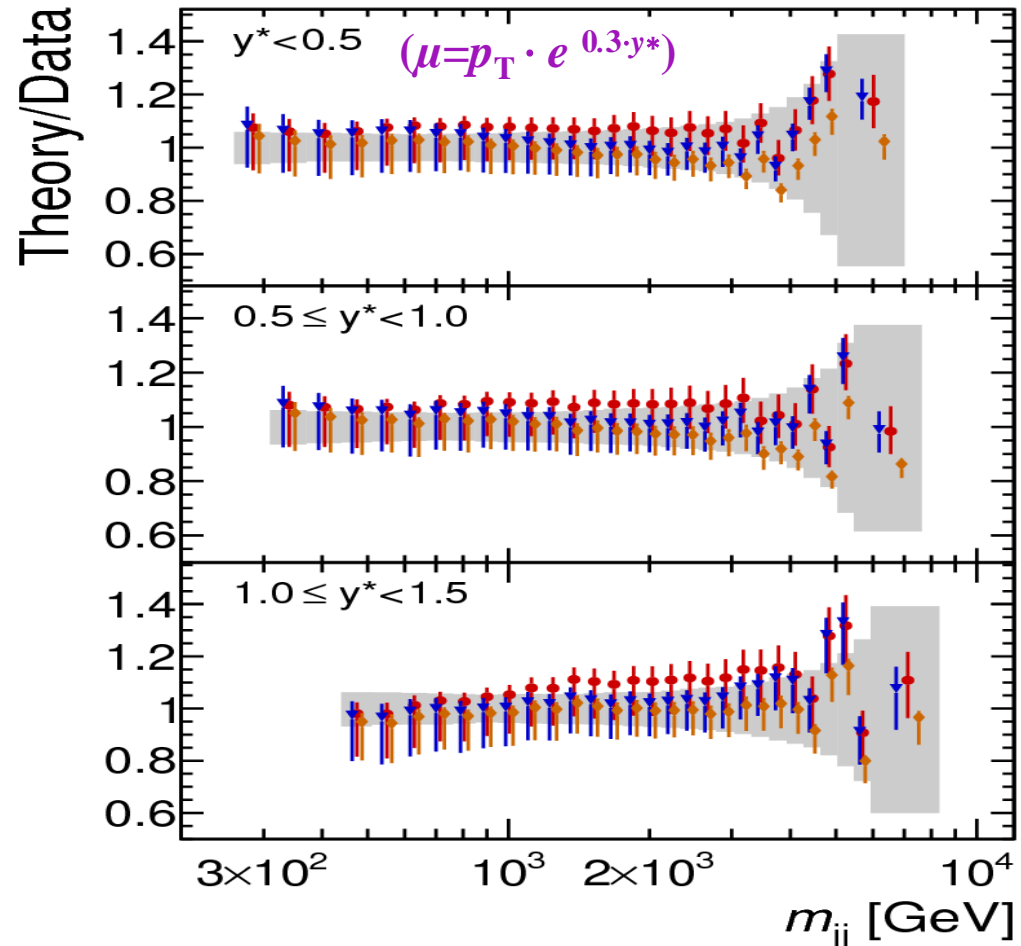
The CT14 case is repeated to serve as a reference for comparison

THEORY/DATA COMPARISON FOR DIJET CROSS SECTION AT 13 TeV

arXiv:1711.02692

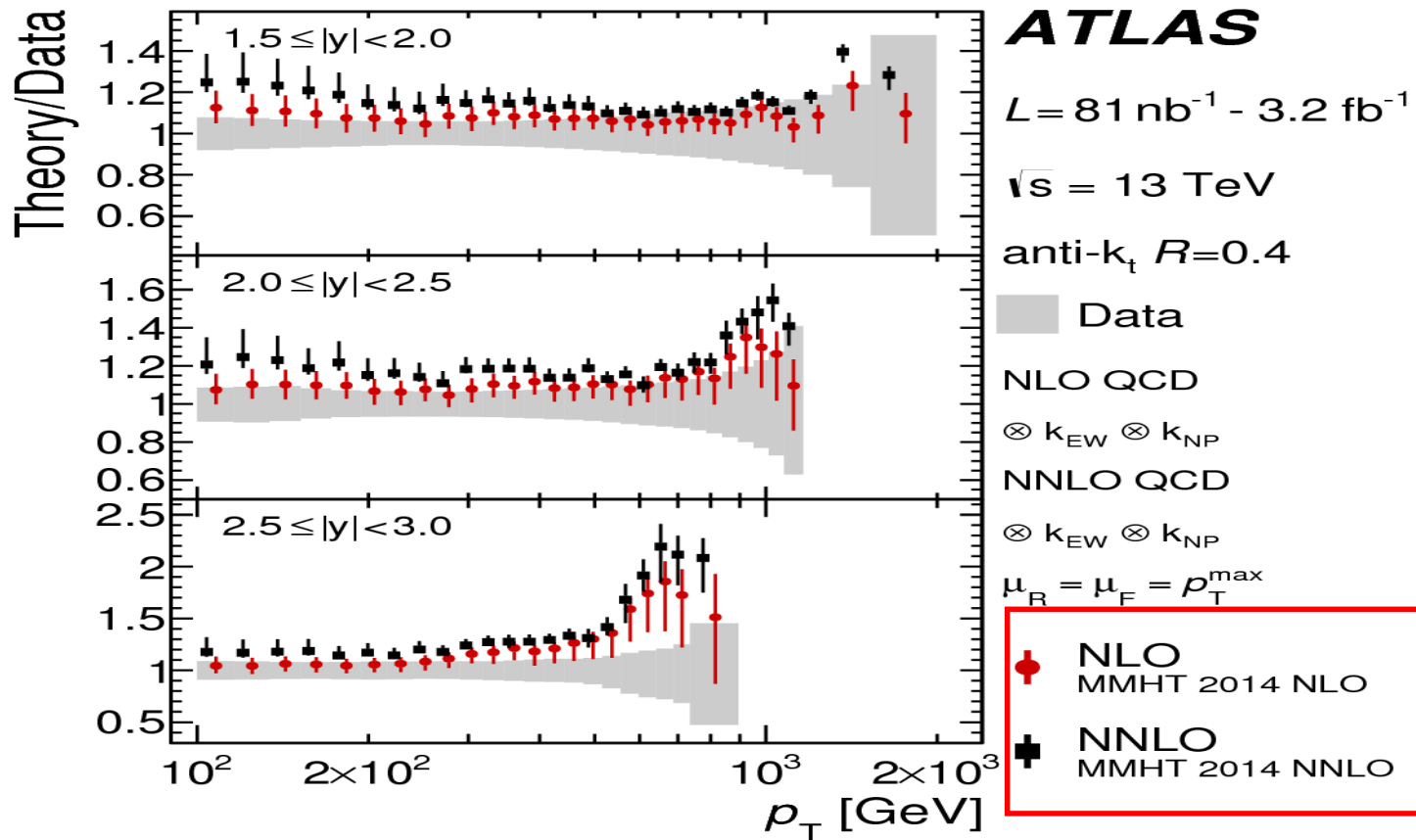
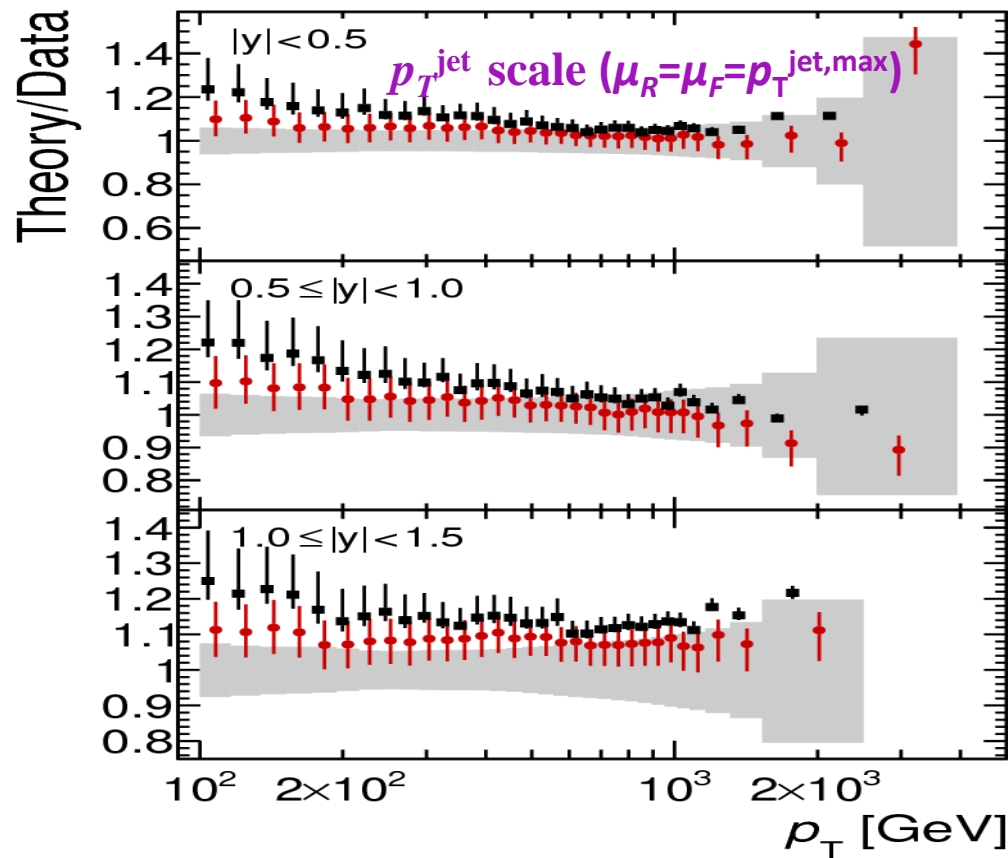


Ratio of **NLOJet++ prediction** to **measurements of Dijet double-diff. cross-sec vs dijet mass**
and y^* PDF sets used: **CT14, HERAPDF2.0, ABMP16**



The **CT14** case is repeated to serve as a reference for comparison

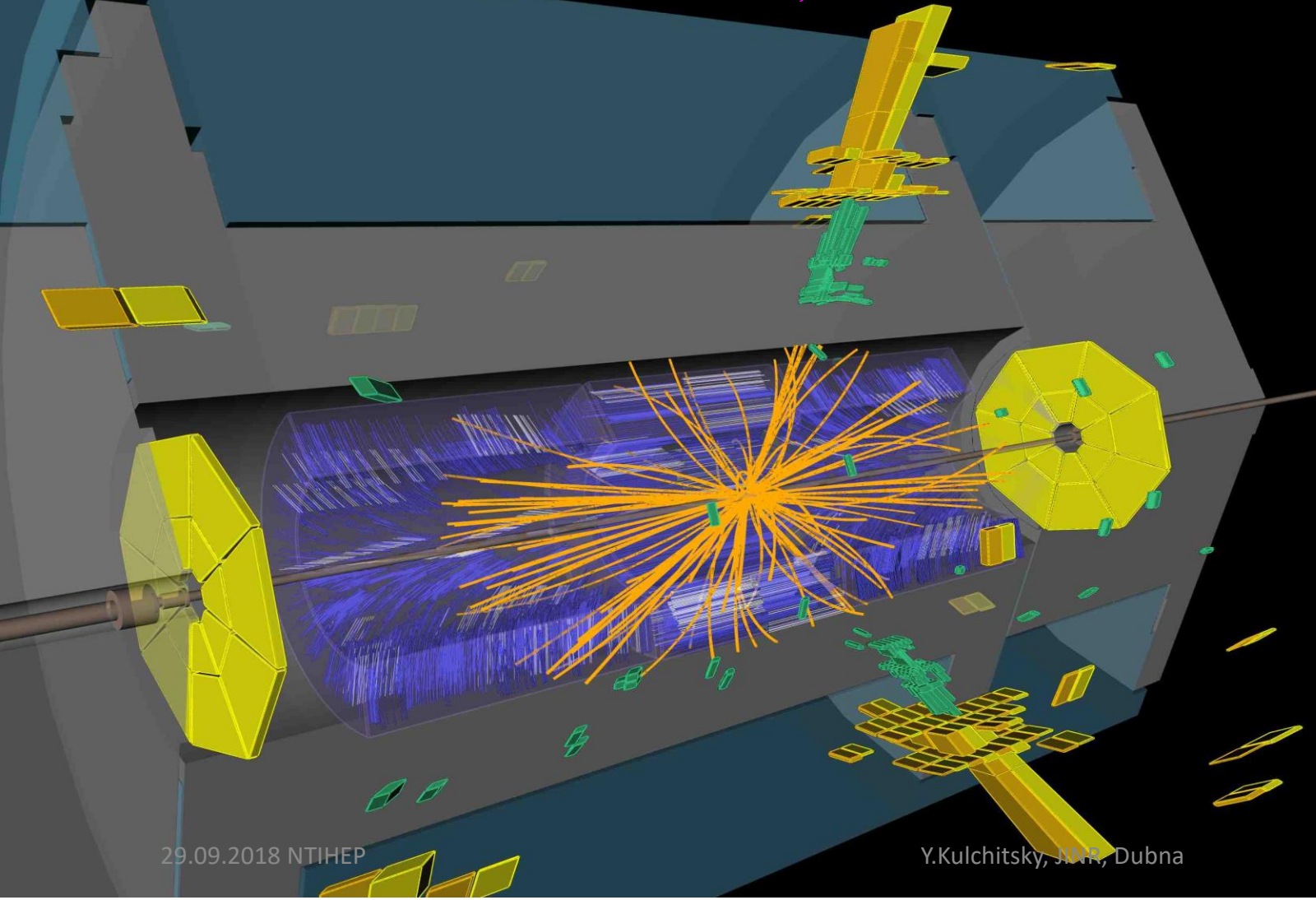
Ratio of NLOJet++ (p_T^{\max} QCD scale) prediction to measurements of Jet double-diff. cross-sec
vs p_T^{jet} and y : PDF sets used: MMHT 2014 NLO, MMHT 2014 NNLO



- ❖ NLO pQCD describes the measurements within uncertainties
- ❖ Toward higher p_T NLO pQCD closer to data
- ❖ $p_T > 300$ GeV and high y rise of NLO pQCD with respect to data (>20%)
- ❖ NNLO above measurements for $p_T < 500$ GeV

The differences between data and the theoretical predictions at NNLO are larger than at NLO for the p_T^{\max} scale choice

INCLUSIVE JET CROSS-SECTION IN $\text{pp} \text{ at } 8 \text{ TeV}$

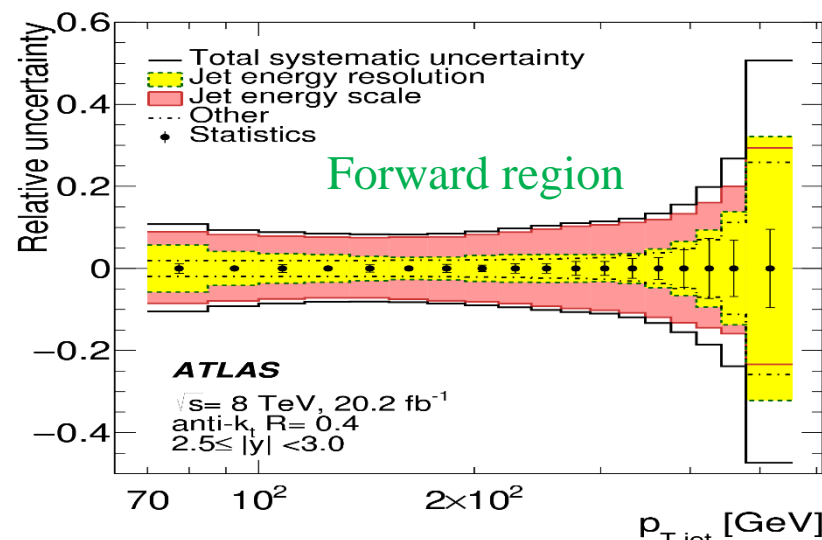
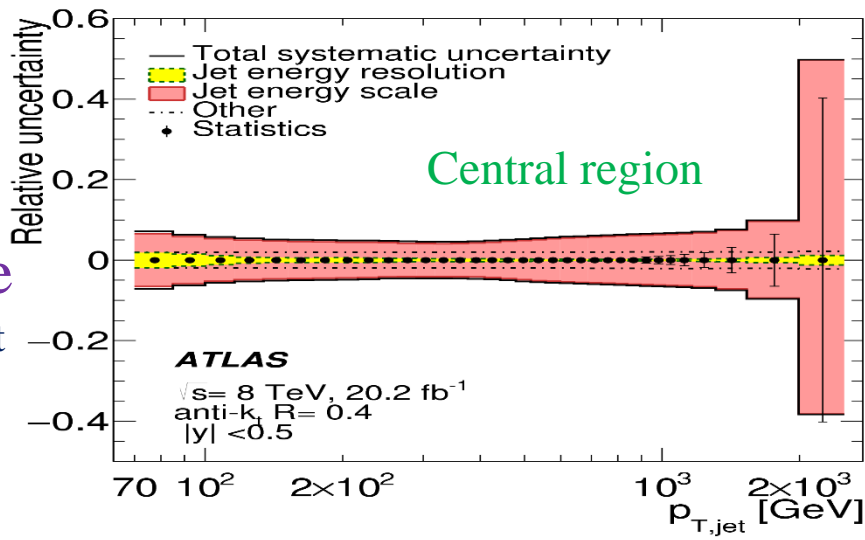


EVENT & JET SELECTION FOR $\text{pp} \rightarrow \text{JET} + \text{X}$ AT 8 TeV

JHEP 09 (2017) 020



- $L_{\text{int}} = 20.2 \text{ fb}^{-1}$
- Pile-up: $\langle \mu \rangle$ increases from $\langle \mu \rangle \sim 10$ to $\langle \mu \rangle \sim 36$
- 3-level jet trigger: events with p_T^{jet} over a threshold, $|\eta| < 3.2$
- Offline data selection and Jet correction: similar to Dijet case
- Cross-sections are measured for **6 rapidities** as function p_T^{jet}
- Data are unfolded to the particle level in a 3-step procedure:
 - ❖ correction for the sample impurities;
 - ❖ unfolding for the p_T migration;
 - ❖ correction for the analysis inefficiencies
- Sources of systematic uncertainty: those associated with jet reconstruction and calibration, unfolding procedure, and luminosity measurement
- Main sources: Jet Energy Scale (JES) & Jet Energy Resolution (JER)
For $|\eta| < 0.5$ & $p_T^{\text{jet}} < 1 \text{ TeV}$ less than 10%



Relative systematic uncertainty

UNCERTAINTY FOR $\text{pp} \rightarrow \text{JET} + X$ AT 8 TeV

JHEP 09 (2017) 020



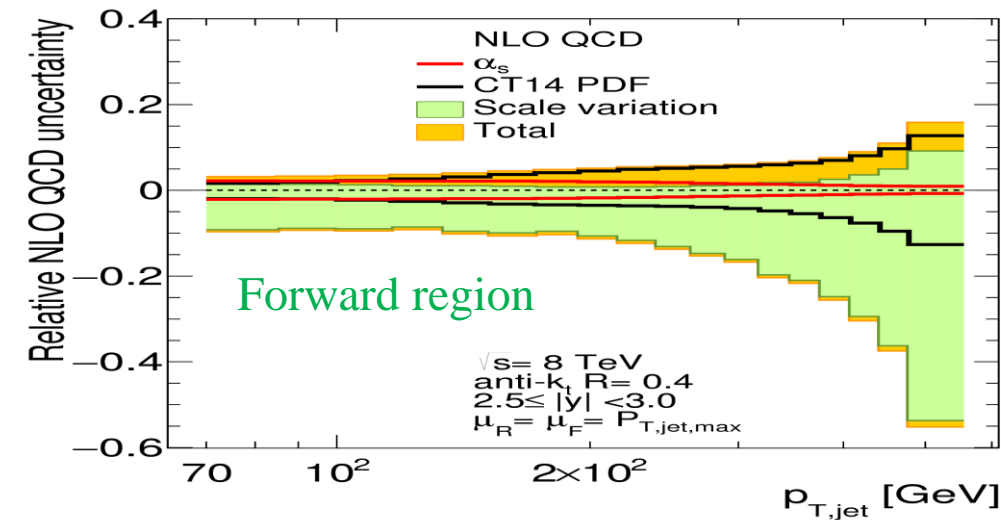
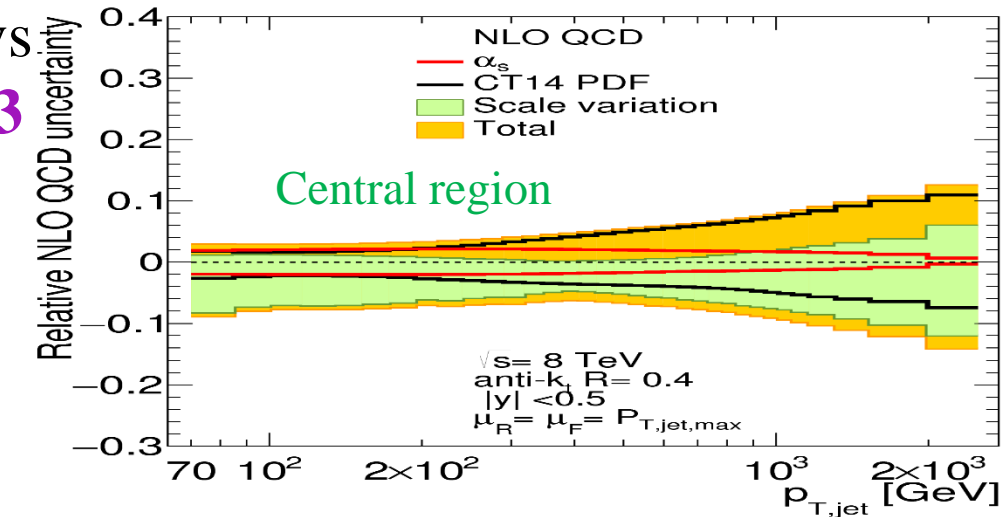
The double-diff. inclusive jet cross-section measurement vs p_T -jet & $|y|$: kinematic region: $70 \text{ GeV} \leq p_T^{\text{jet}} \leq 2.5 \text{ TeV}$ & $|y| < 3$

□ **Motivation:** a test of validity of pQCD and probing of the parton distribution functions (PDFs) in the proton

➤ Jets are identified with the **anti- k_t** using the jet radius, **$R=0.4$ & $R = 0.6$**

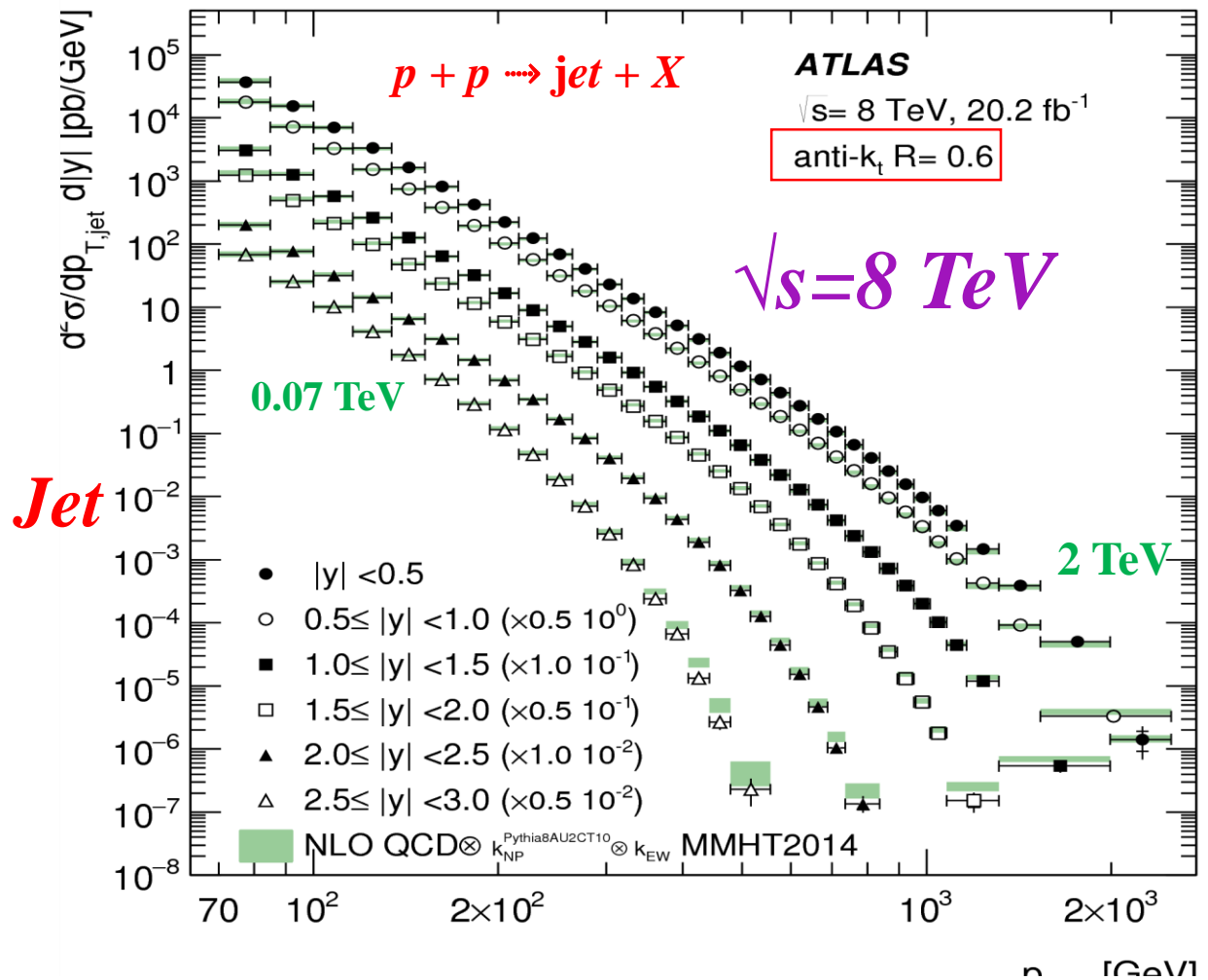
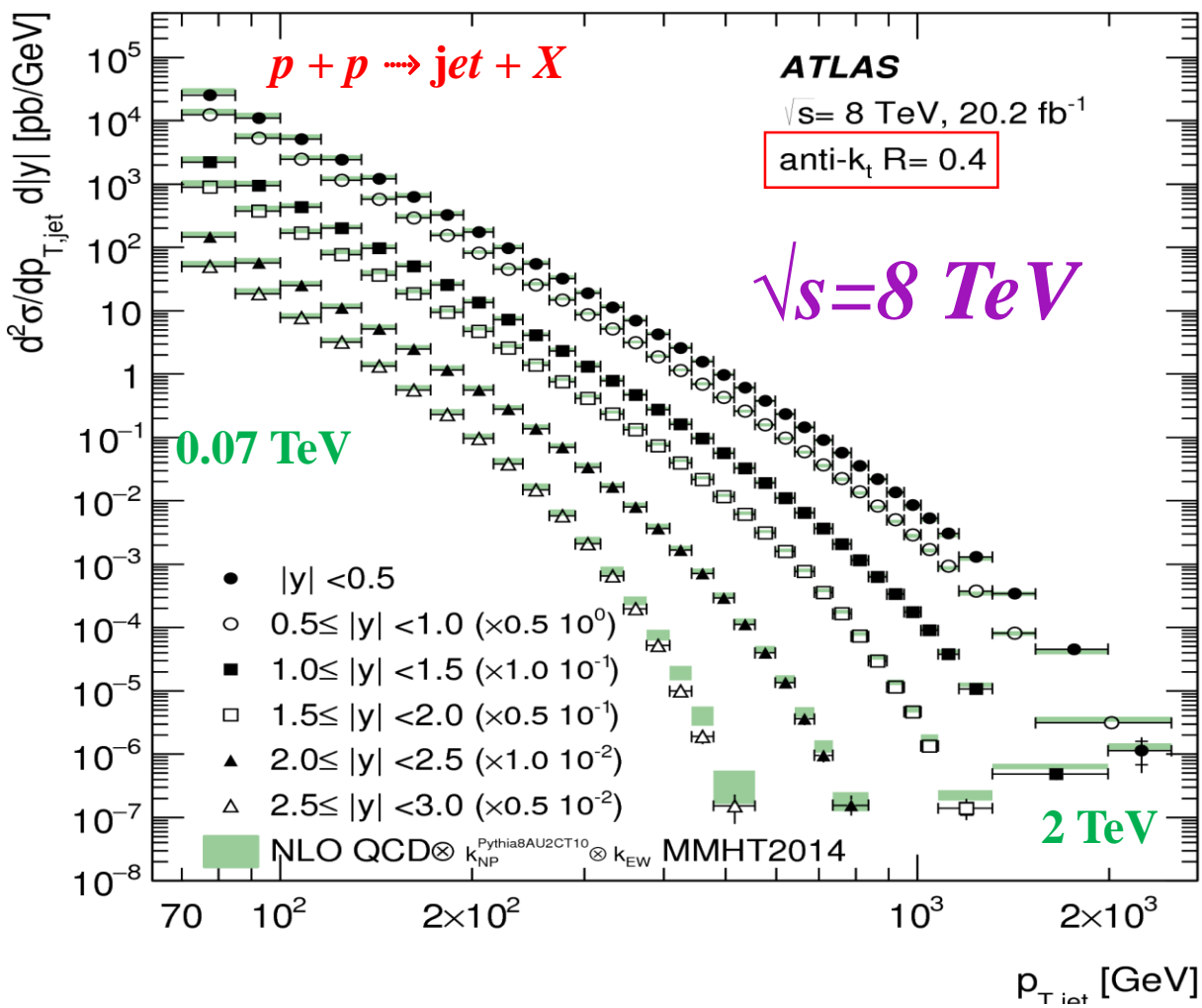
❖ Jet cross section refers to **particle-level jets** and to compare them with NLO pQCD predictions with **parton-level jets**, a correction for **non-perturbative** and **electroweek** effects is done.

□ **Theoretical predictions:** NLO pQCD calculated by **NLOJET++ 4.1.3** with several PDFs and different renormalisation and factorisation scales $\mu_R = \mu_F = p_T^{\text{jet};\text{max}}$ to cover missing higher order corrections.



Uncertainty in the NLO pQCD prediction of inclusive jet X-sec vs jet p_T – potential of jet physics for improving PDFs ⁴⁷

Double-differential *inclusive Jet* cross-sections for *Jets* with $R=0.4$ & 0.6 vs. p_T^{jet} & $|y|$
data vs NLO pQCD prediction corrected for non-perturbative and EW effects



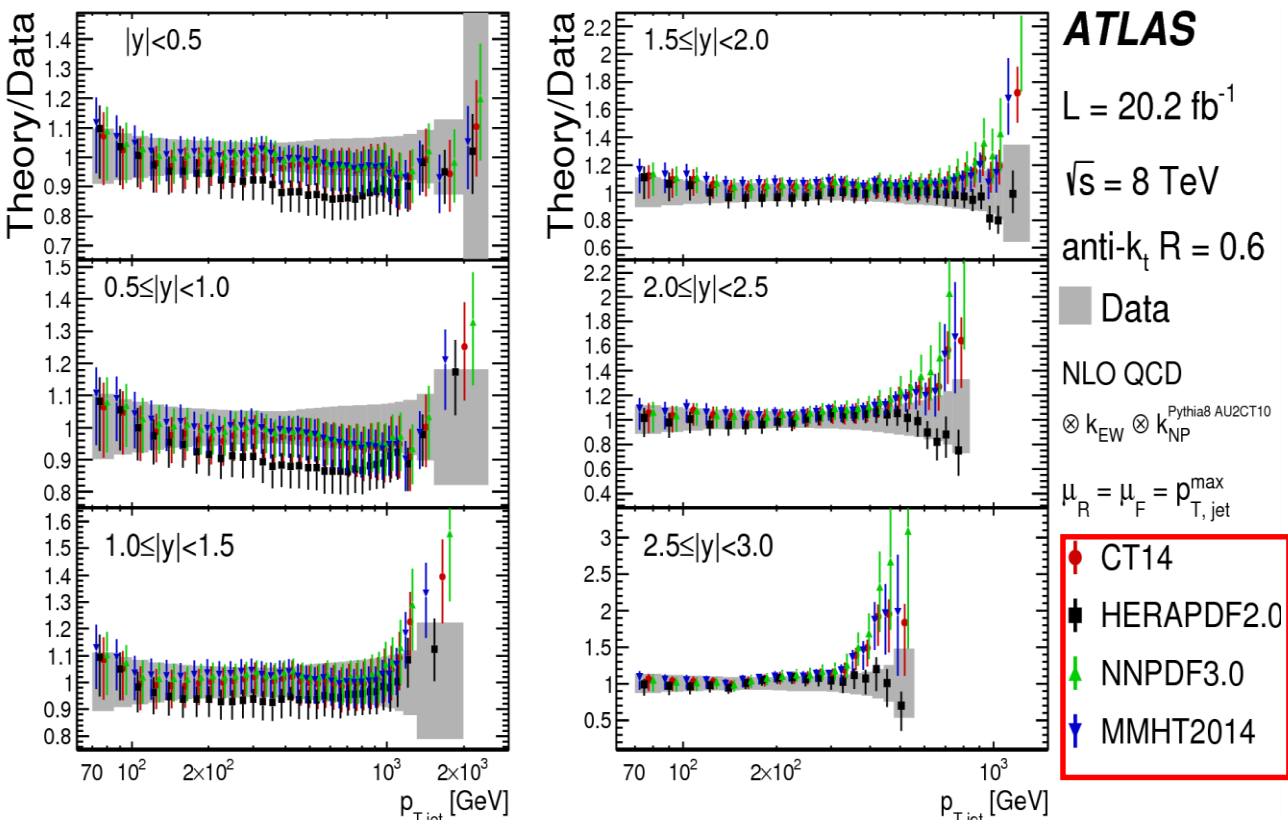
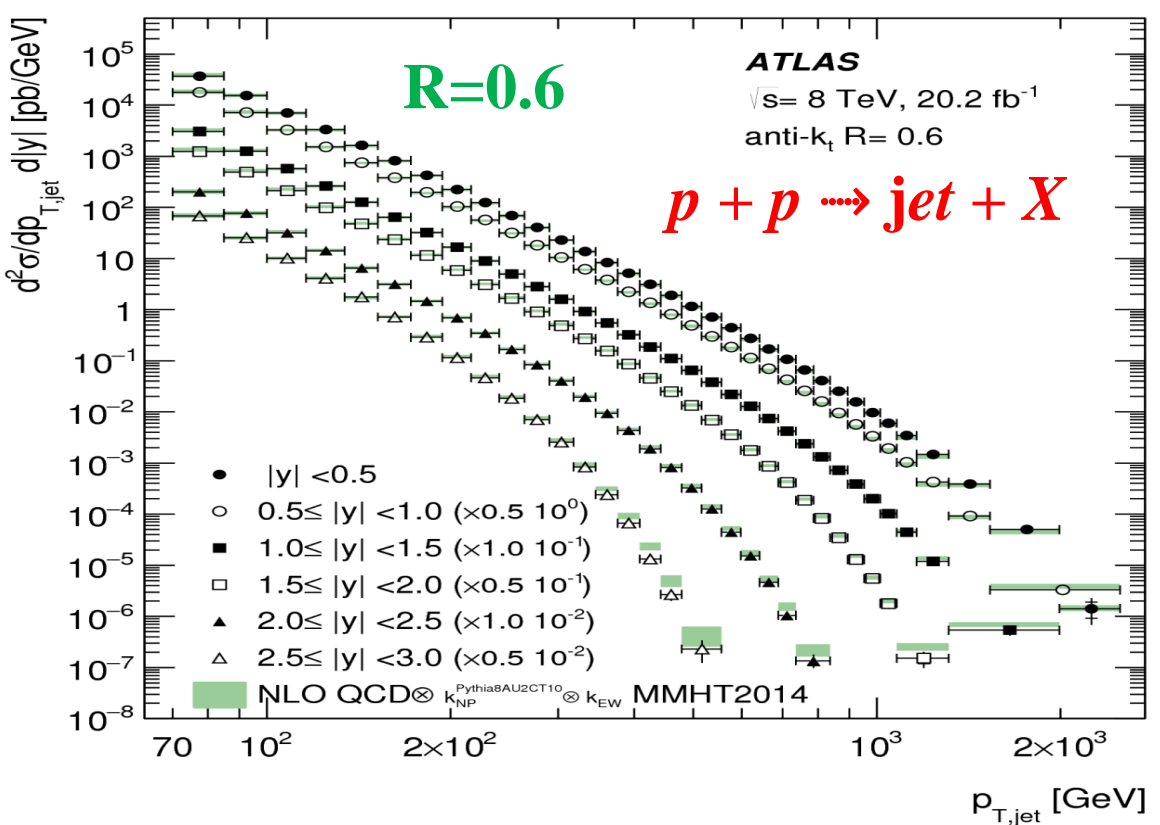
$p_T^{\text{jet}} > 70 \text{ GeV}; |y| < 3; \text{anti-}k_T \text{ jets with } R=0.4 \text{ and } R=0.6$

THEORY/DATA COMPARISON FOR $p + p \rightarrow \text{jet} + X$ AT 8 TeV

JHEP 09 (2017) 020



Double-differential *inclusive Jet* cross-sections for jets with $R=0.6$ vs. *jet p_T* and *rapidities* data vs. NLO pQCD prediction corrected for non-perturbative and EW effects



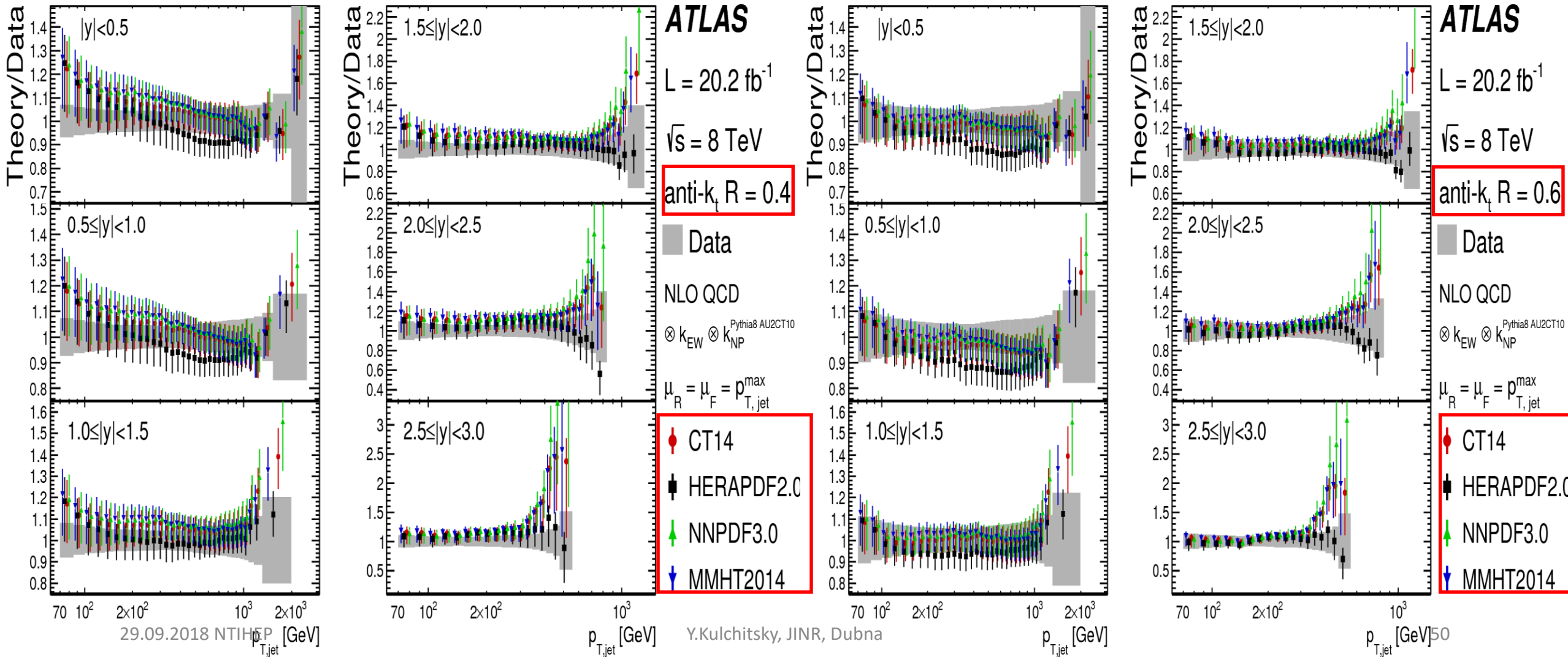
Ratio of NLO pQCD predictions to measured double-diff. inclusive Jet cross-section vs jet p_T and jet rapidity: different NLO PDF sets used CT14, HERAPDF2.0, NNPDF3.0, MMHT2014

RATIO NLO QCD FOR $pp \rightarrow \text{JET} + X$ AT 8 TeV



JHEP 09 (2017) 020

Ratio of **NLO pQCD** predictions to measured double-diff. inclusive jet X-section vs jet p_T and jet rapidity – different **NLO PDF** sets used: **CT14, HERAPDF2.0, NNPDF3.0, MMHT2014**



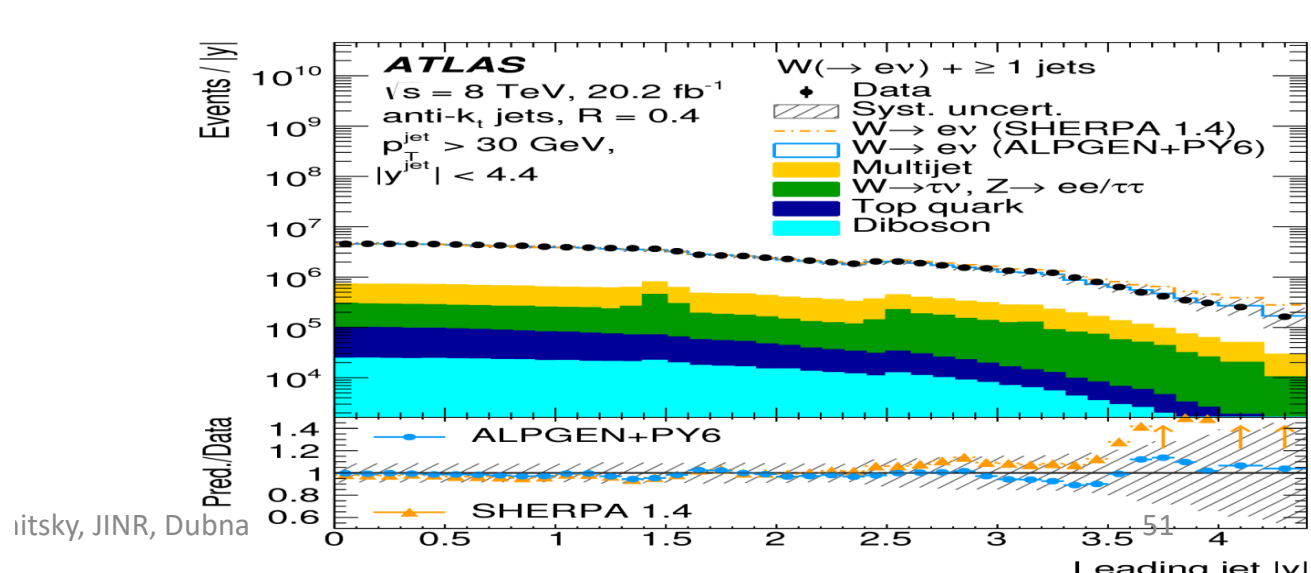
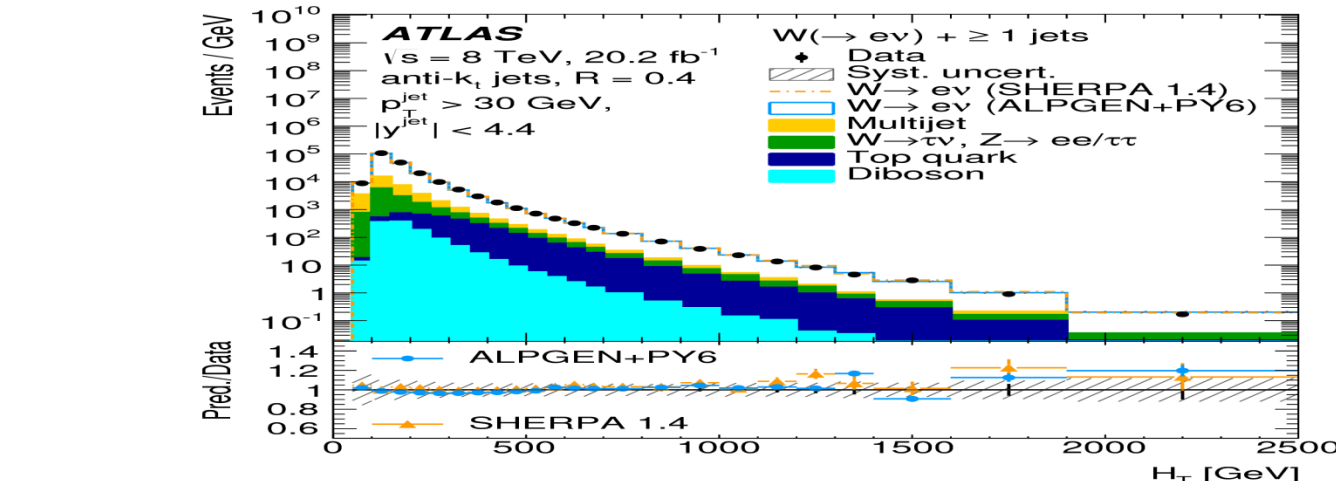
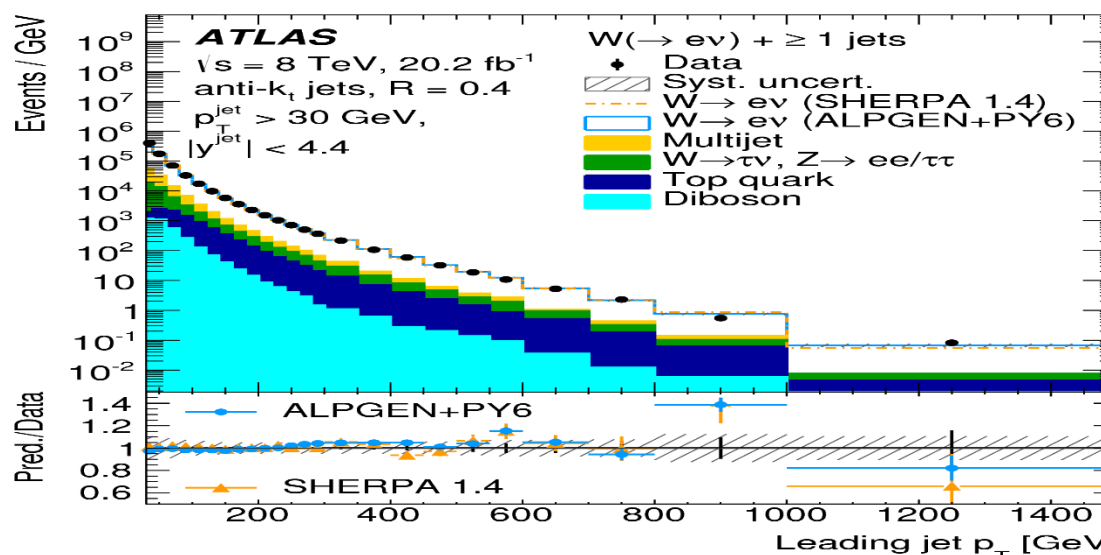
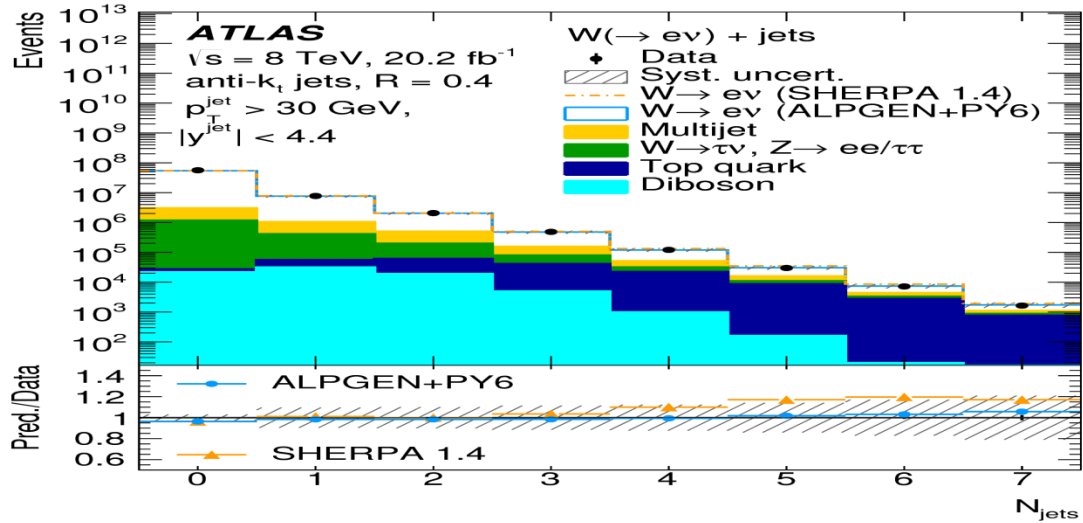
CROSS-SECTIONS OF $\text{pp} \rightarrow W + \text{jets}$, W^+/W^- RATIOS AT 8 TeV

arXiv:1711.03296



- $W(\rightarrow e\nu)$ production in association with jets
- Include forward jets: $|y| < 4.4$

- Challenge – Backgrounds \rightarrow Multijet: Dominant at low N_{jets}
- Suppress by electron isolation & low momentum contributions to E_T^{miss} from tracks, not calorimeter deposits

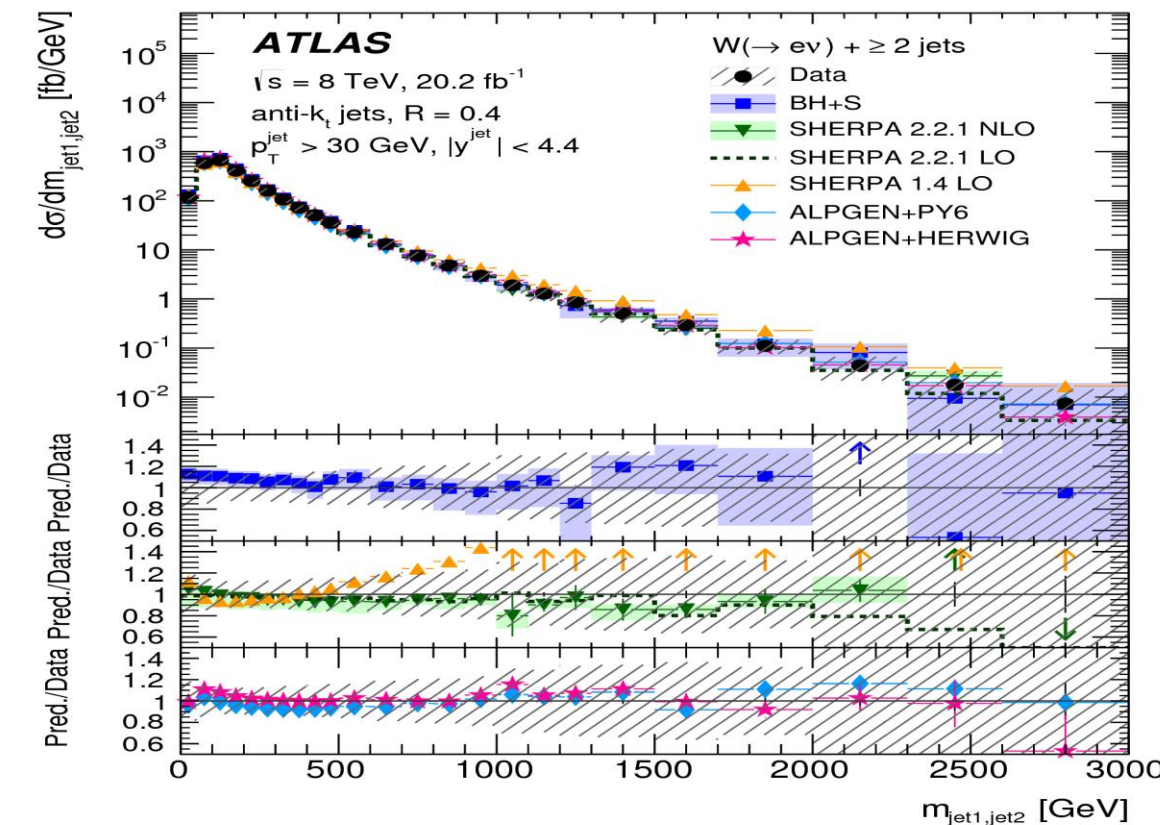
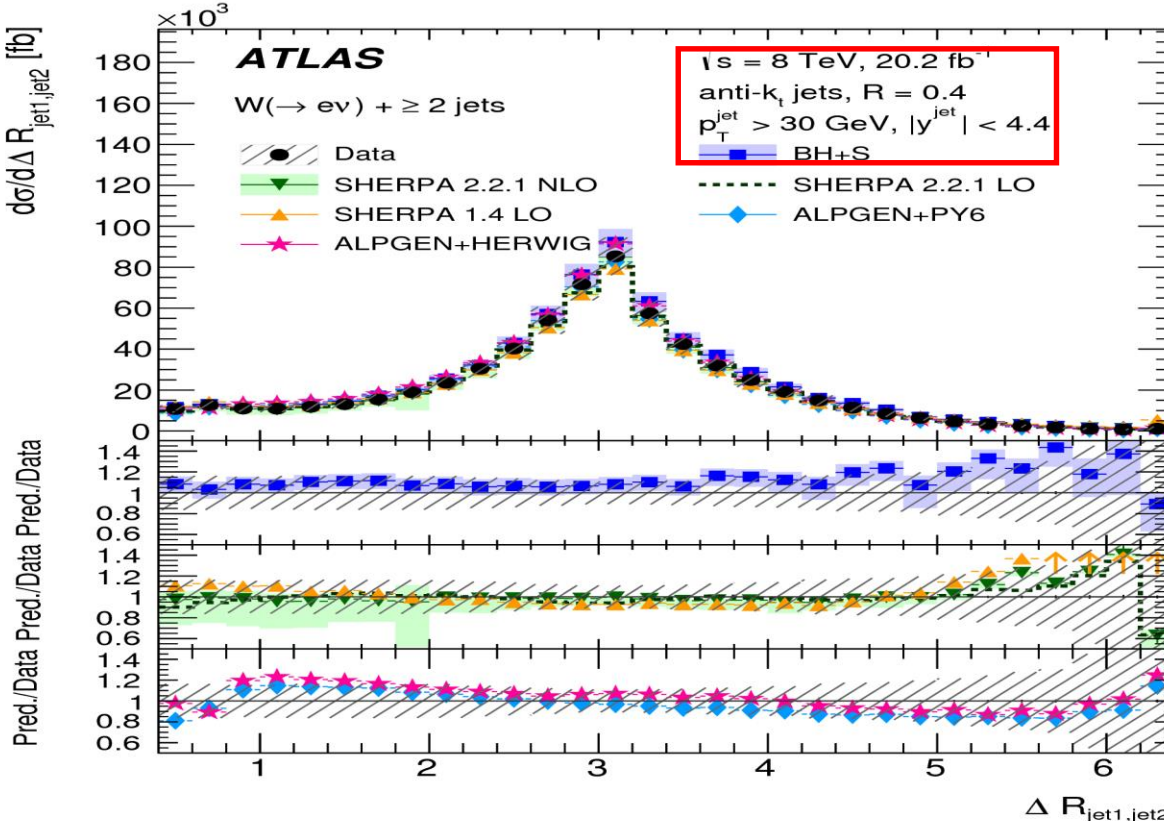


CROSS-SECTIONS OF $pp \rightarrow W + \text{jets}$, W^+/W^- RATIOS AT 8 TeV

arXiv:1711.03296



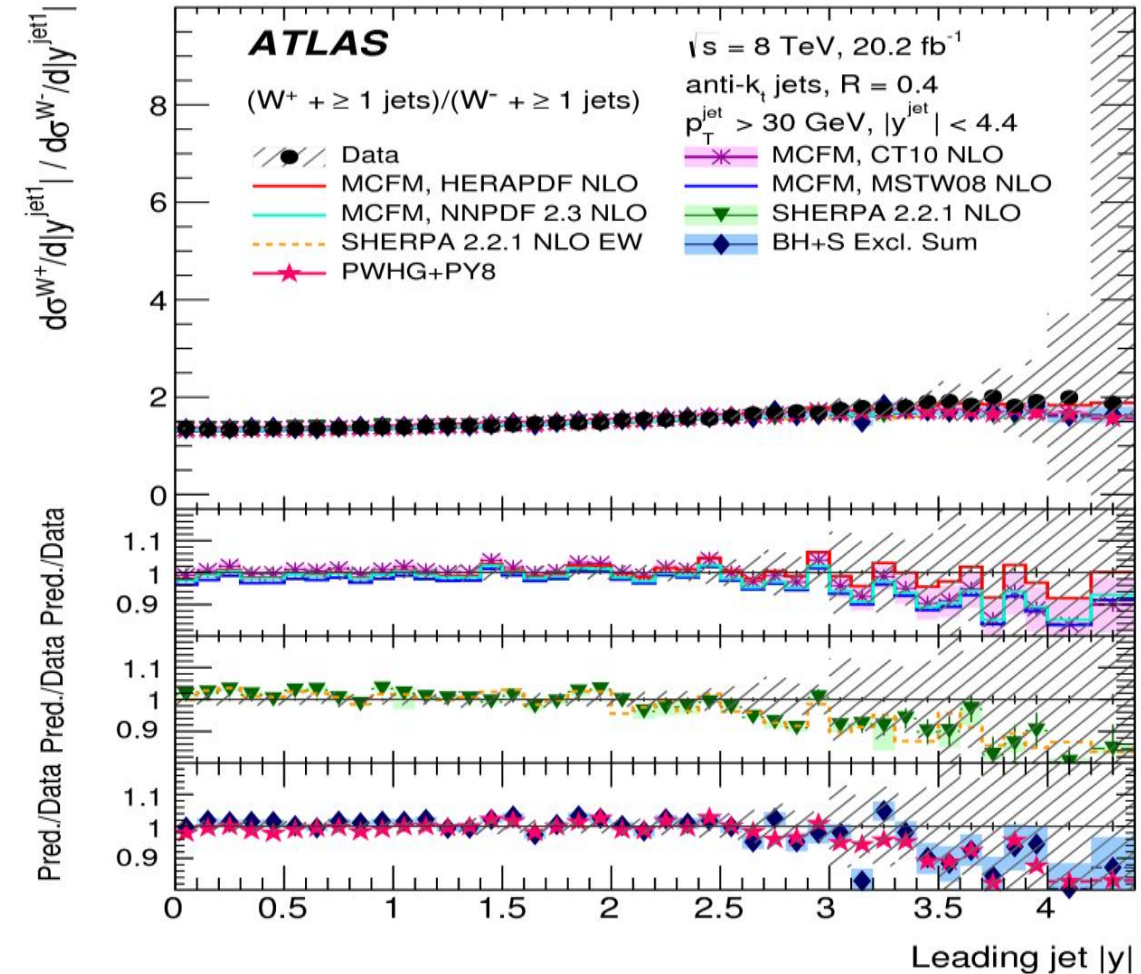
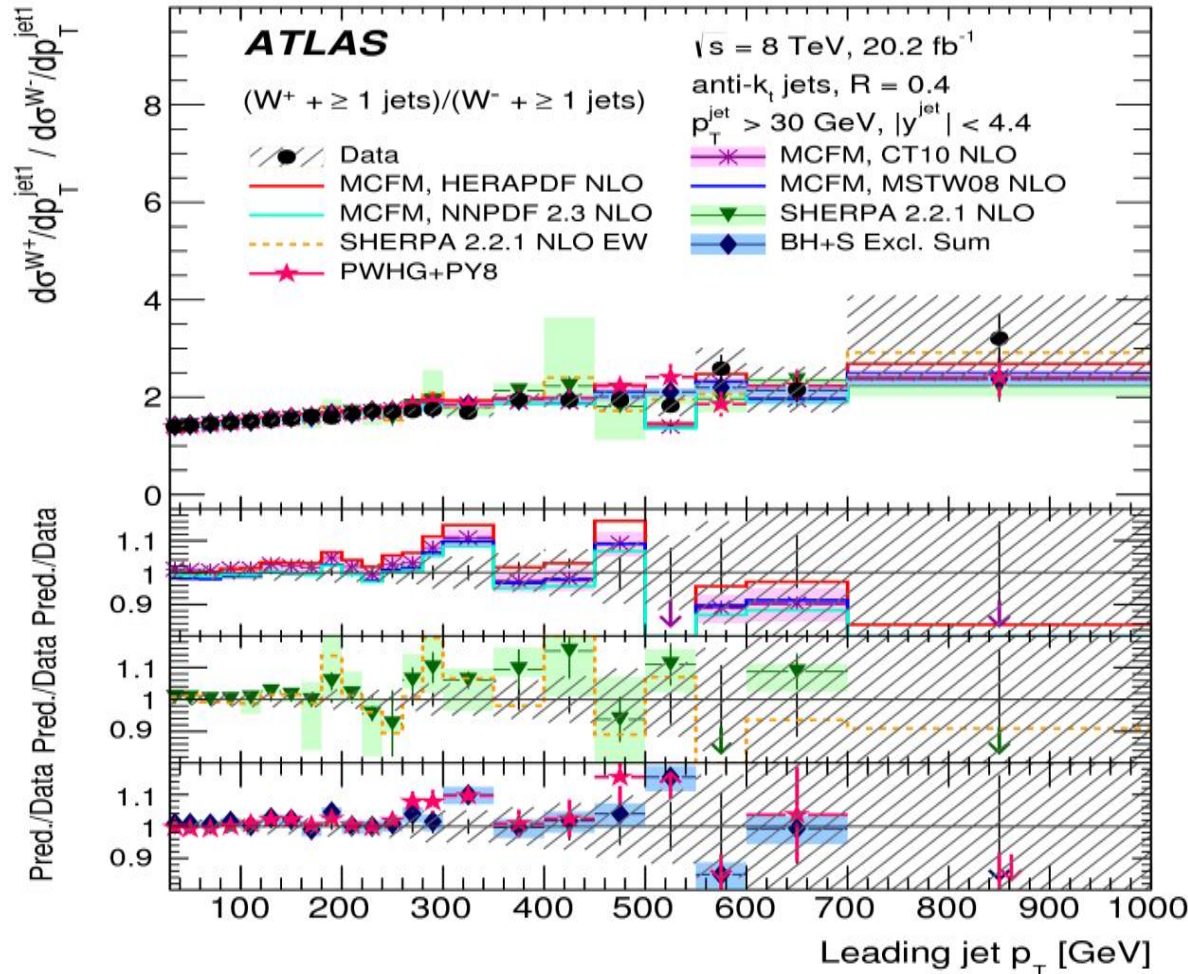
- $\Delta R_{\text{jet1,jet2}}$ and $M_{\text{jet1,jet2}}$ (*Dijet invariant mass*) sensitive to **hard parton radiation** at large angles and different ME/PS matching schemes
- **Sherpa 1.4** predicts too many events at large $\Delta R_{\text{jet1,jet2}}$ and $M_{\text{jet1,jet2}}$
- Both **Alpgen+Herwig** and **Alpgen+Py6** do not describe $\Delta R_{\text{jet1,jet2}}$ well



However, there is no single prediction that is able to describe all distributions well
 29.09.2018 NTIHEP

CROSS-SECTIONS OF $\text{pp} \rightarrow W + \text{jets}$, W^+/W^- RATIOS AT 8 TeV

- MCFM predictions differ by $\sim 2\text{--}5\%$ depending on the PDF set used
- Differences between data and MCFM predictions above experimental uncertainties for W boson $p_T \sim 200\text{--}400$ GeV → results useful for PDF fits

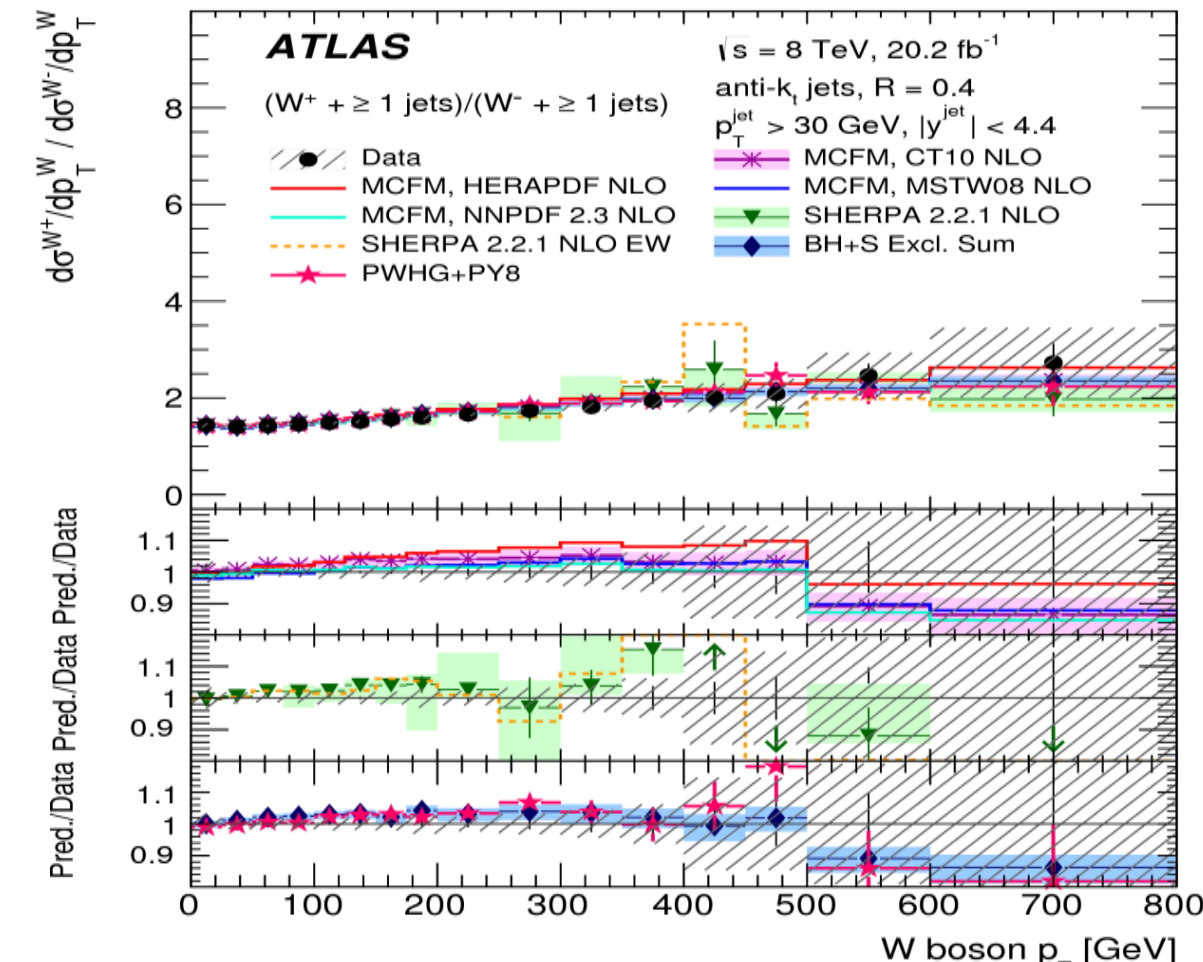
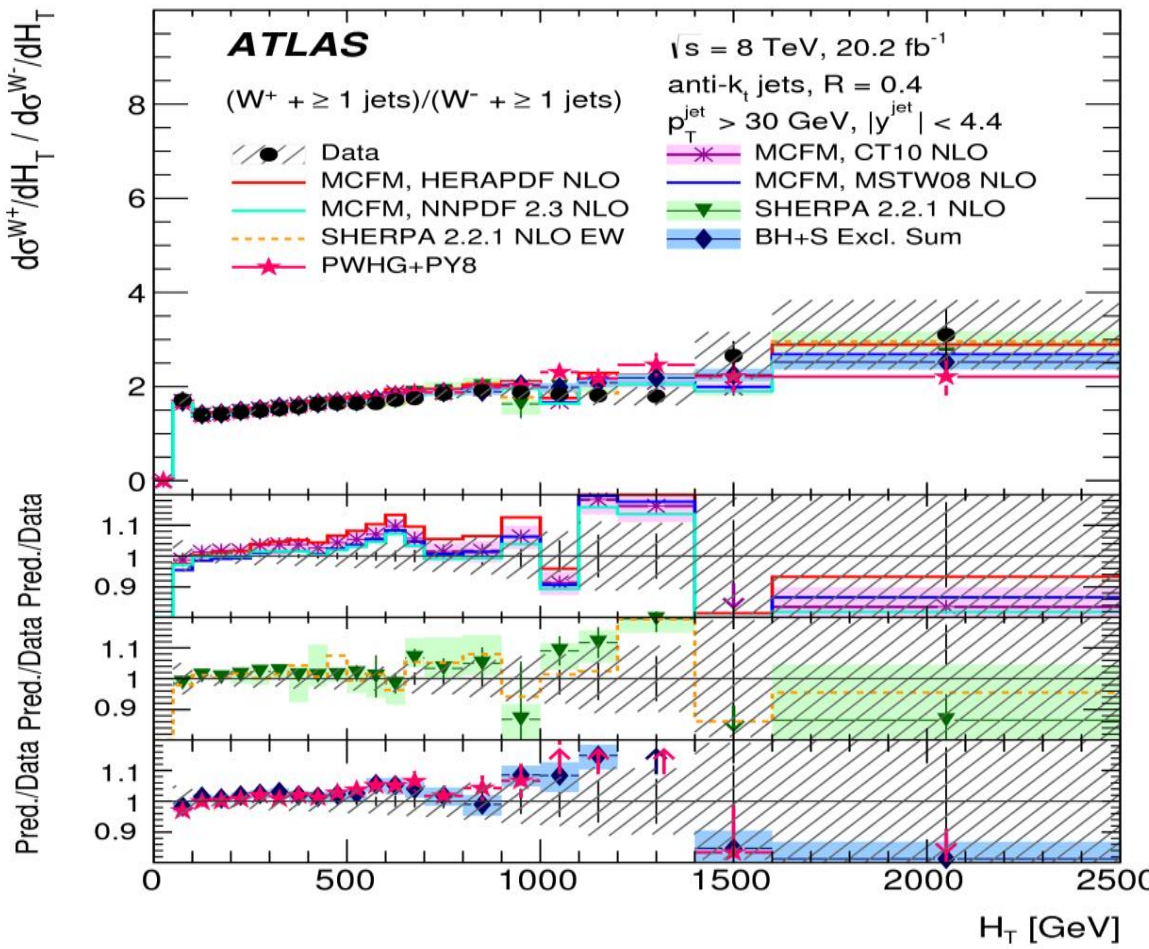


CROSS-SECTIONS OF $pp \rightarrow W + \text{jets}$, W^+/W^- RATIOS AT 8 TeV

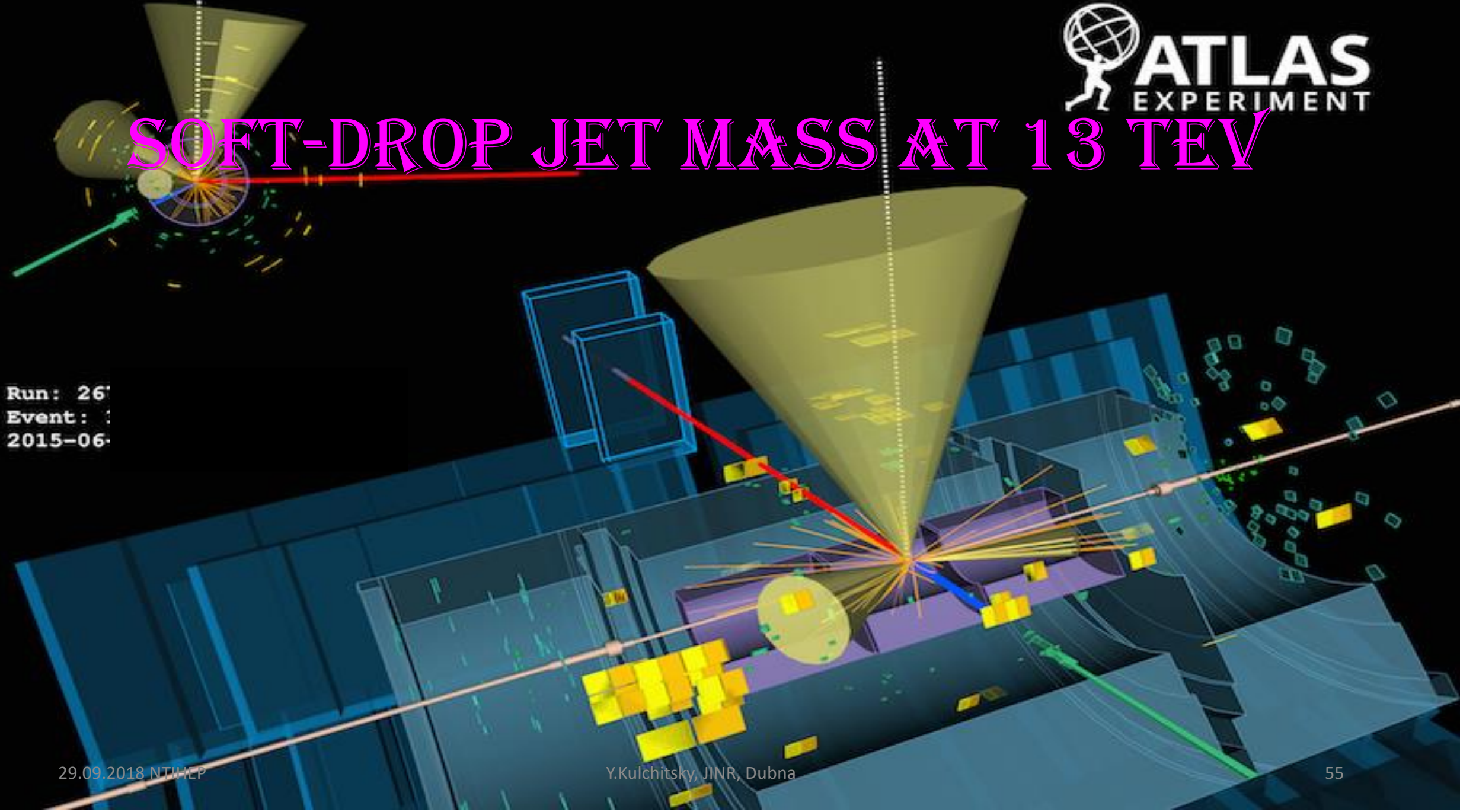
arXiv:1711.03296



- MCFM predictions differ by $\sim 2\text{--}5\%$ depending on the PDF set used
- Differences between data & MCFM predictions above experimental uncertainties for W boson $p_T \sim 200\text{--}400$ GeV → results useful for PDF fits



SOFT-DROP JET MASS AT 13 TEV



Motivation

- Precision calculations of *jet substructure moments* like the jet mass are difficult since they are *sensitive to soft and wide-angle radiation*
- Systematically *removing soft and wide angle radiation* from a jet with the *soft drop grooming algorithm* can allow for *precision calculations* as well as *improved experimental resolution*
- *Probing QCD beyond the parton shower accuracy, starting new era of precision Jet SubStructur (JSS); improving the understanding of JSS properties*

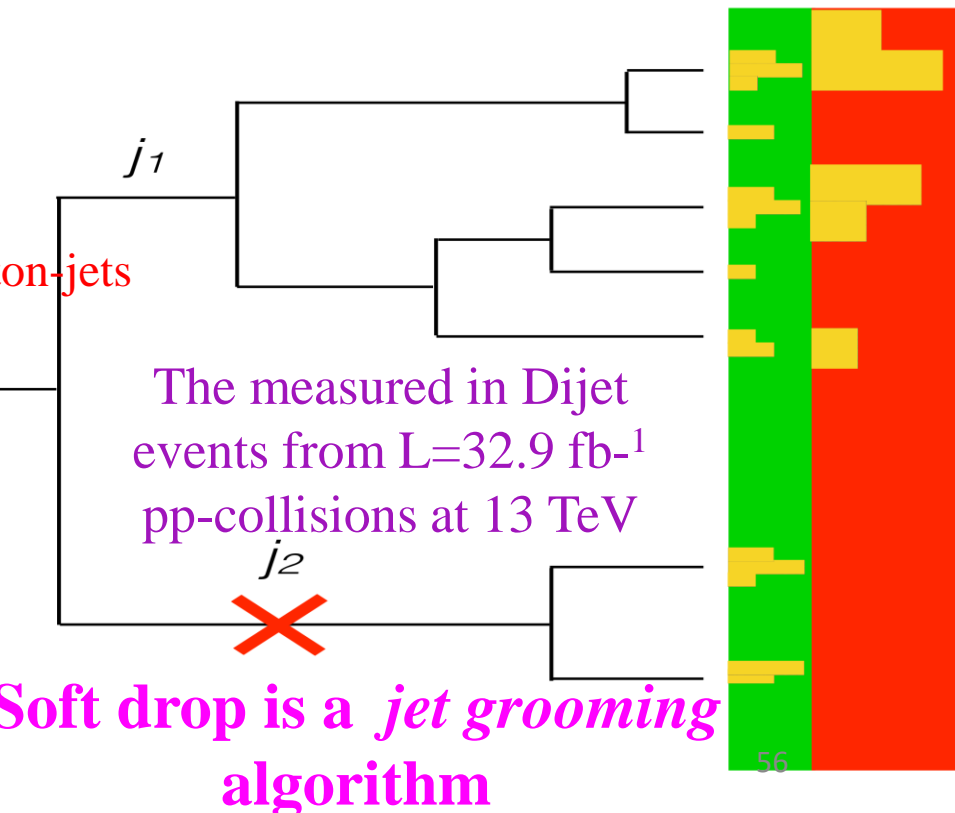
Jet Reconstruction with Soft Drop

- Create $R=0.8$ anti- k_T jets, and recluster their constituents with the *Cambridge/Aachen algorithm*
- Starting from the last branch of the clustering history, check if

$$\frac{\min(p_{T,j1}, p_{T,j2})}{(p_{T,j1} + p_{T,j2})} > z_{\text{cut}} \left(\frac{\Delta R_{j1,j2}}{R} \right)^{\beta}$$

← Distance proton-jets
↑ Scale of energy removed
↑ Sensitivity tuning

- z_{cut} sets the *scale of energy removal*: use $z_{\text{cut}} = 0.1$
- β determines the sensitivity to *wide-angle radiation*: $\beta = 0, 1, 2$
- *If this condition is not satisfied, the softer branch is removed.*
Once this condition is satisfied, the algorithm terminates



Event Selection

- $p_T^{\text{lead}} > 0.6 \text{ TeV}$, to be fully efficient for the lowest unprescaled trigger
- Apply *Dijet* selection: $p_T^{\text{lead}} < 1.5 * p_T^{\text{sublead}}$
- Measure as a function of $\rho = \log_{10} \left[\left(\frac{m^{\text{softdrop}}}{p_T^{\text{ungroomed}}} \right)^2 \right]$; ρ depends logarithmically on p_T , so final result are binned inclusively in p_T ; Soft drop jet mass: $(m^{\text{softdrop}})^2 = (\Sigma E)^2 - (\Sigma p)^2$
- Simultaneously unfold in p_T and ρ and normalize each p_T bin between -3 & -1 in ρ

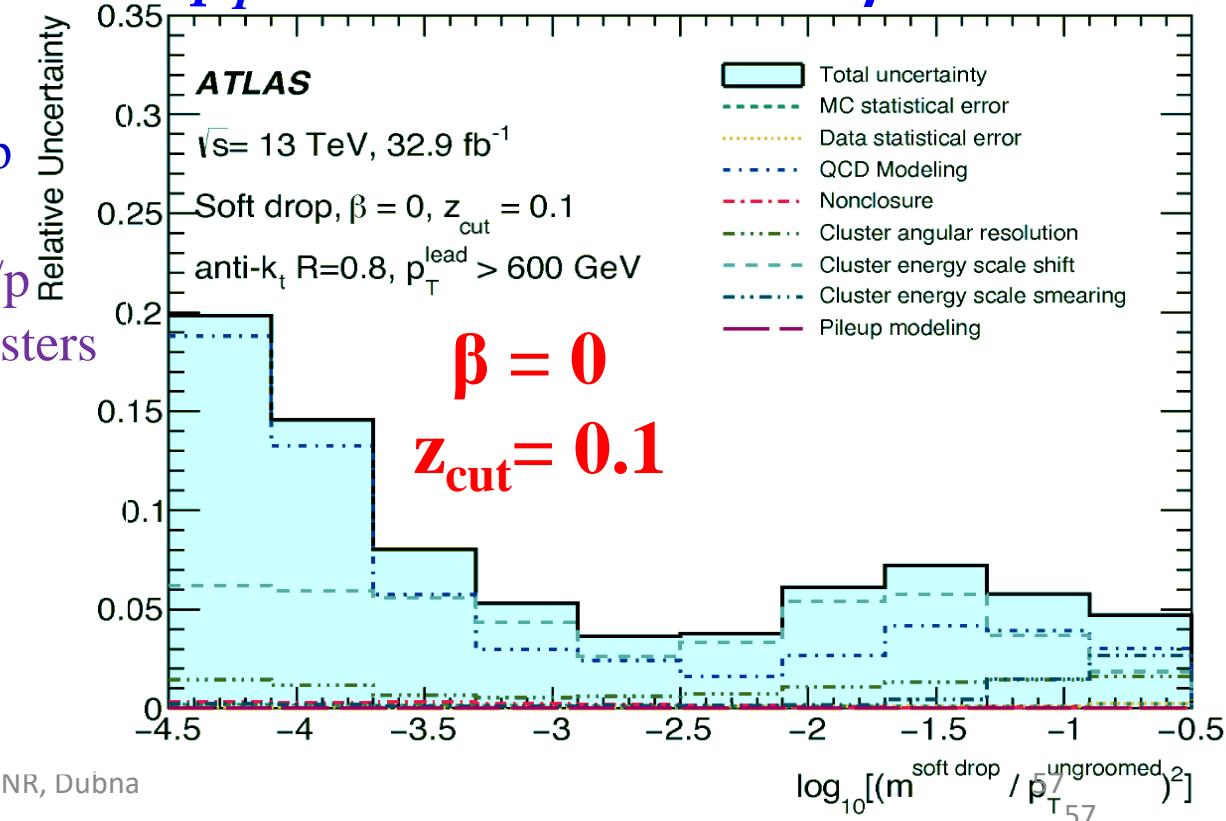
Uncertainties

Cluster Energy Scale Shift: Data/MC difference in the E/p ratio used to determine a shift for clusters

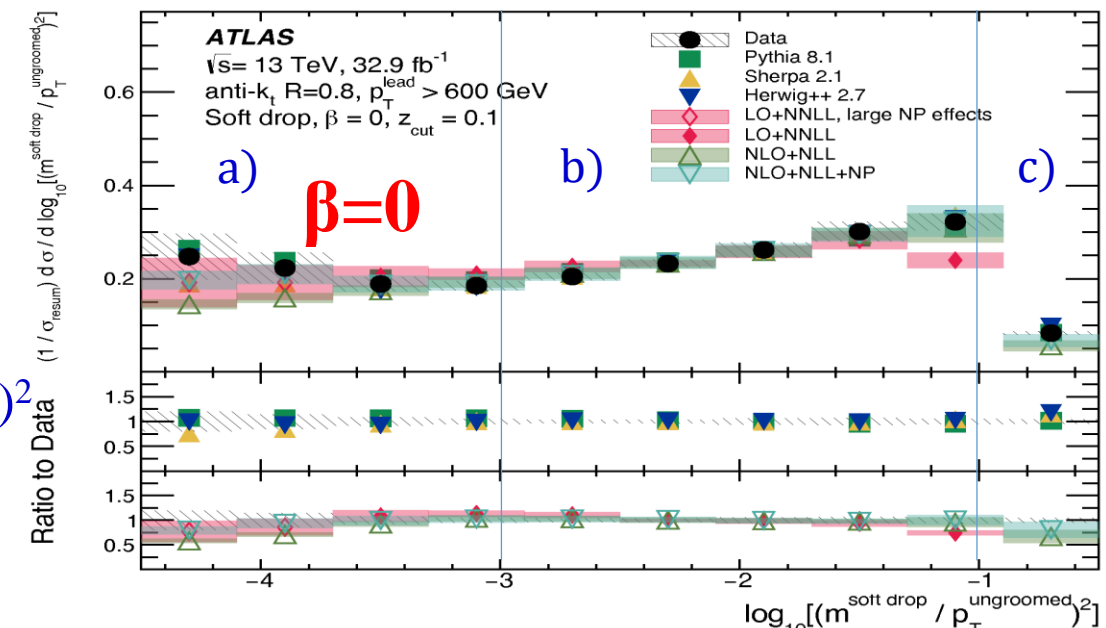
Cluster Energy Scale Smearing: Data/MC difference in E/p ratio used to determine a smearing in the energy scale of clusters

Cluster Angular Resolution:

- Use the distribution of ΔR (track, cluster) to determine an angular smearing of cluster of **5 mrad**;
- Dominated by modeling uncertainties at low mass, with cluster energy scale uncertainties also very important at moderate and high mass



- Measured *the soft drop jet mass* and compared to *two QCD predictions* with accuracy beyond Leading-Logarithm (LL)
- Three main regimes for $\rho = \log_{10} \left[\left(\frac{m^{\text{softdrop}}}{p_T^{\text{ungroomed}}} \right)^2 \right]$
 - a) $\rho < -3$: *non-perturbative regime*; b) $-3 < \rho < -1$: *resummation regime*; c) $\rho > -1$: *fixed order regime*; $(m^{\text{softdrop}})^2 = (\Sigma E)^2 - (\Sigma p)^2$
- *Resummation regime* should be most accurate for MC and Leading Order (LO) + Next-to-Next-to-Leading-Logarithm (NNLL), while *fixed order regime* should be most accurate for Next-to-Leading Order (NLO)+NLL
 - ❖ Predictions agree with measurement in regions where non-perturbative effects are small
 - ❖ Less good agreement with predictions and measurement at small ρ particularly for higher β
- *PYTHIA, SHERPA, HERWIG* all do an excellent job of describing the data over the entire mass range



□ *Larger β means less grooming and less agreement*

